The interaction of lymphogranuloma venereum and oculogenital *Chlamydia trachomatis* with human keratinocytes and cervical epithelium

Bronwyn C. Joubert

Submitted in fulfillment of the requirements for the degree of
Doctor of Philosophy in the Department of Medical Microbiology

As the candidate's supervisor I agree to the submission of this thesis.

Signed:_____ Date:_____

Plagiarism:

DECLARATION

I Bronwyn Joubert declare that

(i) The research reported in this thesis, except where otherwise indicated, is my original work.

(ii) This thesis has not been submitted for any degree or examination at any other university.

(iii) This thesis does not contain other person's data, pictures, graphs or other information, unless specifically acknowledged as being sourced from other persons.

(iv) This thesis does not contain other person's writing, unless specifically acknowledged as being sourced from other researchers. Where other written sources have been quoted, then:
   a) Their words have been rewritten but the general information attributed to them has been referenced;
   b) Where their exact words have been used, their writing has been placed inside quotation marks, and referenced.

(v) Where I have reproduced a publication of which I am an author, co-author or editor, I have indicated in detail which part of the publication was actually written by myself alone and have fully referenced such publications.

(vi) This thesis does not contain text, graphics or tables copied and pasted from the Internet, unless specifically acknowledged, and the source being detailed in the thesis and in the References sections.

Signed: _____ Date: _____

PRESENTATIONS EMANATING FROM THIS THESIS

BC Joubert and AW Sturm. 2008. The "chlamydial" escape from the cell determines clinical presentation of LGV

- 11th International Union against Sexually Transmitted Infections (IUSTI) held in Cape Town, SA from 9 – 12 November 2009
- Poster presentation

BC Joubert and AW Sturm. 2008. The "chlamydial" escape from the cell determines clinical presentation of LGV

- 3rd Joint Congress of the Federation of Infectious Diseases Societies of Southern African (FIDSSA) held in Sun City, SA from 20 – 23 August 2009
- Oral presentation, BEST ABSTRACT AWARD

BC Joubert and AW Sturm. 2008. *Chlamydia trachomatis* infection of human keratinocytes and cervical cells

- 48th Annual Interscience Conference on Antimicrobial Agents and Chemotherapy (ICAAC®) and the Infectious Diseases Society of America (IDSA) 46th Annual Meeting held in Washington, DC, USA from 25 – 28 October 2008
- Poster presentation

BC Joubert and AW Sturm. 2008. *Chlamydia trachomatis* infection of human keratinocytes and cervical cells

- Astrazeneca College of Health Sciences Research Symposium
- Oral presentation

BC Joubert and AW Sturm. 2007. Interaction of lymphogranuloma venereum and oculogenital *Chlamydia trachomatis* with human keratinocytes and cervical epithelium

- 2nd Joint Congress of the Federation of Infectious Diseases Societies of Southern African (FIDSSA) held in Stellenbosch, SA from 28 – 31 October 2007
- Oral presentation

BC Joubert, T Naicker and AW Sturm. 2007. Interaction of lymphogranuloma venereum and oculogenital *Chlamydia trachomatis* with human keratinocytes and cervical epithelium

- Astrazeneca College of Health Sciences Research Symposium
- Poster presentation

BC Joubert, T Naicker and AW Sturm. 2007. Interaction of lymphogranuloma venereum and oculogenital *Chlamydia trachomatis* with human keratinocytes and cervical epithelium

- 17th International Society for Sexually Transmitted Diseases Research (ISSTDR) Conference held in Seattle, USA from 29 July – 1 August 2007
- Poster presentation

BC Joubert, T Naicker and AW Sturm. 2006. Ultrastructural characterization of *Chlamydia trachomatis* pathophysiology on human keratinocytes and cervical epithelium

- 45th Annual Conference of the Microscopy Society of Southern Africa (MSSA) held in Port Elizabeth, SA from 29 November – 1 December 2006
- Oral presentation

BC Hay and AW Sturm. 2005. The interaction of lymphogranuloma venereum and oculogenital *Chlamydia trachomatis* with human keratinocytes and cervical epithelium

- Astrazeneca College of Health Sciences Research Symposium
- Oral presentation

ACKNOWLEDGEMENTS

My supervisor Prof A.W. Sturm for his expert advice and guidance throughout this project Thank you for giving me enough freedom to learn to think, enough guidance to keep me on the right path, and enough encouragement to keep me striving for new heights

Registrars in the Department of Medical Microbiology for the collection of the clinical isolates

Staff of the Sexually Transmitted Diseases Laboratory within the Department of Medical Microbiology for identifying LGV *C. trachomatis* positive specimens prior to culture of the organism

Prof T Naicker of the Optics and Imaging Centre for use of the transmission electron microscope (TEM), fluorescent microscope, digital camera and image analysis software. Thank you not only for your assistance in teaching me how to use this equipment, but also for your advice and encouragement

Gaetan Kabera of the Medical Research Council for providing advice and guidance for the statistical analyses

Fatima Khan for determining the serovar of LGV clinical isolates using sequence analysis techniques

The Department of Physiology for use of their microplate reader for the MTT assay

My husband, Jean-Pierre Joubert. Thank you for your constant understanding and encouragement and for motivating me to keep going. Without your unselfish love and support this would not have been possible

TABLE OF CONTENTS

LIST OF FIGURES AND TABLES

LIST OF ABBREVIATIONS

ANOVA	Analysis of Variance
ADP	adenosine diphosphate
ATCC	American Type Culture Collection
ATP	adenosine triphosphate
CADD	*Chlamydia* protein associated with death domain
CDC	Centers for Disease Control and Prevention
CCM	cell culture medium
CGM-E	Chlamydia growth medium for experiments
CGM-P	Chlamydia growth medium for propagation
CO_2	carbon dioxide
Da	dalton
DAB	diaminobenzidine
dH_2O	distilled water
dUTP	deoxyuracil triphophate
DNA	deoxyribonucleic acid
IDO	indoleamine 2,3-dioxygenase
EB	elementary body
EMEM	Eagle's minimum essential medium
FBS	fetal bovine serum
FITC	fluorescein isothiocyanate
fov	field of view
GM-CSF	Granulocyte-macrophage colony-stimulating factor
HEPES	4-(2-hydroxyethyl)-1-piperazineethanesulphonic acid

IL	interleukin
INF-γ	interferon-γ
kDa	kilodalton
LDH	lactate dehydrogenase
LGV	lymphogranuloma venereum
MHC	Major Histocompatibility Complex
min	minutes
MOI	multiplicity of infection
MoPn	mouse pneumonitis
MTT	3-(4,5-dimethylthiazol-2-yl)-2,5-diphenyltetrazoliumbromide
N-WASP	Neuronal Wiskott-Aldrich Syndrome Protein
NEAA	non-essential amino acids
NF	nuclear factor
NK	natural killer
Nm	nanometers
NO	nitric oxide
OG	oculogenital
PBS	phosphate buffered saline
PCD	programmed cell death
PCR	polymerase chain reaction
PE	polyester
PZ	plasticity zone
RB	reticulate body
RER	rough endoplasmic reticulum
RNA	ribonucleic acid

RPMI	Roswell Park Memorial Institute
SD	standard deviation
sec	seconds
SPG	sucrose-phosphate-glutamate buffer
TC	tissue culture
TCA	tricarboxylic acid
tdH_2O	triple distilled water
TEM	transmission electron microscopy
TdT	terminal deoxynucleotidyl transferase
Th	T helper type
TNF-α	tumour necrosis factor-α
TUNEL	deoxynucleotidyl transferase-mediated dUTP nick end labeling
μm	micrometer

ABSTRACT

Background

Keratinocytes are the first target of infection for lymphogranuloma venereum (LGV) *Chlamydia trachomatis*, yet they have been omitted from pathogenesis studies. We infect keratinocytes and cervical cells with *C. trachomatis* and hypothesize different growth and cytotoxicity profiles among the strains.

Methods

HaCaT human keratinocytes and ME-180 cervical cells were infected with *C. trachomatis* (multiplicity of infection (MOI) 0.025) serovars L1, L2, L3, 3 LGV clinical isolates or serovar E and incubated at 37 or 33°C for 5 days. Cytotoxicity was quantified daily using the CytoTox96® Non-Radioactive Cytotoxicity Assay, cells stained with the MicroTrak *C. trachomatis* Culture Confirmation kit and growth quantified by area of 100X photographs covered by Chlamydia. HaCaT and ME-180 cervical cells were infected with *C. trachomatis* (MOI 0.25) serovar L2 or E, incubated at 37 or 33°C for 48 hours and viewed with a transmission electron microscope (TEM). Mitochondrial activity was quantified using the MTT assay. The DeadEnd™ Colorimetric TUNEL System with *C. trachomatis* Culture Confirmation kit as a counter-stain was used to assess cell death in infected versus uninfected cells. The BioVision™ CaspGLOW Fluorescein Caspase Staining Kit and Transwell® Permeable Supports was used to differentiate between apoptosis mediated by cell-to-cell contact or a secreted molecule.

Results

Growth in ME-180 versus HaCaT cells at 37°C was similar, but slower at 33 versus 37°C in HaCaT cells ($p < 0.05$). By day 5 L2 had grown faster than other strains in HaCaT cells at 37°C ($p < 0.05$), faster than clinical isolates in ME180 cells ($p < 0.01$), and faster than

serovar E, and 2 clinical isolates at 33°C ($p < 0.01$). After 5 days L2 induced cytotoxicty was 11% in ME180 cells, which was higher than the clinical isolates ($p < 0.01$). In HaCaT cells at 33°C L2 EB were identified in a non-membrane state in the cytoplasm but not in the inclusion at 48 hours post infection. Serovar E but not L2 caused mitochondrial swelling at 1 h post infection in HaCaT cells at 37°C. This corresponded with a 16% reduction in mitochondrial activity ($p < 0.001$). TUNEL assay analyses demonstrated numerous dead cells adjacent to chlamydial inclusions for strains L2 and L3 but not L1 and E. An elevated number of caspase positive cells was detected in uninfected cell monolayers exposed to both L2 and E at 37°C but not 33°C.

Conclusions

1. *C. trachomatis* infects human keratinocytes *in vitro.*
2. Fresh clinical isolates behaved differently to the L2 reference strain. This demonstrates the need for fresh clinical isolates in pathogenesis studies of LGV.
3. In HaCaT cells at 33°C serovar L2 EB leave the intact inclusion and migrate through the cytoplasm in a non-membrane bound state
4. *C. trachomatis* induces apoptosis in uninfected cells exposed to infected cells via a secreted molecule at 37°C. This is more marked with serovar L2 exposure than serovar E exposure.

CHAPTER 1 – INTRODUCTION

Chlamydia trachomatis is a sexually transmitted obligate intracellular human pathogen with several different disease manifestations depending on the site of infection and biovar of the microbe present (Ward 2002).

Based on their differences in disease presentation and in vitro cell growth characteristics, the species, *C. trachomatis*, has been divided into two biovars: the oculogenital (OG) biovar and the lymphogranuloma venereum (LGV) biovar (Ward 2002). Due to differences in immunological cross-reactivity with the major outer membrane protein (MOMP) these biovars are further subdivided into different serovars which reflect differences in tissue tropism (Ward 2002). Within the trachoma biovar, serovars A to C cause ocular trachoma, while serovars D to K cause genital tract infections and conjunctivitis (Ward 2002). The LGV biovar, which includes serovars L1 to L3, causes LGV, a more invasive genital tract infection (Ward 2002).

C. trachomatis replicates using a biphasic growth cycle comprising two alternating life forms: the extracellular, metabolically inactive, infective form called the elementary body (EB), and the intracellular, metabolically active, non-infective form called the reticulate body (RB). Infection is initiated by attachment and entry of the EB into the host cell where it remains enclosed in a vesicle called an inclusion. The EB develops into a RB and multiplies within the inclusion before condensing to form an EB which is released from the host cell by exocytosis.

Over the years efforts have been made to determine the exact mode of attachment and entry of *C. trachomatis* EB into their target host cells, however, despite the fact that LGV begins as a genital ulcer on the skin, no previous research has been published on the interaction of *C. trachomatis* with keratinocytes. Since the mode of *C. trachomatis* entry into host cells depends on each host cell type concerned and the biovar investigated, (Bavoil *et al* 2000) it is of paramount importance that chlamydial pathogenesis studies be carried out on the host cell type affected *in vivo*. For the LGV organism keratinocytes are the primary target of infection, while the cervical cells are one of the primary targets of infection for the urogenital OG serovars.

In this study the HaCaT cell line was be utilized since it is a well characterized immortalized human keratinocyte cell line which has retained a similar differentiation pattern to that of normal keratinocytes (Boukamp *et al* 1988). The ME-180 cell line, was used since it is a spontaneously immortalized human cervical carcinoma cell line which has retained the characteristic of its wild type counterparts (Sykes *et al* 1970).

Past research has also been carried out primarily on characterized reference strains whose behaviour may have been altered by many years of *in vitro* propagation in culture systems and cell lines which are not the natural host. To investigate this possibility, fresh LGV clinical isolates were used in addition to the LGV reference strains since the LGV organisms were the focus of these investigations. One serovar E OG clinical isolate was used for comparison purposes.

This work is of relevance in South Africa since LGV is the second most common cause of genital ulcers in our setting (Moodley *et al*, 2003) and is found in 13.6% of men (O'Farrell

et al 2008), and 15.4% of women (Moodley *et al* 2003) with ulcers. Male chlamydial urethritis is also common and is detected in 16% of urethritis patients (Sturm *et al* 2004).

The development of a more appropriate *in vitro* model on which to study the interaction of this microbe with its host cell may lead to a better understanding of *C. trachomatis* attachment and entry, which could ultimately enable the development of new and better methods of patient treatment.

In this study we demonstrate for the first time the ability of *C. trachomatis* to enter and replicate within keratinocytes. This was achieved in the absence of cycloheximide and at both 37 and 33°C. 37°C is core body temperature, while 33°C is the temperature of human skin. *C. trachomatis* was also grown in cervical cells at 37°C. These models of infection were used for the experiments.

Chlamydial growth curves were set up to investigate the rate of replication of several chlamydial strains under conditions described above. The lactate dehydrogenase (LDH) assay was used to quantify chlamydia-induced cell lysis under these same conditions.

Transmission electron microscopy (TEM) was used to monitor the ultrastructural effect of the serovar L2 reference strain and one OG clinical isolate on their host cells.

Because the results of the LDH assay and TEM analyses indicated cytotoxicity and mitochondrial pathology respectively, cytotoxicity assays were used to further investigate these effects.

The TUNEL assay, with counter staining for *C. trachomatis* was used to investigate the spatial relationship between dying and infected cells. The MTT assay was used to quantify the mitochondrial degradation observed on TEM analysis. The caspase assay coupled with Transwell® Permeable Supports was used to investigate whether the cytotoxic effects were apoptotic or not, and to determine if this occurred by cell-to-cell contact or via a secreted molecule.

Methods which quantify apoptosis and necrosis using flow cytometry were not used because unlike other cell lines which are traditionally used for chlamydial studies, HaCaT keratinocytes are difficult to trypsinize. This also leads to the formation of cell clumps which may clog the flow cytometer. The comparatively harsh trypsinization procedure compared to other cell lines would increase the opportunity for the more fragile cells at the late stages of infection to rupture and be omitted from the analyses causing bias.

Furthermore, propidium iodide staining was not used because chlamydial infection produces a rapid transient translocation of phosphatidylserine (Goth and Stephens 2001) which would lead to the detection of false positives. Although this phenomenon is transient, the duration of the chlamydial replication cycle is not exact and new chlamydial inclusions may already begin to develop before 36 hours post infection.

The aims of this study were as follows:

- To investigate whether *C. trachomatis* does infect HaCaT keratinocytes
- To establish differences in infectivity and growth rate at 37 and 33°C

- To investigate differences in growth between the LGV and OG strains with a focus on the LGV strains, and to investigate differences between the LGV reference strains and LGV clinical isolates over 5 days using growth curve analyses
- To investigate the cytotoxic effect of *C. trachomatis* on HaCaT and ME-180 cell monolayers using the lactate dehydrogenase assay
- To investigate the ultrastructural effect that *C. trachomatis* has on HaCaT and ME-180 host cells
- To quantify *C. trachomatis*-induced mitochondrial damage on HaCaT and ME-180 cells using the MTT assay
- To investigate the spatial relationship between dying cells and infected cells using the TUNEL assay with a counter stain for *C. trachomatis*
- To determine whether caspase-mediated cell death (apoptosis) takes place, and if so, whether this occurs via cell-to-cell contact or a secreted molecule

CHAPTER 2 – LITERATURE REVIEW

2.1 Historical aspects and classification of *Chlamydia trachomatis*

Chlamydia trachomatis is a highly specialised, obligate intracellular Gram negative eubacterium (Weisburg *et al* 1986) which has left a trail of taxonomic confusion due to its unique characteristics. In 1907 Halberstaedter and von Prowazek first reported inclusions of the trachoma agent in infected ocular material, but mistaking these organisms for protozoans, conferred the name Chlamydozoaceae to what they saw as "mantled animals" (Ward 1983, Gilbert 1996). Hence the term *Chlamydia* (a cloak) is actually a misnomer, but has precedence in the international rules for bacterial nomenclature (Ward 1983).

Although Durand, Nicolas and Favre recognised LGV as a separate venereal disease in 1913, it was only in 1930 that the causative agent was transmitted to animals by Hellerström and Wassén, and in 1933 Findlay isolated the organism in mice. Findlay also recognised the similarities in the growth cycle of the LGV organism with that of the psittacosis agent which had already been described (Ward 1983).

Chlamydia was later classified, along with other filterable agents that grow in living cells, as viruses (Ward 1983). They were further grouped according to their host and tissue tropisms and referred to as Bedsoniae and trachoma inclusion conjunctivitis (TRIC) agents, however this method of classification was unsatisfactory since a laboratory isolate could only be classified if the clinical source of the isolate was known (Ward 1983).

Later, once Stanier and Lwoff formulated the concepts describing the basic differences between viruses and bacteria, it became accepted that Chlamydiae are bacteria, not viruses, since they posses both DNA and RNA, and multiply by binary fission rather than self-assembly (Moulder 1966). These organisms are distinguished from the rickettsiae, another group of intracellular bacteria, by their developmental cycle, and their requirement for high energy compounds from their host (Weiss and Wilson 1969, Hatch 1975), as well as their lack of cytochromes and other components of the respiratory electron chain (Ward 1983).

Although the family Chlamydiaceae was previously thought to contain a single genus, *Chlamydia*, which comprised four species: *C. trachomatis*, *C. pneumonia*, *C. psittaci* and *C. pecorum*; ribosomal sequence data has incited revision of this classification such that the family Chlamydiaceae comprises two geni: *Chlamydia* and *Chlamydophila*. The genus *Chlamydia* comprises a two species; *C. trachomatis* and *C. muridarum*, while the genus *Chlamydophila* includes all the other Chlamydiaceae species (Ward 2002).

The species *C. trachomatis*, however, is further subdivided into two biovars based on fundamental differences in their involvement in human disease, and invasiveness for cell culture (Ward 2002). The oculogenital (OG) biovar includes those organisms which cause trachoma, inclusion conjunctivitis (TRIC agents) and genital discharge disease, while the lymphogranuloma venereum (LGV) biovar includes those organisms which cause the more invasive disease, LGV (Ward 2002, Gilbert 1996). Each biovar is further subdivided into several serovars or serotypes, based on differences in the epitopes carried on the major outer membrane protein (MOMP) (Ward 2002). Serovars A, B, Ba and C of the OG biovar cause trachoma; serovars D, Da, E, F, G, H, I, J and K of the same biovar cause

genital tract infection or conjunctivitis; and the LGV biovar, which comprises serovars L1, L2, L2a and L3, causes LGV (Ward 2002, Gilbert 1996, Wang and Grayston 1991).

2.2 Clinical manifestations and epidemiology

Despite enormous similarity in the genomic makeup of *C. trachomatis* serovars (Carlson *et al* 2004), these organisms are responsible for a wide range of disease presentations (Ward 2002).

Within the OG biovar strains A-C cause ocular trachoma. Within the same biovar serovars D-K cause discharge diseases (urethritis or cervicitis) which may progress to epididymitis and possibly to prostatitis or pelvic inflammatory disease in males and females respectively. These serovars also cause inclusion conjunctivitis in neonates (Ward 2002).

Serovars L1-L3 within the LGV biovar cause LGV. This more invasive genital tract infection begins as a painless genital ulcer or papule in the skin in the primary stage, and then progresses to the secondary stage which is usually characterised by inguinal lymphadenopathy (Schachter and Osoba 1983). A tertiary stage or genito-anorectal syndrome may follow. This is usually associated with hypertropic and necrotic lymphnode packages, occasionally resulting in elephantiasis. Although patients classically present in the secondary stage (Schachter *et al* 1969), in our setting they usually present in the primary stage with chancroid-like lesions that are usually painful rather than painless (Sturm *et al* 2005). Several cases of proctitis caused by the LGV biovar have recently been reported from developed countries, particularly amongst men who have sex with men (Nieuwenhuis *et al* 2004). This disease is characterised by rectal ulceration with a purulent

anal discharge and fever, lower abdominal pain and tenesmus (Workowski and Berman 2007).

C. trachomatis infection is a world-wide problem. In the USA, about 3 million cases (serovars D-K) occur annually (Workowski and Berman 2007) and the prevalence varies in different parts of the world (Johnson *et al*, 2005, Behets *et al*, 1999).

LGV is of particular interest in South Africa since it is the second most common cause of genital ulcers (Moodley *et al* 2003) and the occurance has increased over the past few years. LGV is found 13.6% of men (O'Farrell *et al* 2008) and 15.4% of women (Moodley *et al* 2003) with genital ulcers. Chlamydia is detected in 16% of male patients with urethritis (Sturm *et al* 2004).

The Centers for Disease Control and Prevention (CDC) treatment guidelines for 2007 indicate azithromycin or doxycycline for the treatment of *C. trachomatis* infection (Workowski and Berman 2007). In South Africa LGV is treated according to local syndromic management guidelines for genital ulcer disease (Moodley *et al* 2003). These guidelines advise the use of erythromycin and benzathine penicillin for the treatment of genital ulcer disease. The spectrum of erythromycin includes LGV.

2.3 Laboratory diagnosis

2.3.1 Specimen collection and transport

Due to the fastidious nature of the organism, proper specimen collection and transport is vital. The collected specimen must contain epithelial cells which harbour the organism, and a cold chain of transport must be maintained to preserve viability of the organism for culture (reviewed in Black 1997).

2.3.2 Cultural methods

Culture has a specificity of almost 100%, and until recently was considered the "gold standard" for the detection of *C. trachomatis* in urogenital specimens (reviewed in Black 1997). Due to its relatively low sensitivity (70 – 85%) compared with DNA amplification tests, stringent requirement of refrigerated specimen transport as well as the fact that it is expensive, requires a high level of technical expertise and takes 3 to 7 days before results are available, culture has largely been replaced by nucleic acid amplification techniques (reviewed in Black 1997).

Before modern day tissue culture technology LGV *C. trachomatis* was cultured in the brains of mice, then later in the yolk sac of hens' eggs (Shaffer *et al* 1944).

Nowadays, *C. trachomatis* is cultured in cell culture monolayers, usually McCoy or HeLa 229 cells. To allow the chlamydia to successfully compete with the host cell's metabolism, the monolayers are pretreated with cycloheximide, DEAE-dextran or irradiation and the inoculum centrifuged onto the monolayer. Both these steps enhance the rate of detection (reviewed in Black 1997). Cultures are incubated for 48 to 72 hours, and inclusions visualized by staining with fluorescently labelled antibodies directed against the chlamydial lipopolysaccharide (LPS) for identification of all chlamydial species, or the

major outer membrane protein (MOMP) for *C. trachomatis*-species identification. It is the distinctive morphology of the inclusions with this fluorescent stain that accounts for the near 100% specificity. This identification test does not differentiate between the serovars (Black 1997).

Although the OG strains target the cervical, urethral and conjunctival epithelium, while the LGV strains target keratinocytes and lymphocytes, infection in *in vitro* cell culture does not always reflect these tissue tropisms. Although the growth rate in *in vitro* cell culture systems does reflect the tissue tropisms of each pathotype i.e. LGV strains replicate more rapidly, followed by OG strains isolated from the genitalia and lastly the trachoma causing-OG strains (Miyairi *et al* 2006).

2.3.3 Non-cultural Methods

In the 1980's antigen and nucleic acid detection technologies were developed and found widespread applications in diagnosis due to the reduced requirements in cost, expertise, preservation of infectivity during transport, and the time required to obtain results (Black 1997). Due to the technical difficulties of culture techniques, many papers report that these tests are more sensitive than culture, revealing that the prevalence of *C. trachomatis* in most populations is higher than was previously believed (Black 1997).

There are numerous non-culture diagnostic tests available based on a wide variety of technologies: nucleic acid amplification, direct visualisation of the organism by staining with fluorescein-labelled specific antibodies, immunohistochemical detection of the antigens and detection of hybridization to a DNA probe (Black 1997).

2.4 Biology of the organism

2.4.1 Morphology

Chlamydia trachomatis is a small Gram negative bacterium suited to its intracellular lifestyle with a biphasic developmental cycle comprising two ultrastructurally and metabolically distinct forms, the elementary body (EB) and the reticulate body (RB).

2.4.1.1 Elementary Body

The EB is responsible for the infectious stage of the developmental cycle and is more compact and osmotically stable than the RB to withstand environmental stress during passage from one host cell to another (Ward 1983, Ward 2002). It is spherical with a diameter of 300-350nm (Ward 2002). Since this developmental form is metabolically and transcriptionally inert, it has a compact DNA core tightly bound to three different DNA binding proteins (Wagar and Stephens 1988). Of these, the Hc1 protein is homologous to eukaryotic histone H1 protein (Hackstadt *et al* 1991, Tao *et al* 1991). This condensed DNA core occupies most of the cell and there is little cytoplasm.

2.4.1.2 Reticulate body

The RB, which is the osmotically fragile, metabolically active intracellular replicating form of *C. trachomatis* is larger than the EB, pleomorphic in shape, and has a diameter of about 1µm (Ward 2002, Ward 1983). Since chlamydial organisms in this stage are metabolically active, the nucleoid is diffuse and does not contain the chlamydial histone analogue found in the EB (Hackstadt *et al* 1991). The diffuse nucleiod allows for transcription and the cytoplasm is rich in ribosomes which synthesise protein (Ward 2002). While replicating, RB are located on the periphery of the inclusion in close association with the inclusion membrane (Peterson and de la Maza, 1988). During this time the region of the RB in contact with the inclusion membrane exhibits an apparently rigid structure (Peterson and de la Maza, 1988). The double trilaminar membrane is well-defined and appears to be septated by electron dense structures which connect the two membranes (Peterson and de la Maza, 1988). Wyrick (2000) suggested that these electron-dense structures connecting the two membranes may be a type III secretion system.

2.4.1.3 Architecture of the cell envelope

Like typical Gram-negative bacteria, chlamydial EB and RB are enclosed in an inner cytoplasmic membrane and an external cell wall covered with projections and rosettes on the external surface (Ward 1983). In addition, the EB cell envelope comprises an additional layer not detected in RB, termed the periplasmic or P layer which is composed of regularly arranged hexagonal subunits located on the internal surface of the cell wall (Matsumoto and Manire 1970).

The chlamydial cell wall is comprised of chlamydial lipopolysaccharide (LPS) which shares 2 of the 3 antigenic domains with typical bacterial LPS (Weisburg *et al* 1986).

Since the primary purpose of the cell wall is to protect the EB while outside the host cell, it is a highly specialised structure which unlike other Gram negative eubacteria, contains almost no detectable muramic acid (Ghuysen and Goffin 1999, Barbour *et al* 1982). Instead, the EB outer envelope is thought to derive its rigidity and resistance to osmotic pressure from sulphur bridges between the cysteine-rich proteins present in the outer envelope (Bavoil *et al* 1984, Newhall and Jones 1983).

The major outer membrane protein (MOMP) is a ~40 kDa protein present on the outer envelope of both EB and RB (Hatch *et al*, 1984). MOMP has heterogeneity in four hypervariable segments which confer different antigenic properties to *C. trachomatis* strains and allow classification of these strains into different serovars (Stothard *et al* 1998). Serovars can be identified by means of the micro-immunofluorescence test (Wang *et al* 1973) or by sequencing of the hypervariable regions in the genome (Stephens *et al* 1988, Sturm-Ramirez *et al* 2000).

Chlamydia also produce a genus specific lipopolysaccharide (LPS) on their outer membrane (Brade *et al* 1985) composed of a linear trisaccharide of 3-deoxy-D-*manno*-octulosonic acid (KDO) linked to a lipid A moiety (Brade *et al* 1987, Rund *et al* 1999, Nurminen *et al* 1985). Chlamydial LPS differs from that of typical Gram negative LPS in that the chlamydial lipid A moiety has five not six fatty acyl groups, its fatty acyl groups are longer, and it contains normal fatty acids instead of hydroxyl fatty acids which are directly linked to the carbohydrate region via an ester linkage (Qureshi *et al* 1997). These differences between typical LPS and chlamydial LPS may be responsible for the reduced level of endotoxic activity which chlamydial LPS produces compared to typical bacterial

LPS (Heine *et al* 2003). This reduced proinflammatroy response due to an altered LPS structure allows chlamydia to establish asympotomatic cervicitis and subsequently ascend up the genital tract to previously sterile sites (Ingalls *et al* 1995) and cause infertility either due to scarring of the fallopian tubes (Ingalls *et al* 1995) or by inducing apoptosis of sperm cells (*Eley et al* 2005).

2.4.2 Developmental cycle

Chlamydial infection is initiated by the attachment of an EB to a host cell, usually at the base of the microvilli (Ward 2002). With the OG biovar entry is facilitated by microfilaments, while entry of the LGV organisms is thought to be independent of the cytoskeleton (Schramm and Wyrick 1995). The organism becomes incorporated into a vacuole termed an inclusion. It escapes the endocytic pathway to the exocytic pathway and the inclusion is translocated to the perinuclear region (Wyrick 2000). This parasitophorous vacuole does not fuse with the hosts lysosomes (Friis 1972, Scidmore *et al*. 1996). At 6 to 9 hours after entry the EB expands, the DNA in the dense core unravels and becomes diffuse, ribosomes are synthesised and a RB is formed (Ward 1983). RB replicate by binary fission with a doubling time of about 2.4 hours (Miyairi *et al* 2006). During this time the chlamydial inclusion intercepts sphingomyelin and cholesterol from the host's exocytic pathway (Hackstadt *et al* 1995). After 24 to 40 hours some RB begin to reorganise and form intermediate bodies that develop into EB. During this time the DNA is recondensed to form a tight core (Ward 1983). EB are then released from infected host cells by exocytosis in the case of the OG strains, or cell lysis in the case of the LGV strains (Todd and Caldwell 1985).

In the presence of nutrient deficiency, and certain antimicrobial agents and immunological factors, the replication cycle may be paused *in vitro* until favourable conditions return. This condition, known as persistence, is characterised by organisms in a non-infectious but viable state. During this time RB display an altered morphology. They may be swollen or fragmented, and "miniature" RB and RB ghosts are seen within the inclusion.

2.4.3 Genome

The chlamydial genome is relatively small. In the case of *C. trachomatis*, the genome comprises a 1042519 base pair chromosome (59% A + T) and 7493 base pair plasmid (Stephens *et al* 1998). Analysis of the sequenced genome identified 894 likely protein coding genes. The functions of 604 putative proteins could be inferred, 35 were similar to hypothetical proteins of other bacteria and 255 were not similar to any sequences deposited in GenBank (Stephens *et al* 1998).

Key genetic features of the *C. trachomatis* genome (Stephens *et al* 1998) are listed in table 1.

Table 1. Key genetic features of the *C. trachomatis* genome

Gene function	**Status within the genome**
DNA replication, repair, transcription and translation, as well as helicases	Genes present
Glycolytic pathway	Genes present except one
Hexose monophosphate shunt	Genes present
Tricarboxylic acid (TCA) cycle	Many genes are missing
Aerobic respiration	Genes present
ADP/ATP translocases	Two genes present
Amino acid biosynthesis	Few genes present
ABC transporters for amino acids and oligopeptides with Na^+ and H^+ amino acid symporters	Thirteen genes present
Permeases for magnesium, phosphate, nitrate and sulphate	Genes present

Fatty acid and phospholipids synthesis	Numerous genes present
Complete peptidoglycan synthesis, membrane assembly and recycling	Genes present
Disulphide bond isomerases	Five genes present
Polymorphic outer membrane proteins	Nine genes present
Complete type III secretion system	Genes present
Complete synthesis of purine and pyrimidine nucleotides	Genes absent except for cytosine triphosphate
Interconversion of deoxyribonucleotides	Genes present except for thymidylate synthase
Transformation and acquisition of exogenous DNA or phage- or transposon-like homologs, or restriction endonucleases	Genes absent

Phylogenetic analyses of the *C. trachomatis* genome indicates that *Chlamydia* represent a distinct bacterial lineage (Stephens *et al* 1998). Several features of the genome suggest horizontal gene transfer from both bacterial ancestors and eukaryotic hosts. There are 35 protein coding sequences, mainly house keeping genes, which are phylogenetically grouped with eukaryotic homologues. This is a higher frequency than detected in the sequenced genomes of other bacterial pathogens (Stephens *et al* 1998).

Genetic variability amongst chlamydial genomes occurs predominantly in a region about 50 kb in length, dubbed the "plasticity zone" (PZ) (Read *et al*, 2000). This region houses the genes for a toxin similar to clostridial toxin B. *C. trachomatis* (mouse pneumonitis (MoPn) strain) encodes the full gene, serovar D possesses a deletion but the region encoding the enzymatic active site remains; while most of this gene is absent in serovar L2 (Belland *et al*, 2001). Both *C. trachomatis* serovar D and MoPn encode genes for phospholipase D-endonuclease in this region (Read *et al*, 2000). Genes encoding purine interconversion are present in the MoPn strain but absent in serovar D (Read *et al*, 2000). Genes encoding tryptophan biosynthesis are present in serovar D but absent in the MoPn strain (Read *et al*, 2000). Clinical isolates obtained from the genitalia have been shown to encode a gene for the production functional tryptophan synthase, while this gene in ocular

isolates has an insertion which results in a frame shift and encodes nonfunctional tryptophan synthase (Caldwell *et al*, 2003).

2.4.4 Gene expression

A study by Shaw *et al* (2000) has indicated the presence of three temporal classes of *C. trachomatis* gene expression. The authors selected 70 genes identified from the published sequence for the serovar D genome (Stephens *et al* 1998), but used serovar L2 for their analyses.

Three temporal classes of gene expression were described (Shaw *et al* 2000). Early genes were transcribed by 2 hours after infection, mid-cycle gene products were not present at 2 or 6 hours post infection, but were present at 12 hours, and late gene expression included those gene products first detected at 20 hours post infection.

Genes involved in DNA replication, transcription, translation and protein modification are transcribed early in the developmental cycle. Many confirmed or putative inclusion membrane proteins (Inc) are expressed by 2 hours post infection. These include IncB to IncG as well as the putative inclusion membrane proteins with their characteristic hydrophobic transmembrane domains. Genes encoding macromolecular synthesis, subunits of RNA and DNA polymerase, 16S ribosomal RNA, *recA* and the chlamydial heat shock protein (HSP) 60 homologue are transcribed early. These findings are consistent with the reported early transcription of ribosomal subunits by Gerard *et al* 1997. The ATP/ADP translocase and ribonucleosidetriphosphate/H^+ symporter was also expressed

early (Shaw *et al* 2000), as was *gigG*, a gene encoding an enzyme necessary for glycogen synthesis, and *yjjK*, which encodes an ABC transporter homologue (Shaw *et al* 2000).

Genes encoding intermediate metabolism, such as *pyk*, *eno* and *sdhA* of the glycolytic pathway and pentose phosphate shunt are not expressed until mid-cycle. This is confirmed by the study of Iliffe-Lee and McClarty (1999) which reported delayed expression of the glycolytic pathway and pentose phosphate shunt enzymes encoded by *gap*, *zwf* and *pgk*, which coincided with *pyk* expression. At mid-cycle genes encoding structural proteins such as MOMP, outer membrane protein 2, peptidoglycan and LPS are expressed, as well as the type III secretion system genes, *yscJ* and *yscN*. IncA is also transcribed and thought to mediate homotypic fusion of chlamydial inclusions (Hackstadt *et al* 1999). Nine other predicted inclusion membrane proteins are also expressed (Shaw *et al* 2000).

Finally, at 20 h post infection genes involved in the switch of RB back to EB are expressed. These include Hc1, the chlamydial histone H1 analogue, and the cysteine rich outer membrane protein ompB (Shaw *et al* 2000).

2.5 Pathogenesis

C. trachomatis exerts a pathogenic effect firstly, by creating an intracellular niche to hide from the immune system while within the host cell (Giles and Wyrick 2008). The organism is pathogenic in its interaction with its host cell, during release from the host cell, and by affecting neighbouring uninfected cells.

2.5.1 Creation of an intracellular niche

EB uptake is initiated when an EB binds to the tips of microvilli on susceptible cells, and becomes internalized via coated pits at the base of the microvilli (Hodinka *et al* 1988, Hodinka and Wyrick 1986, Wyrick *et al* 1989). Serovar E may require host cell microfilaments to internalise clathrin-coated pits on the apicial membrane for endocytosis (Schramm and Wyrick 1995). Since L2 can enter cells without an intact cytoskeleton, these organisms may also enter via a receptor which does not require the cytoskeleton for uptake (Schramm and Wyrick 1995). Molecules which enter without clathrin-coated pits have been shown to enter the same endocytic vesicles as molecules which enter via clathrin-coated pits (Hansen *et al* 1993). The LGV organisms may thus utilize more than one mechanism of entry on apical and basolateral surfaces (Schramm and Wyrick 1995). However, after uptake, the L2 organisms appear to require an intact cytoskeleton for fusion of inclusions in cells where multiple EB have entered, but serovar E does not (Schramm and Wyrick 1995). Several studies have tried to to elucidate the mechanism of attachment of the organism to its host cell. A number of proposed antigens have been described, but their role in chlamydial entry into the cell is not confirmed.

Chlamydia are unique compared to other intracellular bacteria in that its entry into epithelial host cells appears to be silent; proinflammatory cytokines are not secreted on entry but only from 8 hours and continue through the developmental cycle (Rasmussen *et al* 1997). This phenomenon may be due to the small size (350 nm) compared to other bacteria (Rasmussen *et al* 1997).

Once the organism has entered it prevents lysosomal fusion and escapes the endocytic pathway. This is a chlamydia-mediated event which requires chlamydia protein synthesis

(Scidmore *et al*. 1996). Even opsonised *C. trachomatis* EB which enter HeLa 229 cells by Fc-mediated endocytosis have been shown to escape lysosomal death and undergo a normal replication cycle (Scidmore *et al*. 1996). Evasion of the endocytic pathway is likely to occur in two stages: via an intrinsic property of EB, followed by chlamydial protein synthesis (reviewed in Fields *et al* 2002). In a reverse transcriptase PCR based study, 29 of the 39 putative inclusion membrane proteins were already expressed just 2 hours post-infection (Shaw *et al* 2000). This indicates that chlamydia significantly modify their inclusions upon entry to ensure a suitable niche prior to replication (Fields *et al* 2002).

2.5.2 Interaction with host cell processes

A microarray study by Xia *et al* (2003) revealed that *C. trachomatis* serovar L2 infection of HeLa 229 cells alters the expression of 13 host cell genes by 2 h post infection, and 130 genes at 16 h post infection. These genes encode cytoskeletal components, metabolic enzymes, factors which regulate cell differentiation, transcription factors and inhibition of apoptosis factor, as well as proinflammatory cytokines. This clearly indicates that despite being sequestered within a membrane-bound inclusion, *C. trachomatis* is able to modulate numerous host cell processes.

2.5.2.1 Inclusion membrane

The inclusion membrane is important in the pathogenesis of *C. trachomatis* infection since it serves as the interface between the organism and its host cell. Since *C. trachomatis* prevents fusion with host lysosomes, the chlamydial inclusion is non-lysosomal (Friis

1972). Instead it interacts with the exocytic pathway. Sphingomyelin is transported from the *trans*-Golgi to the chlamydial inclusion where it becomes incorporated at the inner face of the inclusion membrane and ultimately becomes part of the chlamydial cell walls (Hackstadt *et al* 1995). Cholesterol (Carabeo *et al* 2003) and phospholipids (Wylie *et al* 1997) are also acquired by the organism.

The *C. trachomatis* inclusion membrane is modified by numerous inclusion membrane proteins termed Incs (Scidmore-Carlson *et al*. 1999). The common feature amongst Inc proteins is a predicted hydrophobic domain comprising about 40 amino acids (Scidmore-Carlson *et al*. 1999), but there is little or no sequence homology even within the hydrophobic domain (Bannantine *et al* 2000). Studies have shown the presence of 5 Inc proteins located on the cytoplasmic face of *C. trachomatis* inclusions (Hackstadt *et al*. 1999, Field and Hackstadt 2002). This allows interaction with host cell proteins such as 14-3-3β, a eukaryotic protein which is part of a highly conserved family of dimeric phosphoserine-binding proteins responsible for signal transduction (Scidmore and Hackstadt 2001). 14-3-3β binds IncG in the *C. trachomatis* inclusion, but neither *C. psittaci* nor *C. pneumoniae* express IncG, and 14-3-3β does not bind to their inclusion membrane (Scidmore and Hackstadt 2001).

Other inclusion membrane proteins without the hydrophobic domain which characterizes Inc proteins have also been associated with the chlamydial inclusion. These include CopN which is part of the chlamydial type III secretion system (Fields and Hackstadt 2000) and Cap1 (Fling *et al*. 2001).

2.5.2.2 Type III secretion system

Like many other pathogenic gram-negative bacteria, *C. trachomatis* encodes (Stephens *et al*. 1998) and expresses (Fields and Hackstadt 2000) genes for a type III or contact-dependent secretion system (TTSS).

Although the exact role of the TTSS in chlamydia has not been demonstrated, such a structure is crucial in the translocation of chlamydial enzymes to the host cytoplasm enabling it to modify host cell processes. Chlamydial antigens including MOMP, LPS and IncA have been detected in the endoplasmic reticulum of the host (Giles and Wyrick 2008).

Although genes encoding a TTSS are only expressed at mid-cycle, the surface projections present on EB and RB may correspond to a TTSS. Purification of projections from EB produced structures similar to the purified parts of a *Salmonella typhimurium* TTSS (Kubori *et al*. 1998). This TTSS may be involved in attachment and entry into susceptible hosts possibly by injecting substances through the host cell to mobilize the cytoskeleton and facilitate uptake of the organism (Wyrick 2000). Wyrick (2000) also suggested that the region of the well defined double trilaminar membrane may represent the TTSS.

2.5.2.3 Acquisition of energy and nutrients

Historically Chlamydiae were classified as energy parasites, but more recent data has indicated that chlamydiae can synthesise ATP (see Read *et al*. 2000, Stephens *et al*. 1998, Iliffe-Lee & McClarty 1999). However, many intermediate metabolic genes are only expressed at mid-cycle (Iliffe-Lee & McClarty 1999, Shaw *et al*. 2000); while the ATP-

ADP exchange mechanism described by Hatch *et al* (1982) is expressed early in the developmental cycle (Shaw *et al*. 2000) and mitochondrial activity has been shown to increase in *C. trachomatis* infected HeLa cells (Hatch & McClarty 1998).

Chlamydia acquire precursors such as nucleotides and amino acids (Hatch *et al* 1982, Hatch 1975), but the method of uptake is not clear. Grieshaber *et al* (2002) demonstrated the possibility that the inclusion membrane may be permeable to cytoplasmic ions, but Heinzen and Hackstadt (1997) report that this membrane is impermeable to molecules ranging from 520 D to 500 kD. Genes encoding peptide transporters are present, but their occurrence on the inclusion membrane has not been confirmed (Stephens *et al*. 1998).

Like other pathogenic bacteria, iron is essential for chlamydial growth (Freidank *et al* 2001, Al-Younes *et al* 2001). Endosomes with transferrin-transferrin receptor complexes have been identified in close association with the chlamydial inclusion (van Ooij *et al* 1997), but since these endosomes do not appear to fuse with the inclusion, the mechanism of iron acquisition by chlamydia is uncertain (Raulston 1997). Endosomes with transferrin-transferrin receptor complexes have been shown to release Fe^{2+} into the cytoplasm upon acidification of the vesicle and reduction (Núnez *et al* 1990). Since these endosomes containing transferrin and its receptor have been identified in close proximity to the chlamydial inclusion (van Ooij *et al* 1997, Al-Younes *et al* 2001) and since the inclusion membrane has been shown to be permeable by ions (Grieshaber *et al*, 2002), Fe^{2+} may be transported to the inclusion membrane by endosomes. Fe^{2+} may then be released into the cytoplasm immediately adjacent the inclusion and enter the chlamydial inclusion by diffusion.

As the number of organisms within the inclusion increases, chlamydia compete with their host cells for nutrients. When many organisms are present host cell replication may be halted (Horoschak and Moulder 1978). Replication is slowed down or unaffected by low numbers of organisms and either one or both daughter cells may house a chlamydial inclusion after mitosis (Horoschak and Moulder 1978, Bose and Liebhaber 1979).

2.5.2.4 Reorganisation of the host cytoskeleton and organelles

The developing chlamydial inclusion affects the ultrastructural organization of its host. As the inclusion of replicating bacteria grows, it pushes the nucleus aside. Mitochondria and endoplasmic reticulum are located in close proximity to the inclusion, to meet the needs of the replicating bacteria (Peterson and de la Maza 1988).

A chlamydia-induced effect on the cytoskeleton occurs before the EB has even been internalized. Attachment of EB to microvilli initiates the phosphorylation of proteins (Birkelund *et al*. 1994) and mobilisation of actin (Fawaz *et al*. 1997), resulting in the internalisation of the organism (OG biovar) (Schramm and Wyrick 1995). Microfilaments, microtubules, and motor protein dynein then mobilise the inclusion to the perinuclear region (Schramm and Wyrick 1995). Annexins located in the peri-inclusion region may facilitate movement or interactions with the inclusion (Majeed *et al*. 1994).

2.5.2.5 Chlamydial toxin

Immediate toxicity of cell culture monolayers infected at a high MOI has been reported (Kuo CC 1978, Moulder *et al* 1976) as well as rapid death of mice infected with a high

inoculum of chlamydia (Rake and Jones, 1944), but until relatively recently a chlamydial toxin was not described.

In 2001 Belland *et al* reported the presence of a preformed cytotoxin located within the EB of *C. trachomatis* serovar D but not L2. This cytotoxin shares significant homology with the large cytotoxins (LCT) A and B produced by *Clostridium difficile* (Busch *et al*, 2000) which disrupts the actin cytoskeleton and intracellular trafficking (von Eichel-Streiber *et al* 1996). While the mouse strain encoded the full-length clostridial toxin B, serovar D encoded a shorter protein which only showed homology to the toxin active site. Serovar L2 exhibited a larger deletion rendering the transcript non-functional.

Cells infected with serovar D EB at high MOI showed cell rounding and actin depolymerization compared to serovar L2 infected cells which retained their shape and cytoskeletal arrangement. This effect occurred independently of EB viability and protein sysnthesis, indicating that the toxin was transcribed prior to infection of the new host cell.

The abridged gene is present in serovars D-K of OG biovar, while a functional gene is absent in serovars L1-L3 of the LGV biovar (Carlson *et al*, 2004).

2.5.3 Release from the host cell

Given that strains from the LGV biovar cause ulcers, the mechanism of release from the host cell can be a pathogenic factor.

C. trachomatis release from host cells occurs via 2 distinct pathways with different outcomes. Host cell lysis causes death of the host cell while extrusion does not (Hybiske and Stephens 2007). Both processes have been investigated by Hybiske and Stephens (2007).

Cell lysis is a relatively rapid process (about 20 min) involving an ordered set of protease dependent events (Hybiske and Stephens 2007). First the inclusion membrane ruptures, followed by permeablisation of cellular organelles and finally the cell membrane. This final step is Ca^{2+} dependent.

Extrusion involves the packaged release of organisms leaving the host cell intact. Three signature events have been described. First, a portion of the membrane bound inclusion projects out of the cell; the inclusion is pinched off into separate compartments; and this pinched off, protruded inclusion is then attached to the cell periphery. This process is dependent on actin polymerisation, the actin nucleation factor Neuronal Wiskott-Aldrich Syndrome Protein (N-WASP), Myosin II and Rho GTPase. After 2-3 hours membrane bound chlamydial particles are released. Extrusion may be beneficial to the organism in that chlamydial particles are shielded from the dangers of the extracellular environment allowing a longer period before invading a new susceptible host.

Prior to the study by Hybiske and Stephens (2007), Todd and Caldwell (1985) described cell lysis and exocytosis as the mechanisms of *C. trachomatis* release from their host cells. Exocytosis may present a third mechanism by which chlamydia are released from their host cells. The large cavern-like crypts observed on the surface of cells infected with an OG isolate late in the developmental (Todd and Caldwell 1985) are unlikely to be

synonymous with the protrusions described by Hybiske and Stevens (2007). It is possible that different methods of release occur *in vitro* depending on the cell type, strain and culture conditions. Hybiske and Stephens (2007) report the occurrence of extrusion and lysis in cell monolayers infected with an OG strain and an LGV strain, while Todd and Caldwell (1985) report lysis as the only method of EB release with the LGV biovar.

These two biovars also show differences in pathogenicity in terms of the surface from which they are released. While the OG strains are released from the apical surface of their host cell, LGV strains may also be released from the basolateral surface of polarised cells (Wyrick *et al* 1989). This would enable the LGV strains to penetrate the epithelium to infect the underlying tissue and ultimately migrate to the lymph nodes.

2.5.4 Effect on neighbouring uninfected cells

The effect of *C. trachomatis* infection on neighbouring uninfected cells has not been widely investigated, however the organism does, either directly or indirectly, result in a pathogenic effect on uninfected neighbouring cells. Schöier *et al* (2001) and Greene *et al* (2004) demonstrated the presence of apoptotic uninfected cells in monolayers infected with *C. trachomatis*. This effect may be mediated indirectly since infected epithelial cells have been shown to secrete proinflammatory cytokines (Rasmussen *et al* 1997). The fact that extra-inclusion vesicles have been detected in the cytoplasm of infected cells (Giles *et al* 2006) indicates the possibility that chlamydia may affect neighbouring uninfected cells via a chlamydial molecule which is secreted by the host cell.

2.6 Interaction with the immune system

Chlamydia attempt to hide from the immune system, but both innate and adaptive immune responses are mounted. While the immune system identifies and eliminates pathogens, in the case of *C. trachomatis* the immune response contributes to tissue pathology and severity of disease (Roan and Starnbach 2008).

2.6.1 Innate immunity

Although they are not professional antigen presenting cells, epithelial cells of the genital tract possess features of innate immunity (Quale 2002). These cells can recognise antigens via the presence of MHC class I and II, mediate bacterial and viral killing, and respond to and secrete chemokines to recruit leukocytes (Quale 2002).

Chlamydia infection can induce the production of a range of proinflammatory cytokines, including interleukin-6 (IL-6), IL-8 and granulocyte-macrophage colony-stimulating factor (GM-CSF) (Rasmussen *et al* 1997), as well as IL-1 and tumour necrosis factor-α (TNF-α) (Dessus-Babus *et al* 2002). IL-8 recruits neutrophils to the site of infection (Taub *et al*, 1996) and these recruited cells secrete more cytokines such as TNF-α (Dessus-Babus *et al* 2002). Although TNF-α can restrict the growth of *C. trachomatis*, elevated levels of TNF-α and IL-6 may cause increased pathology (Darville *et al* 2003). NK cells migrate to the site of infection quickly where they lyse infected cells and produce interferon-γ (INF-γ) (Tseng and Rank 1998).

INF-γ has been shown to inhibit replication of all *C. trachomatis* serovars *in vitro*, but some serovars are more susceptible to INF-γ-induced effects than others (Morrison 2000). INF-γ restricts chlamydial growth in the following ways:

- Up regulation of the IFN-γ-inducible nitric oxide (NO) synthase pathway (Igietseme *et al* 1997). NO has been shown to inhibit the intraepithelial replication of *C. trachomatis* serovars E, H and L2 (Igietseme *et al* 1997).
- Induction of indoleamine 2,3-dioxygenase (IDO) which catabolises tryptophan (Taylor and Feng 1991). A reduction in the intracellular tryptophan pools restricts chlamydia replication (Byrne *et al* 1986) and may induce a state of persistent infection (Beatty *et al* 1994a). Genital isolates of *C. trachomatis* are resistant to this method of INF-γ restriction due to functional tryptophan synthase enabling these strains to synthesise tryptophan from indole unlike the ocular trachoma strains (Caldwell *et al* 2003).
- Inhibition of sphingomyelin acquisition (serovar L2) (Nelson *et al,* 2005)
- Down regulation of intracellular ferritin, the protein responsible for iron storage by cells (Byrd and Horwitz, 1993). This may restrict the growth of *C. trachomatis* due to iron starvation (Freidank *et al*, 2001)
- Increase the phagocytic activity of macrophages by up regulation of MHC class II expression (Zhong and de la Maza, 1988)

The link between the innate and adaptive immune response are dendritic cells (DC) which process and present chlamydial antigens to T cells (Steele *et al* 2004).

2.6.2 Adaptive Immunity

A B cell response is mounted against chlamydia. Although it doesn't prevent subsequent infection, B cell deficient mice are slightly more susceptible to subsequent infection than

wild type mice (Su *et al* 1997, Williams *et al* 1997). Although antibodies can neutralize extracellular organisms, both $CD4^+$ and $CD8^+$ T cells are required for eliminating intracellular chlamydia (Starnbach *et al* 1994, Su and Caldwell 1995, Roan and Starnbach 2006). The $CD4^+$ T cells recognize chlamydial antigen bound to MHC class II on the surface of antigen presenting cells (Roan and Starnbach 2006), while the $CD8^+$ T cells recognise chlamydial antigen bound to MHC class I molecules presented on the surface of the infected cells (Cresswell *et al* 2005).

C. trachomatis has been shown to interfere with antigen presentation. Serovar L2 was shown to down regulate INF-γ-inducible MHC class II by degrading upstream stimulatory factor (USF)-1 (Zhong *et al* 1999). This in turn prevents the induction of class II transactivator (CIITA) which is required for expression of INF-γ-induced MHC class II molecules (Zhong *et al* 1999). The same strain of *C. trachomatis* LGV biovar has been shown to suppress both the constitutive and INF-γ-induced expression of MHC class I molecules on infected cells (Zhong *et al* 2000). This is mediated by the degradation of RFX5 by chlamydial proteasome-like activity in the host cell cytoplasm (Zhong *et al* 2001). Decreased levels of antigen presentation of MHC class I and II molecules would limit the ability of $CD8^+$ and $CD4^+$ T cells to recognise infected cells and professional antigen presenting cells respectively (Roan and Starnbach 2008). This may also increase the likelihood of NK cell mediated lysis which has been shown *in vitro* (Hook *et al*, 2004). It is possible the MHC class I molecule down regulation may also be mediated by deubiquitinases (DUB) encoded by the *C. trachomatis* genome (Misaghi *et al*. 2006). If transcribed these proteins could target host cell ubiquitin thereby interfering with antigen presentation (Roan and Starnbach 2008).

$CD4^+$ T cells exist as two clones, T helper type (Th) 1 and Th2. The Th1 cells produce INF-γ which assists in the clearance of chlamydia (Perry *et al* 1997). Th2 cells enhance antibody production but do not aid clearance of the organism (Perry *et al* 1997, Hawkins *et al* 2002). When the Th1 response is insufficient and the organism is not cleared, sustained high levels of inflammatory cytokines can cause tissue damage (Perfettini *et al*, 2003a). $CD4^+$ T cells also play a role in the activation of B cells and $CD8^+$ T cells (Roan and Starnbach 2008).

Like $CD4^+$ T cells, $CD8^+$ T cells can produce INF-γ to mediate intra-cellular kill of the organism. It is only these chlamydia-specific $CD8^+$ T cells capable of producing INF-γ which have this effect (Roan *et al*., 2006). $CD8^+$ T cells also recognize chlamydia-infected cells via presentation of chlamydial antigens on MHC class I molecules and kill these cells (Starnbach *et al*., 1994). Theoretically this should aid in removal of the organism, but this has not been shown *in vivo* (Roan and Starnbach 2008). This may be due to the presence of small numbers infectious EB relatively early in infection. Lysis of the host cell would enable EBs to enter a new host and continue its replication cycle. Phagocytosis of EB by antigen presenting cells does not guarantee death of the organism. Opsonised *C. trachomatis* EB which enter host cells by Fc-mediated endocytosis have been shown to escape lysosomal death and undergo a normal replication cycle (Scidmore *et al*. 1996).

Activation and proliferation of $CD4^+$ and $CD8^+$ T cells occurs in the nearby lymph nodes which drain antigen from the genital mucosa. These cells develop their INF-γ producing capacity prior to migration to the site of infection where they aid in chlamydial clearance (Roan and Starnbach 2006; Roan *et al*., 2006).

The persistent dormant form of the organism may contribute to disease. Reversible persistence can be induced by INF-γ (Beatty *et al*, 1993). The organism remains dormant until this cytokine is removed, then reactivates and stimulates inflammation and immune cells. Alternating cycles of the persistent dormant form followed by an inflammatory immune response may result in chronic chlamydia-induced disease and tissue damage (Roan and Starnbach 2008).

2.7 Cell death

Cell death is an important part of cellular turnover and plays a role in homeostasis of multicellular eukaryotes (Miyairi and Byrne, 2006), as well as in the elimination of invading organisms (Fink and Cookson 2005). Cell death is generally divided into 2 categories, apoptosis and necrosis, but several other categories of cell death have been proposed (Fink and Cookson 2005).

2.7.1 Apoptosis

Apoptosis is defined as "caspase-mediated cell death with associated apoptotic morphology" (Samali *et al* 1999). It is a regulated process for the removal of unwanted cells without causing damage to neighbouring cells and has distinct morphological characteristics (Boatright and Salvesen 2003).

The caspase family of enzymes, which orchestrate apoptosis, is a group of peptidases with a cysteine residue at the catalytic site (Boatright and Salvesen 2003). These enzymes cleave target proteins at a site adjacent to aspartic acid residues (Boatright and Salvesen

2003). Some members of the caspase family are involved in implementing the apoptotic pathway, while others are responsible for the activation of inflammatory cytokine precursors (Los *et al,* 1999). The group of caspases involved in apoptosis is further classified as initiator and effector caspases to reflect their role in the caspase cascade as well as the structural differences between the two groups (Fink and Cookson 2005).

Apoptosis is a complex biochemical process which can be initiated by numerous stimuli to effect caspase-mediate cell death via a number of pathways.

2.7.1.1 Initiation of apoptosis

Apoptosis may be initiated by a number of stimuli including cellular and DNA damage, withdrawal of growth factors or hormones, receptor-ligand interactions and cytotoxic T cells (Cotran *et al*, 1999). The biochemistry of effector caspase activation varies depending on the type of apoptotic stimulus.

Cellular damage may induce apoptosis via the p53 or the Bcl (B cell leukaemia) -2 family of proteins. In the case of DNA damage p53 arrests the cell cycle to DNA repair (Velculescu and El-Deiry 1996), and if this fails the effector caspases are activated (Cotran *et al*, 1999). In the presence of other types of cell damage, the Bcl-2 family of proteins present in the mitochondrial outer membrane allow the release of cytochrome *c* (Green and Reed, 1998) which recruits and activates the intrinsic pathway of caspase activation (Boatright and Salvesen 2003). Procaspase-9 becomes activated by the apoptosome complex (Zou *et al* 1999) and activates effector caspases (Boatright and Salvesen 2003).

Apoptosis may also occur via receptor-ligand interaction to mediate the removal of unwanted cells which have been tagged, either by the immune system or other processes (Boatright and Salvesen 2003).

Upon attachment of a death ligand, death receptors, such as Fas, at the cell surface trigger the apoptosis cascade (Ashkenazi and Dixit, 1998). Fas-associated protein with death domain (FADD) associates with the cytoplasmic death domains of the Fas receptor (Ashkenazi and Dixit, 1998). The death-effector domain of FADD catalyses the activation of caspase-8 (Ashkenazi and Dixit, 1998). Caspase-8 in turn activates the effector caspases (Boatright and Salvesen 2003).

Caspase-8 may also be activated by other death ligands which bind to other death receptors, but Fas-mediated activation of caspase-8 is the pathway used to kill infected cells by NK cells or cytotoxic T lymphocytes (Ashkenazi and Dixit, 1998).

Cytotoxic T lymphocytes may also mediate apoptosis by another mechanism which bypasses initiator caspase activation (Cotran *et al* 1999). The transmembrane pore forming molecule, perforin, punctures through the membrane and secretes Granzyme B molecules into the cytoplasm which activate effector caspases (Cotran *et al* 1999).

2.7.1.3 Execution of apoptosis

The activated initiator caspases from the intrinsic and extrinsic pathways, caspase-9 and -8 respectively, activate the effector caspases (Boatright and Salvesen 2003). It is caspase-3,

-6 and -7 which disassemble the cell and mediate the morphological changes which characterise apoptosis (Boatright and Salvesen 2003, Fink and Cookson 2005).

Cleavage of structural proteins cause nuclear shrinkage and fragmentation, loss of overall structure of the cell, membrane blebbing, and detachment from the basement membrane and surrounding cells (Fink and Cookson 2005). The genome is dismantled by a caspase activated DNAase (CAD) (Enari *et al*, 1998) which cleaves genomic DNA within the internucleosomal linker regions to produce stepwise DNA fragments of 185 bp in length and multiples thereof (Arends *et al*, 1990). Apoptotic bodies are formed, which in the *in vivo* situation would be phagocytosed by surrounding cells (Fink and Cookson, 2005). The cell membrane of affected cells display phosphatidylserine (PS) on the outer leaflet of their lipid bilayer (Martin *et al*, 1995). This is normally restricted to the inner leaflet in healthy cells (Martin *et al*, 1995).

2.7.2 Necrosis

In the cell death literature, necrosis is the term used to describe non-apoptotic or accidental cell death. This process is characterised by cell and organelle swelling. Ultimately the cell bursts and releases inflammatory contents (Fink and Cookson, 2005). Necrosis thus leads to an inflammatory response and tissue damage (Miyairi and Byrne, 2006)

In the situation where apoptotic bodies are not phagocytosed, they may lose their membrane integrity and lyse (Fink and Cookson, 2005). This would result in an inflammatory response, despite death via the apoptotic pathway (Majno and Joris, 1995).

The term apoptotic necrosis is used to denote apoptotic cellular material which reaches this point via apoptotic pathways (Majno and Joris, 1995).

2.7.3 Chlamydia and cell death

Chlamydia have a complicated interaction with their host cells. In the early and mid stages of their life cycle anti-apoptotic mechanisms predominate, while in the later stages of their developmental cycle these organisms may induce cell death (Miyairi and Byrne 2006).

2.7.3.1 Inhibition of apoptosis

The anti-apoptotic effect of chlamydia is largely shown by its ability to inhibit chemically and spontaneously induced apoptosis (Miyairi and Byrne 2006), and microarray analysis has indicated the up regulation of anti-apoptotic genes such as inhibitor of apoptosis (IAP) homolog B (Xia *et al*, 2003). Although some variability in the levels of anti-apoptotic activity amongst the serovars has been reported (Greene *et al*, 2004), all strains tested demonstrated anti-apoptotic activity in infected cells.

Chlamydia may mediate an anti-apoptotic effect via the Bcl family of proteins (Green and Reed 1998), which consists of three groups of proteins responsible for regulating cytochrome *c* release from mitochondria, Bax, Bcl-2 and BH3 (Miyairi and Byrne 2006). The Bax subfamily of proteins are pro-apoptotic and mediate changes in the permeability of the mitochondrial membrane causing the release of cytochrome *c* into the cytoplasm (Green and Reed 1998). The Bcl-2 subfamily of proteins inhibits mitochondrial cytochrome *c* release (Green and Reed 1998). The BH3-only proteins inhibit Bcl-2

proteins to exert a pro-apoptotic effect (Miyairi and Byrne 2006). *Chlamydia* has been shown to inhibit apoptosis by degradation of the proapoptotic BH3-only proteins (Fischer *et al*, 2004a, Dong *et al,* 2005). In the absence of direct activation of the effector caspases this is sufficient to inhibit apoptosis (Fan *et al*, 1998, Fischer *et al*, 2004b). Although other pathogens modulate gene expression of nuclear factor (NF)κB as an anti-apoptotic mechanism, this has not been conclusively demonstrated for chlamydia.

2.7.3.2 Induction of cell death

Although there have been reports that Chlamydia induces apoptosis late in the developmental cycle the results vary depending on the method used to detect apoptosis (Miyairi and Byrne 2006), as well as the cell line and type of chlamydia (Jungas *et al* 2004).

TNF-α released by infected macrophages has been implicated in the induction of apoptosis of T lymphocytes *in vitro* (Jendro *et al*, 2004).

The gene encoding *Chlamydia* protein associated with death domain (CADD) is expressed and was found to localise with the Fas receptor in infected cells (Stenner-Liewen *et al*, 2002). Despite this association, there was no evidence of apoptosis even in cells where CADD and Fas were co-localised (Stenner-Liewen *et al*, 2002). This indicates that unlike the ectopic expression model in which caspase-mediate apoptosis was detected, CADD may be involved in the inhibition of apoptosis (Stenner-Liewen *et al*, 2002).

The end of the infectious cycle is often characterised by death of the host cell. Although this is described as having morphological characteristics of apoptotic cell death, this occurs without caspase-3 activation (Dumrese *et al*, 2005). Dumrese *et al* (2005) have suggested that cell death at the end of the chlamydial cycle occurs via a process which they call "aponecrosis" since it displays features of both apoptosis and necrosis.

The pro-apoptotic protein Bax may become activated during chlamydial infection independent of the caspase pathway (Perfettini *et al*, 2003b). Wild type mice with functional pro-apoptotic Bax protein produced more infectious progeny with a lower level of inflammation than their Bax-deficient counterparts. This suggests that in *C. muridarum* and possibly other *Chlamydia. spp,* a new round of infection may be mediated by Bax dependent apoptosis. The production of chlamydia containing apoptotic bodies would facilitate the efficient transfer of infectious organisms to a new host cell with minimal inflammation.

2.8 Keratinocytes

2.8.1 Introduction

The epidermis is the multilayered epithelium which forms a boundary between the human body and the surrounding environment (Holbrook 1994). It is comprised of stratified squamous keratinising epithelium (Young and Heath 2000). The main function of skin is protection against dehydration, radiation, mechanical damage and the invasion of microbes (Young and Heath 2000). Because keratinocytes account for more than 80% of the epidermal cells (Holbrook 1994), it is these cells which form the barrier against the

external environment and are probably the first cell type with which *C. trachomatis* of the LGV biovar interacts in its disease pathogenesis.

2.8.2 Structure and development *in vivo*

Keratinocytes undergo maturation and have different features at the stages of its development (Holbrook 1994, Young and Heath 2000) but there are key structural features present at all the stages.

Typical "house-keeping organelles" including the nucleus, rough endoplasmic reticulum (RER), Golgi, ribosomes and mitochondria are present in keratinocytes (Holbrook 1994). The cytoskeleton comprises keratin intermediate filaments which are aggregated into bundles, particularly at the desmosomes and around the nuclear envelope (Holbrook 1994). Microfilaments and microtubules provide order within the cytoplasm, assist in cell motility, and promote intracellular communication as well as communication between the cell and its environment (Holbrook 1994). Desmosomes facilitate cell-to-cell adhesion and attachment of keratin within the cell (Holbrook 1994). Adherens and gap junctions are also present (Holbrook 1994).

The epidermis is a multilayered structure comprising four morphological layers: the *stratum basale*, *stratum spinosum, stratum granulosum* and *stratum corneum*,

As keratinocytes move through these layers from the *stratum basale* on the basement membrane to the *stratum corneum* on the surface of skin they exhibit different features.

The *stratum basale* is the germinal layer where mitosis takes place. These keratinocytes are columnar in shape and rich in ribosomes, mitochondria Golgi and RER (Holbrook 1994). Keratin intermediate filaments are present, but keratin only accounts for 30% of the total protein at this stage (Holbrook 1994).

As cells move up through the *stratum spinosum* they become flattened and polyhedral in shape (Young and Heath 2000) with spiny projections formed by bundles of keratin filaments which insert into the desmosomal plaques (Holbrook 1994). Keratin filaments are present and arranged concentrically around the nucleus and inserted into the desmosomes (Holbrook 1994).

Keratinocytes of the *stratum granulosum* become more flattened and develop irregularly shaped, electron dense keratohyalin granules which are deposited at the points of intersection of the keratin filament bundles (Holbrook 1994).

Once in the *stratum corneum*, keratinocytes become more flattened, lose their nuclei and organelles, and the main cytoplasmic constituent is mature keratin (Young and Heath 2000). The cells in the deeper regions of this layer still possess desmosomes, but these are lost as the cells approach the outermost layers where they will ultimately be sloughed off (Young and Heath 2000).

2.8.3 HaCaT cells

The HaCaT cell line is a spontaneously immortalised human adult skin keratinocyte cell line developed by Boukamp and co-workers in 1988 (Boukamp *et al*. 1988) and has remained nontumorigenic for more than 300 passages (> 6 years in culture) (Boukamp *et al*. 1994). It was developed from a histologically normal male body skin specimen obtained from the distant periphery of a melanoma (second incision) and designated HaCaT to signify its origin from "human adult keratinocytes propagated under low Ca^{2+} conditions and elevated temperature" (Boukamp *et al*. 1988). This cell line has been extensively studied; including differentiation in vitro (stratification and squame formation), and it expresses essentially all epidermal differentiation markers despite the chromosomal changes which occurred during adaptation to autonomous growth in vitro (Boukamp *et al*. 1988). HaCaT cells show a lack of tissue organisation when grown in organotypic cocultures with fibroblasts, but tissue organisation is restored upon supplementation with epidermal growth factor (Maas-Szabowski *et al*, 2003).

HaCaT cells are used in studies of the cell cycle (Chaturvedi *et al*, 1999) and carcinogenesis (Boukamp *et al*. 1994). These cells are susceptible to etoposide-induced apoptosis (Lee *et al*, 2005).

2.9 Cervical Cells

2.9.1 Introduction

There are two distinct cell types present at different regions of the cervix. The endocervical canal is lined by tall columnar mucus-secreting cells (Young and Heath

2000). The ectocervix, which protrudes into the vagina, is lined by a thick layer of stratified squamous epithelial cells with a high glycogen content (Young and Heath 2000).

2.9.2 ME-180 cells

The ME-180 cell line is a spontaneously immortalised human cervical cell line, developed in 1967 by Sykes and co workers (Sykes *et al*. 1970). It was derived from an omental metastasis of a highly invasive squamous cell carcinoma of the cervix. However, after 107 passages, the cells were still characteristic squamous cells with numerous desmosomes, bundles of tonofibrils and occasional keratohyaline granules.

The ME-180 cell line is widely used in carcinogenesis studies and is sensitive to etoposide-induced cytotoxicity (Tanaka *et al*, 2006).

CHAPTER 3 – MATERIALS AND METHODS

3.1 Cell Culture

3.1.1 Cell lines of choice

McCoy cells were used for the propagation of *C. trachomatis*, while HaCaT and ME-180 cells were used for the experimental component.

The McCoy cell line (ATCC® number CRL-1696) is an adherent mouse fibroblast cell line of unknown origin, which is widely utilized for the propagation of Chlamydiae.

The HaCaT cell line, a spontaneously immortalized human keratinocyte cell line, was donated by Professor Norbet E. Fusenig of the Cancer Research Centre, Hiedelburg, Germany, while the ME-180 human cervical cell line (ATCC® number HTB-33™) was purchased from the American Type Culture Collection (ATCC).

3.1.2 Cell culture media

Since all the cells used in this study have different nutritional requirements, 3 different cell culture media were used to ensure optimal growth of each cell line.

For McCoy cells the cell culture medium (CCM) used was Eagles Minimum Essential Medium (EMEM) (BioWhittaker™, Walkersville, USA) supplemented with Earle's balanced salt solution (EBSS), HEPES (25mM) (BioWhittaker™, Walkersville, USA) to facilitate the maintenance of pH 7.4 and L-glutamine (2 mM) (BioWhittaker™,

Walkersville, USA). Glutamine is added separately as this essential amino acid is more labile than other amino acids and is rapidly broken down to ammonia in liquid culture media (ATCC technical information). HaCaT cells were grown in Roswell Park Memorial Institute-1640 (RPMI-1640) medium (BioWhittaker^{TM}, Walkersville, USA) to which L-glutamine (2 mM) and HEPES (10mM) were added. ME-180 cells were grown in McCoy 5a medium. Sterile heat-inactivated fetal bovine serum (FBS) (Gibco, Scientific Group) was added to provide uncharacterised cytokines and growth factors which are essential to regulate cell replication and differentiation. Since the rate of cell growth is proportional to the concentration of FBS in the media all three CCM was supplemented with 10% FBS for cells which had just been thawed or passaged, then reduced 2 to 5 % depending on when the cells were required for use in experiments. Incubation for growth and experiments was carried out in an incubator with 5% CO_2 in 95% air.

3.1.3 Cultivation of cells

All cells were stored in cryovials with storage medium and kept at either -70°C for short term storage or in a liquid nitrogen freezer at -196°C for long term storage. In order to reconstitute frozen cells, the cells were rapidly thawed by placing the cryovial in a beaker containing water at a temperature of 37°C and gently swirled. Once almost thawed, the cryovial was removed from the beaker, swabbed with 70% ethanol and transferred to a class II biosafety cabinet. The cells were seeded into an equilibrated 75cm^2 tissue culture flask which contained cell culture medium supplemented with 10% FBS. The flask was then incubated at 37°C.

Cells were viewed with an inverted microscope daily to monitor the level of cell density and check for any possible contamination or cell deterioration.

Every 2 to 3 days the cell culture medium was replenished. Spent media was discarded, the monolayer was washed with phosphate buffered saline (PBS) (Oxoid) (Dulbecco A without Ca^{2+} or Mg^{2+}, pH 7.3) to remove unattached cells, and fresh cell culture media containing 2 to 5 % FBS was added and the flask reincubated.

3.1.4 Passage

Once the adherent cell monolayer was approximately 90% confluent it was passaged and the cells either seeded into several new flasks to propagate more cells, seeded into a 24- or 96-well plate or Trak vials with coverslips for experiments, or cryopreserved.

The passage procedure was the same for all three cell types except the HaCaT cells required an additional step:

1. Spent cell culture medium was discarded and the monolayer washed thrice with prewarmed (37°C) PBS to remove unattached cells and to ensure that all FBS was removed since this would inhibit the action of the proteolytic enzyme trypsin.

2. HaCaT cells only:

   Two millilitres of 0.05% ethylenediaminetetraacetic acid (EDTA) solution (Sigma, Steinheim, Germany) was added to the washed monolayer in the flask and incubated at 37°C for 5 to 10 minutes or until intercellular spaces were visible between the cells on

microscopic examination. Since EDTA is a chelating agent (Petrucci and Harwood 1997), it binds Ca^{2+} thereby loosening the desmosomal attachments between the HaCaT cells (Hennings and Holbrook 1983, Kitajima 2002). Once the intercellular spaces were visible the EDTA solution was removed (Makakole and Sturm 1999).

3. About 1ml of 0.05% trypsin - 0.02% versene (EDTA) solution (BioWhittaker™) was added, the flask gently tilted from side to side to ensure the solution covered the entire monolayer and the excess solution discarded. After about 1 minute incubation on a warm surface the flask was gently tapped to dislodge the cells.

4. One millilitre of FBS was added immediately and allowed to cover the entire monolayer to neutralise the action of trypsin before it caused cellular damage. The FBS was aspirated with a Pasteur pipette and squirted against the base of the flask to remove most of the remaining attached cells and to break up cell clumps. Following this the cell-FBS suspension was aspirated and decanted into a sterile centrifuge tube.

3.1.5 Cryopreservation of cells

For cryopreservation of cells, cell suspensions were produced as described and an equal quantity of the appropriate freezing fluid (Appendix) was added drop by drop to the cell-FBS suspension. The suspension was gently swirled between drops to slowly mix the cells with the freezing fluid. The resulting cell suspension was aliquoted into cryovials (1.0 – 1.5ml per cryovial) which were tightly capped and sealed with Parafilm. Date of storage, passage number and concentration of cells was recorded on each vial. Cells were slowly frozen to -70°C by placing the cryovials in a closed polystyrene rack at -70°C. Long term

storage of cells was carried out by transferring the vials into a liquid nitrogen freezer (-196°C) once they had reached -70°C.

3.1.6 Determination of cell numbers

The Trypan blue dye exclusion assay, using a Neubauer haemocytometer, was used to enumerate viable and nonviable cells.

A haemocytometer was wiped with 70 % ethanol and covered with a square coverslip. Twenty microlitres cell suspension was added to 20 µl 0.4% trypan blue solution (Sigma) (1:2 dilution) and mixed well by pipetting up and down. A pipette was used to place a drop of this Trypan blue-cell suspension at the edge of the coverslip such that it was drawn under the coverslip by capillarity to fill the counting chamber. Since trypan blue dye is actively removed from viable cells but remains in dead cells, viable and dead cells can be differentiated when visualised under a light microscope and the cells enumerated using the haemocytometer. The number of viable (colourless) and non-viable (blue) cells were counted in the 5 primary squares: each corner square and the centre square. Cells touching the top and left borders of the square were included in the count for that square, while those touching the bottom and right borders were not. (Maleka *et al* 1996) Cells in clumps were counted as individual cells, but if there were too many clumps, the suspension was mixed more thoroughly, the haemocytometer cleaned and refilled and the count repeated.

The number of viable and dead cells was then used to calculate the concentration, total cell number and percent cell viability.

Since each primary chamber has a volume of 1 x 10^{-4} ml, the concentration of cells per millilitre was determined using the formula:

$$\text{Concentration} = \frac{N}{5} \times 10^4 \times \text{dilution factor}$$

Where N = total number of cells in 5 primary squares

Total cell number was calculated by multiplying the concentration in cells per ml by the total volume in ml:

$$\text{Total cell number} = \text{concentration} \times \text{total volume}$$

The percent cell viability was calculated by dividing the number of viable (unstained) cells by the total number of cells (viable and nonviable) then multiplying by 100 as follows:

$$\% \text{ cell viability} = \frac{\text{no. of viable cells}}{\text{total no. of cells}} \times 100$$

If the cells in each primary square were too numerous to count, the cell suspension was diluted with PBS, and the trypan blue dye exclusion assay repeated.

3.2 Bacterial Culture

3.2.1 Bacterial strains of choice

Experiments were conducted using 3 LGV reference strains originally isolated from bubonic aspirates of a group of military servicemen or seamen who had recently returned from Asia, and presented with classical LGV symptoms (Schachter *et al*, 1969). These strains are: L1 strain 440 (ATCC® number: VR-901B™), L2 strain 434 (ATCC® number: VR-902B™) and L3 strain 404 (ATCC® number: VR-903™). These strains are widely used for pathogenesis studies of LGV.

We isolated three fresh clinical isolates from patients presenting in the primary stage of LGV (genital ulcers) at the Prince Cyril Zulu Communicable Diseases Clinic in Durban, South Africa for use in this pathogenesis study. These strains are designated Ulcer Study (US)151, US162 and US197. They were all shown to be serovar L2 using sequence analysis techniques. The OG serovar E strain was isolated by Maleka and coworkers (1996) in our laboratory from a male patient presenting at the same clinic with urethritis. This strain was typed in the Division of Allergy and Infectious Diseases, Department of Medicine, University of Washington, Seattle, USA (Dr. M Lampe) using monoclonal antibody microimmunofluoresence.

This study was approved by the Research Ethics Committee of the Nelson R. Mandela School of Medicine, University of KwaZulu Natal; reference number: H184/04

3.2.2 Propagation, isolation and storage

3.2.2.1 Monolayer preparation

Since *C. trachomatis* is an obligate intracellular pathogen, in order to propagate this organism, a suitable host cell, such as the McCoy cell line, was required.

McCoy cells were cultured in tissue culture flasks and passaged as described above. Approximately 8 x 10^4 cells suspended in 1ml CCM with 10% FBS were seeded into Trak vials, each containing a round glass coverslip. After overnight incubation at 37°C with 5% CO_2 in 95% air, the glass coverslip was removed from 1 vial, placed on a clean glass slide, and viewed at 100x magnification to verify integrity of the cells and ensure that the monolayer had become 80 to 90% confluent.

3.2.2.2 Infection

Once the McCoy cells were ready for infection, CCM was aspirated from each Trak vial, the monolayer washed once with PBS, and 500µl chlamydia growth medium for propagation (CGM-P) was added. CGM-P comprised EMEM (BioWhittaker™) with EBSS, nonessential amino acids (NEAA) and sodium pyruvate which had been enriched to yield final concentrations of the following: 10mM HEPES, 2mM L-glutamine, cycloheximide (1µg/ml), gentamicin (10µg/ml), Amphotericin B (5µg/ml), glucose (5.4mg/ml) and 10% FBS.

Chlamydia EB suspended in 100µl sucrose-phosphate-glutamate buffer (SPG) was introduced into each Trak vial, except the negative control vial, to which 100µl sterile SPG was added. Vials were centrifuged at 1200 x g for 1 hour, then incubated at 37°C for a further 1 hour. The residual inoculum was aspirated and replaced with 1ml fresh CGM-P and the vials incubated for 2 days.

3.2.2.3 Isolation and storage

After the incubation period, the negative control monolayer and 1 positive monolayer was stained and viewed using a fluorescent microscope to verify the presence of chlamydial inclusions in the positive monolayer, and eliminate the possibility of any crossover chlamydial contamination (negative monolayer).

Once this had been verified, the excess CGM-P in the remaining vials was aspirated and replaced with SPG containing 10% FBS. A few sterile glass beads were added and the vials vortexed to disrupt the McCoy cell monolayer and release the chlamydial EB. The EB-SPG suspensions from all the vials of the same batch were pooled, mixed and aliquoted into sterile safe-lock Eppendorf tubes for storage at -70°C. When more than 1 serovar was to be harvested on the same day, this was done sequentially, not simultaneously, and the biosafety cabinet and all equipment used was swabbed with 70% ethanol between serovars. The safety cabinet's air circulation system was allowed to run for 5-10 minutes to prevent cross contamination between chlamydial strains.

3.2.3 Determination of the infectious titre

Since the viability of chlamydial EB decreases during freezing (Aarnaes *et al* 1984), frozen EB suspensions from the same batch to be used for experiments were applied to determine the infectious titre on 80 to 90% confluent McCoy cell monolayers grown in a 24-well plate with a 12 mm round glass coverslip (Marienfield) in each well.

One vial EB suspension per batch was thawed, and 10-fold serial dilutions prepared in SPG. These serial dilutions were used to infect the 80-90% confluent McCoy cell monolayers in the 24-well plate using the infection procedure described. One hundred microlitres of SPG was used for the negative control in place of the 100µl EB-SPG suspension.

After 2 days incubation, coverslips were stained then viewed with a fluorescent microscope.

The number of inclusions per field was enumerated at 400x magnification and the average number of inclusions per field of view calculated. The dilution at which the inclusions were counted was the dilution at which 5 to 40 inclusions were present in each field of view.

The infectious titre was then calculated using the following formula:

$$\text{Concentration (IFU/ ml)} = \frac{\text{inclusions}}{n} \times \frac{1'000\mu l}{V} \times C \times D$$

Where: n = number of fields counted

V = volume of inoculum (µl)

C = objective lens conversion factor

D = dilution (ml)

The objective lens conversion factor is the numerical factor used to convert from the number of inclusions seen in a field of view with a certain objective lens, to the number of

inclusions present in the whole well. Since conversion factors are affected by the area of the well and the area of the field of view visualised with each objective, the conversion factors vary and are calculated by dividing the area of the field of view by the area of the well.

3.3 Fluorescent Microscopy

3.3.1 Principle

The chlamydial major outer membrane protein (MOMP) is present in all known serovars of *C. trachomatis*, and in both the EB and RB. In MicroTrak® *C. trachomatis* Culture Confirmation Test kit (Trinity Biotech) monoclonal antibodies directed against this protein are conjugated to fluorescein isothiocynate (FITC) to specifically identify these organisms. The anti-*C. trachomatis* antibodies bind to the MOMP antigen, and cause chlamydial particles to fluoresce apple-green in contrast the host cells which stain red with the Evan's Blue counter stain when viewed with a fluorescent microscope with the appropriate filter.

3.3.2 Staining method

The staining procedure was performed as outlined by the manufacturer with slight modifications.

Excess media in the well or Trak vial was aspirated and monolayers fixed by the immediate addition of 1ml 95% ethanol in distilled water for about 10 minutes. It was imperative that the monolayer did not dry out before the fixative was added; otherwise the

inclusions may have burst and become reduced in number. After the fixation step, excess fixative was aspirated and the monolayers rinsed once with PBS to remove any unattached cellular debris. While the monolayer was still moist 30µl equilibrated stain reagent (Appendix) was applied to the coverslip, and incubated at 37°C in a humidified chamber for 30 minutes. The monolayer needed to be moist to ensure that the stain reagent covered the whole coverslip, and coverslips were incubated in a humidified chamber to prevent the stain drying on the monolayer which would cause non-specific binding. After this incubation step, the coverslips were rinsed in distilled water with agitation for 10 seconds. Excess water was blotted off and the dry monolayers placed cell side down onto a drop of DPX mountant on a clean, labelled microscope slide. Slides were either read immediately or stored in the dark at -20°C until read.

3.3.3 Visualisation and photography

Slides were visualised using a fluorescent microscope with a filter system for FITC (λ = 520nm) and magnification at 100-400x (dry objective) for scanning and 500-1000x (oil immersion objective) for confirmation of morphology.

3.4 Collection and propagation of clinical isolates

3.4.1 Participants

Specimens were collected from adult male or female patients presenting with genital ulcer disease and/or lymphadenopathy at the Prince Cyril Zulu Communicable Diseases Clinic

in Durban. Exclusion criteria for participation in the study were the use of antimicrobial agents in the preceding 4 weeks and refusal to participate.

3.4.2 Specimen collection

After consent was obtained, the specimen was collected by a registrar from the Department of Medical Microbiology who was trained in the collection of such specimens. The base and edge of the ulcer/s was cleaned with a sterile dry gauze swab and a sterile disposable plastic loop was used to scrape the edge and base of the ulcer. The material was suspended in 1 ml chlamydia transport medium and the plastic loop was left in the container. This was stored and transported on ice. In addition a Dacron swab was also rolled over the ulcer then placed in 1 ml PBS for aetiological diagnosis by PCR (Sturm *et al*. 2005). The specimens were transported to the laboratory within 4 hours of collection. Specimen in chlamydia transport media were immediately frozen at -70°C, while the specimen in PBS was refrigerated and processed within 48 hours.

3.4.3 Identification *C.trachomatis*, LGV biovar

A *C. trachomatis* specific PCR was used to determine the presence of chlamydia in the ulcer specimens. An endonuclease restriction was employed to confirm that the organism was of the LGV biovar (Watson *et al.* 1991).

3.4.4 Isolation and propagation

Ulcer specimens testing positive in the chlamydia PCR and with the LGV biovar restriction pattern were seeded on McCoy cell monolayers in CGM-P. The frozen specimen was thawed immediately prior to use. Three sterile glass beads were added to the specimen in chlamydia transport media then vortexed for 2 minutes with the disposable plastic loop still in place. The loop was then removed with sterile forceps and discarded. The specimen suspension was transferred to a sterile cryovial. Prepared McCoy cell monolayers with CGM-P were infected with 200 µl specimen suspension in duplicate. A negative control comprising 200 µl sterile SPG was also prepared. Cultures were processed as described for the reference strains. After the 2 day incubation step, one Trak vial from each specimen, as well as the negative control was fixed and stained using the MicroTrak® *Chlamydia trachomatis* Culture Confirmation Test kit. Slides were examined using a fluorescent microscope with a filter system for FITC to confirm the presence of chlamydial inclusions in the specimens and absence of chlamydial inclusions in the negative control. EB were harvested and passaged onto prepared McCoy cell monolayers approximately 3 times until a sufficient titre was obtained for use in experiments.

3.5 Lactate Dehydrogenase Detection

3.5.1 Principle

The CytoTox96® Non-Radioactive Cytotoxicity Assay (Promega) was used to quantify the level of chlamydia-induced cytotoxicity in HaCaT and ME-180 cells. This assay quantifies the level of lactate dehydrogenase (LDH), a cytosolic enzyme which is released upon cell lysis (Sepp *et al* 1996). The level of LDH released into the culture supernatent is detected using a coupled enzymatic reaction in which the tetrazolium salt is converted to a

red formazan product. The wavelength absorbance data recorded are used to calculate the percentage cytotoxicity.

Since there are several factors which affect the absorbance at the wavelength used in this assay, including FBS and phenol red which were both present in the chlamydia growth medium for experiments (CGM-E), four controls were set up:

- The **host cell spontaneous LDH release** utilizes the supernatant from uninfected cells and corrects for the spontaneous release of LDH from the host cells.
- The **host cell maximum LDH release** utilizes the supernatant from uninfected cells which have been lysed. It is required in calculations in order to determine 100% LDH release.
- The **volume correction control** comprises culture medium without cells to which the lysis solution has been added in order to compensate for the volume change caused by the addition of lysis solution to the host cell maximum LDH release control.
- A **culture medium background** control comprising only cell culture medium without cells corrects for the LDH activity contributed by serum in the cell culture medium, as well as the presence of phenol red.

3.5.2 Methodology

HaCaT or ME-180 cells were seeded (1.5×10^4 cells in 100µl CCM per well) into flat-bottom 96-well TC microtitre plates and incubated at 37°C overnight to yield an 80% confluent monolayer the following day. Three wells for each cell line were trypsinized and the cell count used to calculate an appropriate dilution of the stock chlamydial inoculum to

produce a MOI of 0.025. This low MOI ensured that only a few cells became infected in the first instance, allowing sufficient uninfected neighbouring cells for the progeny EB to infect after completion of the chlamydial lifecyle.

CCM was aspirated from the wells and replaced with 100µl CGM-E comprised of RPMI-1640 (BioWhittaker^{TM}) with 10mM HEPES, 2mM L-glutamine, gentamicin (10µg/ml), Amphotericin B (5µg/ml), glucose (5.4mg/ml) and 10% FBS. Cycloheximide was not used in any experiments, because it inhibits eukaryotic cell replication by interfering with the 60S ribosomal subunit (Elela and Nazar, 1997), which would prevent eukaryotic host cells from behaving as they would in an *in vivo* situation.

Cells were infected in triplicate with 3 *C. trachomatis* reference strains (serovars L1, L2 and L3), 1 OG strain (serovar E), 3 LGV clinical isolates or 50µl sterile SPG for the negative control and maximum LDH release control. After addition of the inoculum or SPG, plates were centrifuged at 1200 x g for 1 h, incubated at 37°C or 33°C for 1 h, then the inoculum removed and replaced with 150µl fresh CGM-E. At this point 150µl CGM-E was added to 6 empty wells for subsequent use as the volume correction control and culture medium background control. Plates were incubated at 37°C or 33°C for 5 days.

Each day post-infection, 1 plate from each cell line and both temperatures for the HaCaT cell line, was removed from the incubator for use in the LDH assay and chlamydial growth curve study. The remaining plates were centrifuged at 1200 x g for 1 h each day then returned to the incubator. On the second day post-infection 100 µl fresh CGM-E was added to all remaining wells, while 50 µl fresh CGM-E was added on day 4.

For the LDH assay, lysis solution was added to the volume correction and maximum LDH release control. The volume added was 10% of the volume of CGM-E in the well, therefore on days 1 and 2, 15µl was added, on days 3 and 4, 25µl lysis solution was added, while 30µl lysis solution was added on day 5. The solution in each well was mixed by stirring with a pipette tip, and the plates returned to the incubator for 45 minutes until the cells had lysed. The solution was mixed by pipetting up and down, then cellular debris pelleted by centrifugation at 250 x g for 4 minutes.

Twenty-five microlitres supernant was transferred from each well to a clean well on a new flat-bottom 96-well TC plate. Because of the high LDH activity, the superant was diluted with 25µl PBS to produce a final volume of 50µl. Reconstituted substrate mix (50 µl) was added to each well. The plates were covered with foil and incubated at room temperature for 20 minutes. The reaction was stopped with 50µl stop solution (1M acetic acid) and the absorbance read at λ 492nm using an Anthos 2010 version 1.7 microplate reader.

Before calculation of the percentage cytotoxicity, the average absorbance of the volume correction control was subtracted from the maximum LDH release control, and the average absorbance values of the culture medium background control subtracted from all other absorbance values.

The corrected absorbance values were used to calculate the percent cytotoxicity in the following calculation:

$$\% \text{ cytotoxicity} = \frac{\text{Experimental} - \text{Host Spontaneous}}{\text{Host Maximum} - \text{Host Spontaneous}} \times 100$$

This experiment was performed 3 times in triplicate.

No effector cell (chlamydia) spontaneous LDH release was measured since *C. trachomatis* is an obligate intracellular organism, and thus unable to replicate in the absence of a eukaryotic host. These organisms rely on adenosine triphosphate (ATP) from their host, and there are no reports of this organism possessing LDH, an enzyme of the glycolytic pathway.

3.6 Chlamydial Growth Curves

3.6.1 Principle

Although chlamydial growth rates are known to differ between the biovars and reflect tissue tropisms, previous studies do not accurately reflect the *in vivo* situation. Cells that were not the native host cell treated with cycloheximide or DEAE-dextran were used to grow the organisms and the isolates have been passaged for decades under conditions different to those from which they were isolated originally.

Here we eliminate some of those variables by growing *C. trachomatis* in cell lines derived from tissue affected *in vivo* under conditions which do not impair the host cells from functioning normally (neither cycloheximide nor DEAE-dextran are used), and in addition to the reference strains, we used recently collected isolates from our setting. To approach the *in vivo* situation as close as possible, a very low MOI (0.025) was used. This ensured the availability of a sufficient number of uninfected cells for the progeny EB to infect and replicate in, mimicking a natural infection.

3.6.2 Methodology

The same 96-well TC plates set up for the LDH assay in 5.2 were used for the chlamydial Growth Curve studies.

After the supernatant was removed for use in the LDH assay, the remaining supernatant was aspirated and discarded. The cells in the wells were immediately fixed with about 200 µl 95% ethanol for 5 minutes. The ethanol was removed and the plates allowed to dry, before being frozen at -70°C until needed.

The experiment was performed 3 times in triplicate.

On the day that the plates were visualised, they were allowed to reach room temperature. The cell monolayers were then moistened with 200µl PBS. Plates were inverted to remove the PBS, then 15µl *C. trachomatis* Reagent from the MicroTrak® *C. trachomatis* Culture Confirmation Test was added immediately before the monolayers dried. Following this the plates were incubated in a humidified chamber at 37°C for 30 minutes with manual agitation every 10 minutes. The reaction was stopped by washing the monolayers with 200µl dH_2O twice for 10 sec each then allowed to dry.

3.6.3 Visualization and enumeration

The 96-well TC plates were inverted and viewed at low magnification (100-400x) with an Olympus BH2-RFCA fluorescent microscope. The number of chlamydial inclusions per

field of view (FOV) was enumerated using the 10, 20 or 40× objective lens depending on which objective yielded a countable number of inclusions. For the 10 and 20× objectives, 5 FOV were counted and averaged; for the 40x objective 10 FOV were counted and averaged.

Objective lens conversion factors were calculated by dividing the area of 1 well in a 96-well plate by the area of each objective lens FOV. The number of inclusions per well was calculated by multiplying the average number of inclusions per FOV by the objective lens conversion factor.

3.6.4 Photography and image analysis

The 96-well TC plates were inverted and viewed at low magnification (100×) with a Nikon eclipse E600 fluorescent microscope using a filter with an excitation wavelength of 450-490 nm and an emission wavelength of 520 nm. Images were captured in colour using a Nikon ColorView Soft Imaging System digital camera with an exposure time of 2.500 sec and the red, green, blue balance set to 1.00, 2.00 and 2.00 respectively. Images were analysed using Soft Imaging System version 3.2.

In order to calculate the area of each image occupied by *C. trachomatis* (stained green) and the area occupied by cells (stained red), colour thresholds were set. Two phases were defined, one to detect green and the other to detect red. For phase green the thresholds were defined as follows: hue, saturation and intensity were 60-255, 140-255 and 20-255 respectively; and in phase red, hue, saturation and intensity were 0-65.16, 100-200 and 10-106 respectively. These values were attained by reading the pixel value at various points

on numerous images, and the accuracy of the resultant phase definitions confirmed using the phase colour coding function which colour-coded the green phase blue, and the red phase pink. The original image was compared with the colour-coded image to ensure that all the correct areas were selected, and the undesired areas omitted. The ranges were then broadened or restricted until the colour thresholds were optimal. The area occupied by *C. trachomatis* and the area occupied by cells was calculated using the phase analysis function on each 100× image captured.

Chlamydial inclusion size was measured for the HaCaT cells at 33°C for days 2 to 5 post infection. Inclusions were too small to be visually detected 1 day after infection under these conditions. The detection parameters were setup to include particles with a minimum size of 60 pixels. Inclusions touching the border were excluded. Each image was separated into its red, green and blue components and the new image of the green component selected. The detect function was utilized to select chlamydial inclusions. Each image was carefully compared with the original to ensure that only chlamydial inclusions were selected. Since the software could not discriminate between 2 or more inclusions in contact with each other, any inclusions that were touching each other were excluded from the analysis using the delete particle function. The particle results function was used to analyse each selected inclusion and measure various parameters, including the area (μm^2), diameter (μm) and mean level of green that was detected per inclusion. Results were output in a Microsoft Excel spreadsheet and the inclusion parameters of the chlamydial strains compared.

3.7 Transmission electron microscopy (TEM)

The ultrastructural development of the chlamydial inclusion in human keratinocytes and cervical epithelial cells, and the effect of the organism on the infected and exposed cells compared to an unexposed negative control over 48 hours, was investigated using transmission electron microscopy.

3.7.1 Monolayer preparation and infection

HaCaT and ME-180 cells were grown in tissue culture flasks. Once confluent cells were trypsinised and 1 x 10^5 cells seeded to 24 well plates (Greinier) to which 12mm round Thermanox coverslips (Nunc) had been inserted into each well. After 2 days, the cells were about 90% confluent. Trypsinization and enumeration using the Trypan Blue dye exclusion assay and a haemocytometer revealed a cell count of approximately 2.5 x 10^5 cells per well. The residual CCM was aspirated, the monolayer washed once with PBS, then chlamydial growth medium added. The chlamydial inoculum was thawed immediately prior to use, and diluted with SPG buffer. Cells were infected with 100 µl chlamydial suspension at an MOI of 0.25, which equated to 1 chlamydial EB per 4 cells to ensure the presence of both infected and uninfected exposed cells in each well. For the unexposed negative control, cells were treated with 100 µl sterile SPG buffer. Cells were immediately centrifuged at 1200 x g for 1 hour, then transferred to an incubator. This point was defined as T_0. HaCaT cells were incubated at 37°C and 33°C to compare the effect of *C. trachomatis* on the host cell at core body temperature (37°C) versus the temperature of human skin (33°C), while the ME-180 cells were only incubated 37°C because these cells could not survive at 33°C. The residual inoculum was removed after 2 hours in the incubator and replaced with 1 ml fresh CGM-E.

3.7.2 Monolayer processing

At 1, 3, 9, 18, 24, 36 and 48 hours post-infection, 1 well for each strain, cell type and temperature combination was fixed and processed for transmission electron microscopy (TEM). After washing with EMEM, the cell monolayers were transferred to a fresh 24-well plate using sterile forceps and a dissecting needle. The original plate was returned to the incubator, while the harvested coverslips with their cell monolayers were processed within the 24-well plate until the final step. Cells were fixed with 2% gluteraldehyde in EMEM for 30minutes, then washed with EMEM twice for 5 minutes. The fixed monolayers were covered by a layer of sterile EMEM and refrigerated until they could be processed (no more than 20 hours). Cells were post-fixed, dehydrated and infiltrated directly in the 24-well plate (table 1). In order to embed the cells in Spurr resin, a beam capsule was filled with Spurr resin and the coverslip placed on top of the beam capsule with cell-side down touching the resin. The beam capsules were incubated at 60°C for 48 hours to allow the resin to solidify.

After 48 hours the coverslip was quickly removed while the resin was still warm allowing the cells to remain embedded in the Spurr resin.

Table 2. Processing schedule for TEM

Step	Process	Solution	Temperature	Time
1	Fixation	2% gluteraldehyde in EMEM	24°C	30 min
2	Wash	EMEM	24°C	5 min
3	Wash	EMEM	24°C	5 min
4	Wash	Sodium cacodylate buffer	24°C	5 min
5	Post-fixation	1% osmium tetroxide[a]	24°C	45 min
6	Wash	Sodium cacodylate buffer	24°C	5 min
7	Wash	Sodium cacodylate buffer	24°C	5 min
8	Dehydration	50% ethanol	24°C	10 min
9	Dehydration	70% ethanol	24°C	10 min

10	Dehydration	90% ethanol	24°C	10 min
11	Dehydration	100% ethanol	24°C	10 min
12	Dehydration	100% ethanol	24°C	10 min
13	Dehydration	100% ethanol	24°C	10 min
14	Infiltration	Ethanol : Spurr resin (1:1)[b]	24°C	30 min
15	Infiltration	Spurr resin[b]	60°C	1 hour
16	Infiltration	Spurr resin[b]	60°C	1 hour
17	Embedding	Spurr resin	60°C	24-48 hours

[a] protected from light

[b] procedure carried out uncovered to allow polypropylene to evaporate

3.7.3 Ultramicrotomy

The section of the resin block containing cells was sawed off and trimmed to produce a "mesa" with a trapezoidal shape. Ultrathin sections (50-60nm) were cut and collected onto uncoated copper 200 mesh grids, then double stained with uranyl acetate and Reynold's lead citrate for 3 and 2 minutes respectively (Reynolds 1963). Uranyl acetate and Reynolds lead citrate was decanted and centrifuged to pellet any debris or solute crystals. Grids were floated on a drop of uranyl acetate for 3 minutes, rinsed twice with triple distilled water and blotted dry on Whatman filter paper. They were then placed in a drop of Reynolds lead citrate, rinsed twice with triple distilled water and blotted dry.

3.7.4 Visualization and photography

Sections were viewed using a Jeol 1011 transmission electron microscope at an accelerating voltage of 100 kV. The TEM was interfaced with a Megaview III Software Imaging Systems camera unit. Images were captured digitally and measurements performed using iTEM analySIS (Germany) image analysing software.

3.8 MTT Assay

3.8.1 Principle

The 3-(4,5-dimethylthiazol-2-yl)-2,5-diphenyltetrazoliumbromide (MTT) assay was used to determine the level of mitochondrial activity in infected versus uninfected cell populations.

The MTT assay is a colorimetric cell culture assay based on the principle that dehydrogenase enzymes in the intact mitochondria of metabolically active cells reduce the insoluble pale yellow tetrazolium MTT salt to slightly soluble, dark blue formazan crystals allowing the assay to detect living cells but not dead cells with the signal generated proportional to the level of activation (Mosmann, 1983). This assay is used to determine cell proliferation, or the rate of cell survival in various medical, microbiological and toxicological fields (Hanelt *et al*. 1994).

3.8.2 Methodology

HaCaT or ME-180 cells were seeded (1.5 x 10^4 cells in 100µl CCM per well) to flat-bottom 96-well TC plates and incubated at 37°C overnight to yield an 80% confluent monolayer the following day. Three wells for each cell line were trypsinized and the cell count used to calculate an appropriate dilution of the stock chlamydial inoculum to produce a MOI of 0.25. Cells were infected in triplicate with *C. trachomatis* serovar L2, L3 or E in 50 µl SPG. Sterile SPG was used for the uninfected control, while the positive control contained 20 µM etoposide. Etoposide is a cytotoxic compound shown to induce

caspase mediated apoptosis in HaCaT cells (Lee *et al*. 2005). After addition of the inoculum or SPG, plates were centrifuged at 1200 x g for 1 h, incubated at 37°C or 33°C for 1 h. The inoculation medium was then removed and replaced with 150µl fresh CGM-E.

At 1, 3, 9, 18, 24, 36 and 48 hours post-infection the level of mitochondrial activity was measured using the MTT assay. Ten microlitres of MTT salt solution (5µg/ml in PBS) was added to each well, and the cells were incubated at the experimental temperature for 2 hours 30 minutes. The culture media was aspirated, and the purple formazan crystals were dissolved in 150µl DMSO by pipetting up and down 5 times. This solution was transferred to a fresh 96-well plate and the absorbance data read at test wavelength of 570 nm with a reference wavelength of 630 nm.

The experiment was performed 3 times in triplicate.

3.9 TUNEL assay

3.9.1 Principle

The terminal deoxynucleotidyl transferase (TdT)-mediated dUTP-biotin nick end labeling (TUNEL) assay was first developed in 1992 by Gavrieli *et al.* This method detects cells undergoing programmed cell death (PCD) *in situ* at the single cell level without destroying cell and tissue architecture. Apoptosis is associated with the activity of endogenous endonucleases which cleave double stranded genomic DNA at regular intervals and yield numerous 3'hydroxyls (3'-OH) available for TdT to label (Bortner *et al*. 1995; Didenko and Hornsby, 1996). In the TUNEL assay, cells are treated with protease to expose the

nuclear DNA. Thereafter TdT is added which binds to the 3'-OH ends of the cleaved DNA and facilitates the incorporation of biotinylated deoxyuridine (dUTP). If this is the case, horseradish peroxidase (HRP)-labeled streptavidin is bound to dUTP. These biotinylated nucleotides are detected using hydrogen peroxide, the substrate for HRP, and diaminobenzidine (DAB), which is a stable chromagen detectable by light microscopy.

3.9.2 Methodology

HaCaT or ME-180 cells were grown on glass coverslips in 24-well tissue culture plates for 2 days until confluent. The residual CGM-E was removed and replaced with 500µl CGM-E, then infected with *C. trachomatis* serovar L2, L3, E, or the clinical isolates US151, US162 and US197 in 100 µl SPG at an MOI of 0.25. One hundred microlitres sterile SPG was used for the uninfected control, TUNEL positive control, and TUNEL negative control (provided with the kit). Monolayers were centrifuged at 1200 x g for 1 hour, then incubated at 37°C or 33°C for 1 hour. The residual inoculum was aspirated, replaced with 1ml CGM-E and the monolayers incubated at 37°C or 33°C for 2 or 5 days.

After 2 days (or 5 days for the HaCaT cells at 33°C), the cells were fixed and stained for the TUNEL assay using the DeadEnd™ Colorimetric TUNEL System (Promega) and *C. trachomatis* detection using the MicroTrak® *Chlamydia trachomatis* Culture Confirmation Kit (Trinity Biotech) as described below.

Procedures were carried out according to manufacturer's instructions with the following adaptations:

- Cells were processed on coverslips within the wells of a 24 well plate and mounted to glass slides after the staining procedure, instead of being processed on glass slides
- Cells were fixed with 4 % formalin in PBS in stead of 10% buffered formalin, 4% paraformaldehyde solution or 10 % buffered formalin in PBS
- Cells were permeabilized with 0.4% Triton® X-100 in PBS for 10 min at room temperature for ME-180 cells, and 37°C for HaCaT cells. The manufacturer's recommendation of 0.2% Triton® X-100 in PBS for 5 min did not permeabilize the HaCaT cells sufficiently.
- Ten units per millilitre RQ1 DNase was used as the TUNEL positive control
- At the end of the TUNEL assay staining procedure, the same slides were stained with the MicroTrak® *C. trachomatis* Culture Confirmation Test Kit

Cells were processed directly in the wells at room temperature unless otherwise stated.

Procedure:

1. Wash with PBS
2. Fix with 4% formalin in PBS for 25 min
3. Wash twice with PBS for 5 min
4. Permeabilize with 0.4% Triton® X-100 in PBS for 10 min (room temperature for ME-180 cells; 37°C for HaCaT cells)
5. Wash twice with PBS for 5 min
6. DNase treatment for TUNEL positive control:
    a. Wash with 200µl DNase I buffer for 5 min

b. Treat with 200µl RQ1 RNase free DNase (10 unit/ml) (Promega) in DNase I buffer for 10 min at 37°C

c. Rinse with tdH_2O 4 times

d. Wash with PBS for 5 min

7. Equilibrate with 100µl equilibration buffer for 5-10 minutes
8. Prepare rTdT reaction mix by combining the following components per well:

   98µl equilibration buffer

   1µl biotinylated nucleotide mix

   1µl rTdT enzyme or 1µl autoclaved tdH_2O for the TUNEL negative control
9. Label with 100µl rTdT reaction mix for 60 min at 37°C with each glass coverslip covered with a plastic coverslip to ensure even distribution of the reagent and prevent evaporation
10. The plastic coverslips were removed and the reaction stopped with 200µl 2X SSC for 15 min
11. Wash thrice with PBS for 5 min
12. Block endogenous peroxidases with 0.3% hydrogen peroxide for 4 min
13. Wash thrice with PBS for 5 min
14. Bind with 200 µl streptavidin horse radish peroxidase (HRP) (1:500 in PBS) for 30 min
15. Wash thrice with PBS for 5 min
16. Prepare DAB stain solution:

   950 µl tdH_2O

   50 µl 20x DAB substrate buffer

   50 µl DAB 20x chromagen

   50 µl 20x hydrogen peroxide

17. Stain with 100µl DAB solution for 15 min with each glass coverslip covered with a plastic coverslip to ensure even distribution of the reagent and prevent evaporation
18. Remove plastic coverslips
19. Rinse monolayer 5 times with tdH_2O
20. Counterstain for *C. trachomatis* detection using the MicroTrak® *Chlamydia trachomatis* Culture Confirmation Kit (Trinity Biotech)
    a. Moisten with PBS for 5 min
    b. Stain with 30µl stain reagent for 30 min at 37°C in a humidified chamber
    c. Wash with tdH_2O for 10 sec
21. Remove glass coverslip from well
22. Blot
23. Mount to glass slide with DPX mounting fluid

Once the mounting fluid had solidified, the slides were viewed with a Nikon eclipse E600 fluorescent microscope. Slides were examined using bright field microscopy to identify cells with fragmented DNA and DAB positive nuclei; then switched to fluorescence (excitation wavelength 450-490 nm; emission wavelength 520 nm) and the same field of view examined for the presence and location of *C. trachomatis*-infected cells relative to DAB positive cells.

Images were captured in colour using a Nikon ColorView Soft Imaging System digital camera. For each field of view, DAB positive cells were captured in a bright field photograph, and the same field of view captured under fluorescence. Each pair of images was examined to identify relationships between DAB positive and *C. trachomatis* infected cells.

3.10 Caspase detection in uninfected but exposed cells

3.10.1 Principles

Because apoptosis has been defined as "caspase-mediated cell death with associated apoptotic morphology" (Samali *et al* 1999), a caspase detection assay was performed using the BioVision™ CaspGLOW Fluorescein Caspase Staining Kit (BiocomBiotech). The broad spectrum caspase family inhibitor Val-Ala-Asp-α-fluoromethylketone (VAD-fmk) binds irreversibly to Caspase-1 through to Caspase-10 (Garcia-Calvo *et al*. 1998). After conjugation to the fluorescent marker FITC, this cell permeable VAD-fmk-FITC conjugate enters viable cells and binds activated caspases. Apoptotic cells are directly detected upon fluorescent microscopy examination.

In order to elucidate whether or not chlamydia-induced molecules affect neighbouring uninfected cells, the caspase assay was coupled with the use of Transwell® Permeable Supports (Corning). This allows the separation of a layer of infected cells from a layer of uninfected cells. This made it possible to differentiate between cytotoxicity caused by cell-to-cell interaction with an infected neighbouring cell or by secreted molecules.

Transwell® Permeable Supports with a polyester (PE) membrane were used, since the PE membrane allowed better cell visibility than the polycarbonate or polytetrafluoroethylene membranes. The membrane is compatible with histological fixatives, as well as many other chemicals and solvents. The pore size was 0.4 μm, with a density of approximately 4×10^6 pores/cm^2, to allow diffusion of molecules which may be secreted.

3.10.2 Methodology

ME-180 or HaCaT cells were cultured in wells of a 24-well plate overnight at 37°C until 90% confluent.

The following day, cells within the wells were infected, and cells seeded to the upper chamber of Transwell® Permeable Supports. A well of each cell line was trypsinized and a cell count performed. The number of cells obtained was used to calculate the number of chlamydial EB to be added to achieve an MOI of 2. The CCM was aspirated from each well and replaced with 500µl CGM-E. Cells were infected with *C. trachomatis* serovar E, L2 or L3, suspended in 100µl SPG or sterile SPG for the uninfected control and the caspase positive control. Plates were centrifuged at 1200 x g for 1 hour, incubated at 37°C for the ME-180 cells, and 37 or 33°C for the HaCaT cells for 1 hour. The residual inoculum was aspirated, 1ml fresh CGM-E added and the plates incubated overnight.

On the same day, 2 x 10^4 ME-180 or HaCaT cells were seeded to the upper chambers of Transwell® Permeable Supports. The appropriate CCM with 10% FBS was prepared; 600µl and 100µl CCM was added to the lower and upper chambers respectively, and incubated at 37°C with 5% CO_2 for 1 hour. After this time, the CCM in the upper chamber was aspirated, and 2 x 10^4 cells suspended in 100µl CCM was added to the upper chamber of each well. Plates were incubated for at least 24 hours at 37°C to allow cells to attach.

Late the following afternoon, the Transwell® permeable supports were transferred to the 24-well plates containing ME-180 or HaCaT cells incubated at 37 or 33°C. CCM from the

upper chamber was aspirated, and the Transwell® immediately lifted out of the well and transferred to a well containing the appropriate cell monolayer infected with *C. trachomatis* or uninfected cells for the negative control. Four hundred microlitres of CGM-E was aspirated from the surface of the liquid in each well to prevent overflow when the Transwell® was inserted. The upper chamber was immediately replenished with 100µl CGM-E. For the caspase positive control, an uninfected HaCaT and ME-180 cell monolayer grown on a 12 mm round glass coverslip (Marienfield) at the appropriate temperature was treated with 100µl CGM-E to yield a final concentration of 20mM etoposide. The plates were returned to the incubators overnight. Sixteen hours later, the BioVision™ CaspGLOW Fluorescein Caspase Staining Kit was used to identify apoptotic cells in the upper chamber which were exposed, but not infected. The staining procedure was modified for use with adherent cells. Two hundred microlitres stain solution (1µl FITC-VAD-fmk per 300µl CGM-E) was added to the wells of a fresh 24-well plate. CGM-E was removed from the upper chambers of the Transwells® which were then immediately transferred to the wells prepared with the stain solution, and an additional 100 µl stain solution added to the upper chambers. For the caspase positive control, CGM-E was removed and 300 µl stain solution added directly into the appropriate well on the original cell monolayer. All plates were incubated at 37°C for 1 hour. A Transwell® insert was not used for the caspase positive control due to significant background fluorescence of the PE membrane when subjected to fluorescence microscopy after incubation with etoposide.

After 1 hour, plates were removed from the incubator, and the PE membrane was washed twice by aspirating the stain solution. The Transwell® inserts were then transferred to a fresh well of the 24-well plate containing 200µl wash buffer; 100µl wash buffer was added

to the upper chamber. Plates were incubated for 5 minutes at room temperature. The Transwells® were removed from the wells 1 at a time, and the PE membrane carefully cut off the Transwell® support using a scalpel blade. The membrane was placed on a glass slide with 2 drops of wash buffer, and covered by a glass coverslip. For the caspase positive control, the coverslip was washed twice with 300µl wash buffer for 5 minutes each directly in the original well of the 24-well plate. The round glass coverslip was removed from the well, and placed cell side down on a glass slide. All slides were read with a Nikon eclipse E600 fluorescent microscope using a filter with an excitation wavelength of 450-490 nm and an emission wavelength of 520 nm. Images were captured in colour using a Nikon ColorView Soft Imaging System digital camera.

3.11 Statistical analyses

Preliminary statistical analyses were performed with GraphPad Instat® version 3.00. The method of Kolmogorov and Smirnov was used to test for Gaussian distribution to indicate whether the data was parametric or not. Bartlett's test was used to investigate significance amongst the standard deviations (SD) of the groups.

After the preliminary statistics, analyses were performed using SPSS version 15.0. One-way Analysis of Variance (ANOVA) with Tukey's post test was used when data was parametric and the standard deviations were similar for all groups. When the data was parametric but the SD were not equal, or when the data was non-parametric, the Kruskal-Wallis non-parametric ANOVA was used. If there was a significant difference amongst the medians, GraphPad Instat was used to perform Dunn's multiple comparison's test

which only reports the range of significance, not the exact P value. Significance was set at $P \leq 0.05$.

Data was transformed by log 10 for inclusions per 10 thousand cells, area green and size of individual inclusions before analyses were conducted. Transformations did not affect the normality of the data, nor the variation amongst the SD for percentage cytotoxicity or the MTT assay, therefore these results were not transformed for analyses.

CHAPTER 4 - RESULTS

4.1 Chlamydial growth curves

ME-180 and HaCaT cells were infected with *C. trachomatis* and incubated at 37°C only for the ME-180 cells, and 37 and 33°C for the HaCaT cells. Growth was analysed using two different indicators: area occupied by chlamydia, and number of inclusions per 10 thousand cells. Counting the number of inclusions is the more commonly used techinique, but it does not take into account the size of the inclusion, which in turn reflects the number of organisms.

All strains tested were able to enter, and replicate in both cell lines at both temperatures. This is indicated by the presence of green fluorescent inclusions in the cell culture monolayers (figures 1 to 3), and by an increase in the area occupied by chlamydia, and number of inclusions per 10 thousand cells from 1 to 5 days post infection (figure 4).

The mean area occupied by chlamydia (figure 1) and mean number of inclusions per 10 thousand cells (figure 4) was plotted against days post infection for each strain, cell type and temperature. Growth curves are the same regardless of whether the means or medians are plotted.

Null hypothesis 1: *C. trachomatis* replicates at the same rate in ME-180 cells at 37°C, HaCaT cells at 37°C and HaCaT cells at 33°C.

Alternate hypothesis 1: *C. trachomatis* does not replicate at the same rate under all conditions tested.

When overall chlamydial growth in culture was compared there was an extremely significant difference in chlamydial growth ($P < 0.001$) with parametric and non-parametric methods. This difference was observed using either area occupied by chlamydia, or inclusions per 10 thousand cells. Growth in HaCaT cells at 37°C was significantly different to growth in HaCaT cells at 33°C ($P < 0.001$). There was no significant difference between chlamydial growth in HaCaT and ME-180 cells at 37°C (P values 0.5 and 1.0 for area occupied by chlamydia and inclusions per 10 thousand cells respectively). Null hypothesis 1 was rejected and alternate hypothesis 1 accepted.

Null hypothesis 2: All strains of *C. trachomatis* replicate at an equal rate in ME-180 cells at 37°C.

Alternate hypothesis 2: Some strains of *C. trachomatis* replicate more rapidly than others in ME-180 cells at 37°C.

There was an overall significant difference amongst the strains for both area occupied by chlamydia and inclusions per 10 thousand cells ($P<0.001$ for both). Using area occupied by chlamydia (Figure 5A), serovar E was significantly different to L1, L2 and L3 ($P < 0.001$, $P < 0.001$ and $P < 0.05$ respectively). No differences were found between serovar E and any of the clinical isolates ($P < 0.05$). The serovar L2 reference strain was significantly different ($P <0.01$) from all 3 clinical isolates, although sequence analysis techniques indicated that these isolates were also serovar L2. Serovar L1 was significantly different to US162 and US197 ($P < 0.001$ and $P < 0.01$ respectively). Serovar L3 was significantly different to US162 and US197 ($P < 0.001$ and $P < 0.05$ respectively).

The number of inclusions per 10 thousand cells yielded a different set of results (Figure 5B). Serovar E was not significantly different to L1, L2 or L3, and US162 was significantly different ($P < 0.01$) to all other strains except US197. Null hypothesis 2 was rejected and alternate hypothesis 2 accepted.

The ME-180 cell growth curves for 5 days post infection (figures 4A and 4B) indicated that the LGV reference strains, most notably serovar L2, replicated more rapidly than the clinical isolates or serovar E. The area occupied by chlamydia increased each day for all strains tested. But the number of L2 inclusions per 10 thousand cells increased steadily until 4 days post infection, followed by a sharp decline between day 4 and 5, despite an increase in area occupied by chlamydia during the same time frame. Fluorescent micrographs of serovar L2 infected ME-180 cells 5 days post infection illustrated many green chlamydial particles (figure 1B). Some inclusions were still intact, but numerous free chlamydial particles were dispersed across the monolayer which no longer appears intact. This is in contrast to the clearly defined serovar E inclusions (figure 4C) on a typical intact ME-180 cell monolayer.

Null hypothesis 3: All strains of *C. trachomatis* replicate at an equal rate in HaCaT cells at 37°C.

Alternate hypothesis 3: Some strains of *C. trachomatis* replicate more rapidly than others in HaCaT cells at 37°C.

In the HaCaT cells at 37°C all strains of *C. trachomatis* replicated as indicated by a steady increase in the area occupied by chlamydia and the number of inclusions per 10 thousand

cells (figure 4C and 4D). However, both growth curves demonstrate a more rapid increase in the number of L2 organisms.

The mean of the combined area occupied by chlamydia and combined number of inclusions per 10 thousand cells is plotted in figure 5 for each strain of *C. trachomatis* used.

There was an overall significant difference amongst the strains for both area occupied by chlamydia and inclusions per 10 thousand cells ($P = 0.001$ and $P = 0.019$ respectively). Post tests revealed a significant difference when L2 was compared with E, US162 or US 197 (P values 0.020, 0.000 and 0.024 respectively). Inclusions per 10 thousand cells only indicated a significant difference between L2 and US162 ($P < 0.01$). Null hypothesis 3 was rejected and alternate hypothesis 3 accepted.

Differences amongst the strains were also analysed for each day post infection. There was no significant difference in area occupied by chlamydia at 1 day post infection, but this became extremely significant ($P < 0.001$) from days 2 through to 5. At day 2 there was an extremely significant difference when serovar E or US162 was compared with the 3 LGV reference strains ($P < 0.001$ for all). These remained significant at day 3. However, at day 4 there was no longer a difference between E and L1 or L3 (P values 0.460 and 1.000 respectively). There was a significant difference between L2 and L1 ($P = 0.004$), and an extremely significant difference between L2 and all other strains ($P < 0.001$). The significant difference was sustained through to day 5.

With inclusions per 10 thousand cells L2 was significantly different to E, L1, L3, US151, US162 and US197 (P values 0.012, 0.019, 0.000, 0.016, 0.000 and 0.000 respectively) at day 4. At day 5 there was only a significant difference between L2 and E, L1, L3 and US 197 ($P < 0.01$), but not between L2 and US151 or US197.

Null hypothesis 4: All strains of *C. trachomatis* replicate at an equal rate in HaCaT cells at 33°C.

Alternate hypothesis 4: Some strains of *C. trachomatis* replicate more rapidly than others in HaCaT cells at 33°C.

In the HaCaT cells at 33°C, the area occupied by chlamydia increased from day 1 to day 5 (figure 4E). For L1 and L2, this was a steady increase, while the area occupied by the other strains reached a plateau or decreased slightly from day 4 to 5. At day 1, all strains began with zero inclusions per 10 thousand cells (Figure 3C) due to inclusions being too small to visualise at low power so soon after infection under these conditions. The day 1 zero values were excluded from statistical analyses to prevent skewing of the data.

With the exception of L1 and L2, the number of inclusions per 10 thousand cells remained steady for the duration of the experiment (figure 4F). The number of L2 inclusions per 10 thousand cells remained the same from days 2 to 3, then doubled from day 3 to day 5. The number of L1 chlamydial inclusions per 10 thousand cells was higher than any other strain at day 2. It increased slightly from day 2 to 3, but the number of inclusions decreased substantially from days 3 to 5, and at day 5 there were less inclusions than at day 2.

In the HaCaT cells at 33°C, area occupied by chlamydia and inclusions per 10 thousand cells indicated a significant difference in the overall growth between strains (P = 0.024 and P < 0.001 respectively) (figure 5E and 5F). Overall, area occupied by chlamydia indicated a significant difference between L2 compared to E or US162 (P values 0.036 and 0.011 respectively). The number of inclusions per 10 thousand cells revealed significant differences between L2 and E (P = 0.014), as well as significant differences for US162 compared with all other strains (P < 0.001 for all except L3 where P = 0.028).

At 5 days post infection the number of serovar L2 inclusions was significantly different to E, L1 and L3 (P values 0.018, 0.029 and 0.001 respectively), but only 1 clinical isolate, US162 (P <0.001). There was no significant difference between L2 and the clinical isolates US151 and US197 (P values 0.355 and 0.088 respectively). However, when area occupied by chlamydia was used as an indicator of growth at 5 days post infection, serovar L2 was significantly different (P < 0.001) to all strains except L3, which was not quite significant (P = 0.056). L3 was also significantly different (P < 0.01) to all strains except L2. Null hypothesis 4 was rejected and alternate hypothesis 4 accepted.

Visual inspection of the fluorescent micrographs revealed a difference in the maximum inclusion size attained by different chlamydial strains in HaCaT cells at 33°C. Chlamydial inclusions begin small, but as the bacteria within inclusions replicate, the inclusions swell and increase in size. However, not all strains of *C. trachomatis* appeared to reach the same maximum size.

Null hypothesis 5: There is no difference in the size of chlamydial inclusions produced by different strains of *C. trachomatis* grown in HaCaT cells at 33°C.

Alternate hypothesis 5: Some strains of *C. trachomatis* produce larger inclusions than others when grown in HaCaT cells at 33°C.

The size of chlamydial inclusions was quantified by measuring the area (μm^2) of individual inclusions in HaCaT cells at 33°C from 2 to 5 days post infection. In figure 6, the median inclusion size, as indicated by area (μm^2) was plotted against the number of days post infection for each strain of *C. trachomatis*. At day 2, most inclusions were about 100μm^2. The L2 inclusions grew rapidly from days 2 to 4, and the L3 inclusions grew rapidly from day 3 to 4, while the other strains exhibited more moderate inclusion growth. There was however a sharp decline in the median inclusion size from days 4 to 5 for both L2 and L3. Despite the low median inclusion size, the maximum inclusion size for these strains at day 5 was still higher than the maximum inclusion size produced by any other strain. The data are skewed by the presence of numerous smaller inclusions at this time point. The spread of area values is plotted for each day post infection in figure 6.

The overall data indicated an extremely significant difference in inclusion size amongst the strains ($P < 0.001$), and post testing revealed extremely significant differences between most pairs of strains. There were also extremely significant differences between the strains at each day post infection ($P < 0.001$). The P values for individual strains summarized in table 2. Null hypothesis 5 was rejected and alternate hypothesis 5 accepted.

4.2 Transmission electron microscopy

TEM was used to investigate the ultrastructural effect that LGV and OG *C. trachomatis* had on their host cells, and to assess the replication cycle under conditions different to those described in the literature.

In HaCaT and ME-180 cells at 37°C, both biovars exhibited the typical biphasic chlamydial replication cycle comprising both EB and RB.

The spherical EB were approximately 350 nm in diameter with an electron-dense core of about 200 nm diameter. Within this core was a darker region surrounded by aggregates of electron dense material (figure 8A). The core was encased by a single 7nm membrane. The surrounding periplasmic space of 8-17 nm was enclosed by a prominent trilaminar outer envelope which was about 8 nm thick.

With maturation, the RBs are larger at almost 1μm in diameter and more pleomorphic in shape. The RB cell envelope exhibited a "ruffled-ballerina-skirt" (Peterson and de la Maza 1988) appearance with some RB having a region of well-defined double trilaminar cell envelope while undergoing binary fission (figure 8B). In this region the periplasmic space appeared septated with electron-dense structures perpendicular to the two membranes.

Figure 9A illustrates a membrane-bound chlamydial inclusion in the cytoplasm of the cell at 18 hours post infection. The infectious EB has already developed into a RB and undergone several rounds of binary fission. Eleven RBs are seen within this inclusion. The inclusion is located adjacent to the nucleus, and has been pushed aside and become crescent-shaped as the inclusion of replicating bacteria grew. By 24 hours post-infection some RB had already developed into EB, while others continue to replicate at the

periphery of the inclusion. At 36 hours post infection (Figure 9B) the inclusion occupied most of the cell. The nucleus had been pushed aside and the inclusion, which comprised a mixture of RB, intermediate bodies (IB) and EB, is surrounded by a thin layer of cytoplasm.

In the HaCaT cells at 33°C, serovar E replicated in the typical manner described above for HaCaT cells at 37°C, albeit slightly slower – EB were first seen at 36 hours post infection compared to 24 hours post infection at 37°C. With serovar L2, some intermediate bodies were present at 36 hours post infection, but EB were not detected. At 48 post infection, no EB were detected within the chlamydial inclusion, instead 2 EB were seen migrating through the cytoplasm in a non-membrane bound state (figure 10C). Both of these EB displayed the typical morphological characteristics and size of EB that were observed within inclusions.

The ultramicroscopic effect of *C. trachomatis* on their host cells was also investigated.

Uninfected ME-180 cervical cells were polygonal or round in shape, with some giant cells. Adjacent cells were connected by numerous desmosomal attachments. The spherical nucleus was centrally located and encapsulated by a thin ring of tonofilaments. Two or 3 nucleoli were present. In the cytoplasm, mitochondria were located in close proximity to the nucleus, while polyribosomes tended to be concentrated on the periphery of the cell. Several small vacuoles were also noted in the cytoplasm of uninfected cells.

In this cell line, infection with either serovar resulted in similar cytopathic changes within the host cell. At 1, 3 and 9 hours post-infection, organelle and cytoplasmic degeneration

were present. Figure 11B shows the cytoplasm of a serovar E infected ME-180 cell with a degenerate mitochondrion with sparse cristae and a lucent matrix; whorled membranous myelin bodies indicative of involuting mitochodria, and regions of cytoplasmic lysis.

Although chlamydia were usually compartmentalised within an inclusion in infected cells, in some instances there was no distinct division between the host cell cytoplasm and inclusion matrix with its associated chlamydial particles. Figure 11C illustrates the close association between several mitochondria and chlamydial RB and EB. In figure 11D two EB appear to migrate through the cytoplasm towards the host cell plasmalemma.

At 48 h after serovar L2 infection, an ME-180 cell housed numerous EB within membrane-bound vesicles (figure 12A, 12B). Since this cell only had one small immature inclusion with RB only, it is likely that these EB were taken up by the cell after an inclusion in a neighbouring cell burst. At this time point some mitochondrial pathology was noted in a serovar L2 infected cell with a non-membrane bound EB in the cytoplasm (figure 12C). Mitochondria were swollen, the cristae were fragmented and electron dense deposits were present in the mitochondrial matrix.

Uninfected HaCaT keratinocytes at 37 or 33°C were polygonal in shape, with a centrally located nucleus containing 1 to 4 nucleoli. Invaginations of the nucleus were common as well as regions of nucleoli margination, which are indicative of active protein synthesis. The cytoplasm contained numerous mitochondria and polyribosomes, as well as a few small vacuoles. Tonofilaments were usually located in regions of cell-to-cell attachments, and adjacent cells abutted on each other with numerous projections and desmosomal attachments.

Cytopathic changes were noted in HaCaT cells at 37°C as early as 1 hour post infection. With serovar E infection the mitochondrion was the main organelle involved. At 1 hour post infection swollen mitochondria with a lucent matrix and reduced cristae were noted. This phenomenon was not observed from 3 to 24 hours post infection but appeared again at 36 and 48 hours post infection (figure 13C). This corresponds with the time at which new immature inclusions with RB only were beginning to form. This gross mitochondrial pathology was not observed in serovar L2 infected nor in uninfected cell monolayers. In serovar E infected monolayers, myelin figures indicative of degenerate mitochondria were present from 3 hours post infection (figure 13B). In contrast, organelle integrity in serovar L2 infected monolayers was maintained for longer – myelin figures were first observed at 18 hours post infection (figure 14B). However, the markedly swollen mitochondria described for serovar E infected cells were not observed in serovar L2 infected monolayers at any of the times tested.

Many chlamydial inclusions contained a diffuse electron dense granular substance in a lucent matrix. Vacuoles which appeared to contain this same substance were observed. In figure 14C a serovar E infected HaCaT cell at 37°C is captured releasing the contents of one such vacuole into the extracellular space.

There were no noticeable morphological differences between the uninfected HaCaT cells incubated at 33°C versus those incubated at 37°C.

Apart from the formation of inclusions, *C. trachomatis* did not exert noticeable ultrastructural pathological changes on HaCaT cells at 37°C during the time period investigated. Some myelin figures were present in the early stages post infection, but

generally mitochondria were intact. Like the HaCaT and ME-180 cells, mitochondria were located in the vicinity of the chlamydial inclusion.

Mitotic figures were observed in the ME-180 cell monolayers and HaCaT cell monolayers at both 37 and 33°C regardless of whether or not the monolayers had been infected.

4.3 MTT assay

The MTT assay was used to quantify the level of mitochondrial activity in chlamydia infected cells relative to uninfected cells for 48 hours post infection. Data are expressed as a percentage of the level of mitochondrial activity in uninfected cells. The etoposide treated positive control exhibited the expected decrease in percentage mitochondrial activity over 48 hours under all experimental conditions (figure 15). These data are excluded from the analyses. Data from the uninfected untreated negative control is included since it represents a baseline of 100% mitochondrial activity under the conditions tested.

Null hypothesis 6: There is no difference in the level of mitochondrial activity in ME-180 cell at 37°C when infected with various strains of *C. trachomatis* compared to each other and uninfected cells

Alternate hypothesis 6: There is a difference in the level of mitochondrial activity in ME-180 cell at 37°C when infected with various strains of *C. trachomatis* compared to each other and uninfected cells

Chlamydia infected ME-180 cell monolayers generated 92 to 102% mitochondrial activity compared to the negative control. There was no overall significant difference in the level of mitochondrial activity amongst the strains and negative control ($P = 0.102$). Nor was there a significant difference amongst mitochondrial activity assessed at any of the time points measured. Null hypothesis 6 was accepted and alternate hypothesis 6 rejected.

Null hypothesis 7: There is no difference in the level of mitochondrial activity in HaCaT cells at 37°C when infected with various strains of *C. trachomatis* compared to each other and uninfected cells

Alternate hypothesis 7: There is a difference in the level of mitochondrial activity in HaCaT cells at 37°C when infected with various strains of *C. trachomatis* compared to each other and uninfected cells

In the HaCaT cells at 37°C the level of mitochondrial activity 1 hour after *C. trachomatis* infection was 84%, 90% and 93% for serovars E, L2 and L3 respectively, compared to the negative control, which by definition, produced 100% mitochondrial activity. Differences amongst the groups was significant at this time point ($P = 0.001$). Serovars E and L2 were significantly different to uninfected cells ($P < 0.001$ and $P = 0.027$ respectively), but serovar L3 was not ($P = 0.243$). There was also a slight significant difference between serovars E and L3 ($P = 0.049$), but not serovars E and L2 ($P = 0.360$). Mitochondrial activity was partially restored by 3 hours post-infection and remained between 92% and 105% compared to uninfected cells for all chlamydial strains tested from 3 to 48 hours post infection. The difference in mitochondrial activity, regardless of the time point post infection at which this was measured, reached significance ($P < 0.001$). Serovar E was

significantly different to the uninfected cells ($P < 0.01$), but no other comparisons reached significance. Null hypothesis 7 was rejected and alternate hypothesis 7 accepted.

Null hypothesis 8: There is no difference in the level of mitochondrial activity in HaCaT cells at 33°C when infected with various strains of *C. trachomatis* compared to each other and uninfected cells

Alternate hypothesis 8: There is a difference in the level of mitochondrial activity in HaCaT cells at 33°C when infected with various strains of *C. trachomatis* compared to each other and uninfected cells

In the HaCaT cells at 33°C, the level of mitochondrial activity in chlamydia infected cells at various time points post infection ranged from 94% to 104%. No significant differences were detected amongst the overall levels of mitochondrial activity ($P = 0.424$) or at any of the time points tested. Null hypothesis 8 was accepted and alternate hypothesis 8 rejected.

4.4 Lactate dehydrogenase detection

ME-180 and HaCaT cells were infected with *C. trachomatis* and incubated at 37°C only for the ME-180 cells, and 37 and 33°C for the HaCaT cells, and the percentage cytotoxicity assessed each day post-infection for 5 days. In figure 16, the percentage cytotoxicity is plotted against days post infection.

Null hypothesis 9: *C. trachomatis* is equally cytotoxic to ME-180 cells at 37°C, HaCaT cells at 37°C and HaCaT cells at 33°C.

Alternate hypothesis 9: *C. trachomatis* more cytotoxic to some cell lines tested than others.

There was an overall significant difference in the median level of *C. trachomatis* induced cytotoxicity amongst cell lines and temperatures ($P = 0.006$). There was a slight significant difference between the HaCaT cells at 37°C and 33°C ($P < 0.05$), and no significant difference between the ME-180 cells and HaCaT cells at 37°C. Null hypothesis 9 was accepted and alternate hypothesis 9 rejected.

In both cell lines, at both temperatures, the median percentage cytotoxicity was close to 0 for the first 2 days post-infection (figure 16). In the HaCaT cells at 33 and 37°C, the median percentage cytotoxicity did not exceed 2% and 4% respectively, while *C. trachomatis* had a more dramatic effect on the ME-180 cell line.

Null hypothesis 10: All strains of *C. trachomatis* are equally cytotoxic to ME-180 cells at 37°C.

Alternate hypothesis 10: Some strains of *C. trachomatis* are more cytotoxic to ME-180 cells at 37°C than others.

In the ME-180 cells, the initial level of cytotoxicity was about 1%. At day 3, there was a slight increase in the level of cytotoxicity for most strains. By the fifth day post-infection, serovar L2 had induced 11.9 % cytotoxicity on the cell line, in contrast to all the other strains which exerted a protective effect, indicated by the negative percentage cytotoxicity.

The overall percentage cytotoxicity exerted on ME-180 cells at 37°C did not reach significance ($P = 0.283$). But when the effect of the *C. trachomatis* strains was assessed on a day-by-day basis there was a significant difference ($P < 0.001$) amongst the strains in this

cell line 5 days post infection. Serovar L2 was significantly different to all 3 clinical isolates. Post-tests indicated a significant difference between serovar L2 and all 3 clinical isolates ($P < 0.01$), but not the other strains. Null hypothesis 10 was rejected and alternate hypothesis 10 accepted.

In the HaCaT cells, the median percentage cytotoxicity approximated zero for the first 3 days after infection, and even at 5 days post infection, the median percentage cytotoxicity did not exceed 2 and 4 % for the HaCaT cells at 33 and 37°C respectively.

Null hypothesis 11: All strains of *C. trachomatis* are equally cytotoxic to HaCaT cells at 37°C.

Alternate hypothesis 11: Some strains of *C. trachomatis* are more cytotoxic to HaCaT cells at 37°C than others.

In general there are differences in the percentage cytotoxicity exerted on HaCaT cells at 37°C by the strains of *C. trachomatis* tested. The overall median percentage cytotoxity was 4%. If only 4% of cells in an area of approximately $30mm^2$ (area of one well in a 96 well plate) in the skin lyse and die this is unlikely to cause a noticeable ulcer. US162 produced significantly less cytotoxicity than serovar E or L3 (P values 0.016 and 0.049). Null hypothesis 11 was rejected and alternate hypothesis 11 was accepted.

Null hypothesis 12: All strains of *C. trachomatis* are equally cytotoxic to HaCaT cells at 33°C.

Alternate hypothesis 12: Some strains of *C. trachomatis* are more cytotoxic to HaCaT cells at 33°C than others.

In the HaCaT cells at 33°C differences in percentage cytotoxicity amongst the strains was not quite significant (P = 0.053). Null hypothesis 12 was accepted and alternate hypothesis 12 rejected.

4.5 TUNEL Assay

The TUNEL assay was used to investigate the spatial relationship between chlamydia infected cells and cells undergoing cell death.

Figure 17 illustrates the TUNEL assay controls for the ME-180 cell line. Figure 17A indicates the DNAase treated positive control. Note the presence of numerous brown DAB positive nuclei (arrow heads). Apoptotic cells are also present. The nuclei of these cells are smaller and darker than the cells which were DAB positive due to DNAase treatment. The TUNEL negative control (figure 17B) omits the TdT enzyme; no dark brown DAB positive nuclei are present. The uninfected cell monolayer (figure 17C) demonstrates only a few DAB positive nuclei as would be expected in normal cell turnover. The controls for the HaCaT cell line at 37°C and 33°C are similar (not shown).

In both the ME-180 cells and HaCaT cells at 37°C, more DAB positive cells were observed 2 days after infection with the LGV reference strains and clinical isolates than with the serovar E OG strain. Images of light micrographs and fluorescent micrographs of the same field of view indicated that cells with DAB positive nuclei were often located immediately adjacent to infected cells (figure 18). This was occasionally observed in

serovar E infected ME-180 or HaCaT cell monolayers. Infected cells with a DAB positive nucleus were also observed.

With the HaCaT cells at 33°C, chlamydial inclusions at day 2 were small for all strains tested. There was about the same number of DAB positive cells in the infected and uninfected monolayers. When the incubation step was extended to 5 days, the inclusions were larger, but there was still no increase in the number of DAB positive cells except for serovar L3 which exhibited a slight increase in the number of DAB positive cells, while the serovar E OG strain exhibited a slight decrease.

At high magnification (X 1000), small non-nuclear DAB positive particles were observed in ME-180 and HaCaT cells monolayers grown at 37°C, but not in HaCaT cells at 33°C. These particles appeared to be housed within the chlamydial inclusion and had a diameter of about 0.7 μm (figure 19).

4.6 Caspase detection

The caspase assay coupled with Transwell® permeable inserts was used to elucidate whether chlamydia-induced cytotoxicity occurred in infected and neighbouring cells alone, or whether *C. trachomatis* infection could cause apoptotic activity in uninfected cells over a distance. This was assessed in ME-180 and HaCaT cells at 37°C, as well as HaCaT cells at 33°C.

Figure 20 illustrates caspase positive cells in uninfected cell monolayers. The cells in C, D, G, H, K and L have been exposed to chlamydia-infected cells via shared culture

medium across a permeable membrane. The cells in A, E and I were exposed to uninfected cells, while the cells in B, F and J were treated with the apoptotic agent, etoposide.

Under all conditions tested, the etoposide treated positive controls housed at least 10 times the number of caspase positive cells observed in the untreated unexposed negative control. With the ME-180 cells, the average number of caspase positive cells per 200 X field of view was 1.8 and 2.7 for serovar E and L2 respectively, compared to 1.0 for the negative control. With the HaCaT cells at 37°C there were 1.9 and 3.1 caspase positive cells for serovars E and L2 respectively, compared to 1.1 for the negative control. In the HaCaT cells at 33°C there was an average of between 1 and 2 caspase positive cells per 200 X field of view for the negative control and both serovar E and L2. These results indicate that chlamydia-infected ME-180 and HaCaT cells at 37°C may exert a cytotoxic effect on cells over a distance via a secreted molecule. This is not so for the HaCaT cells as 33°C.

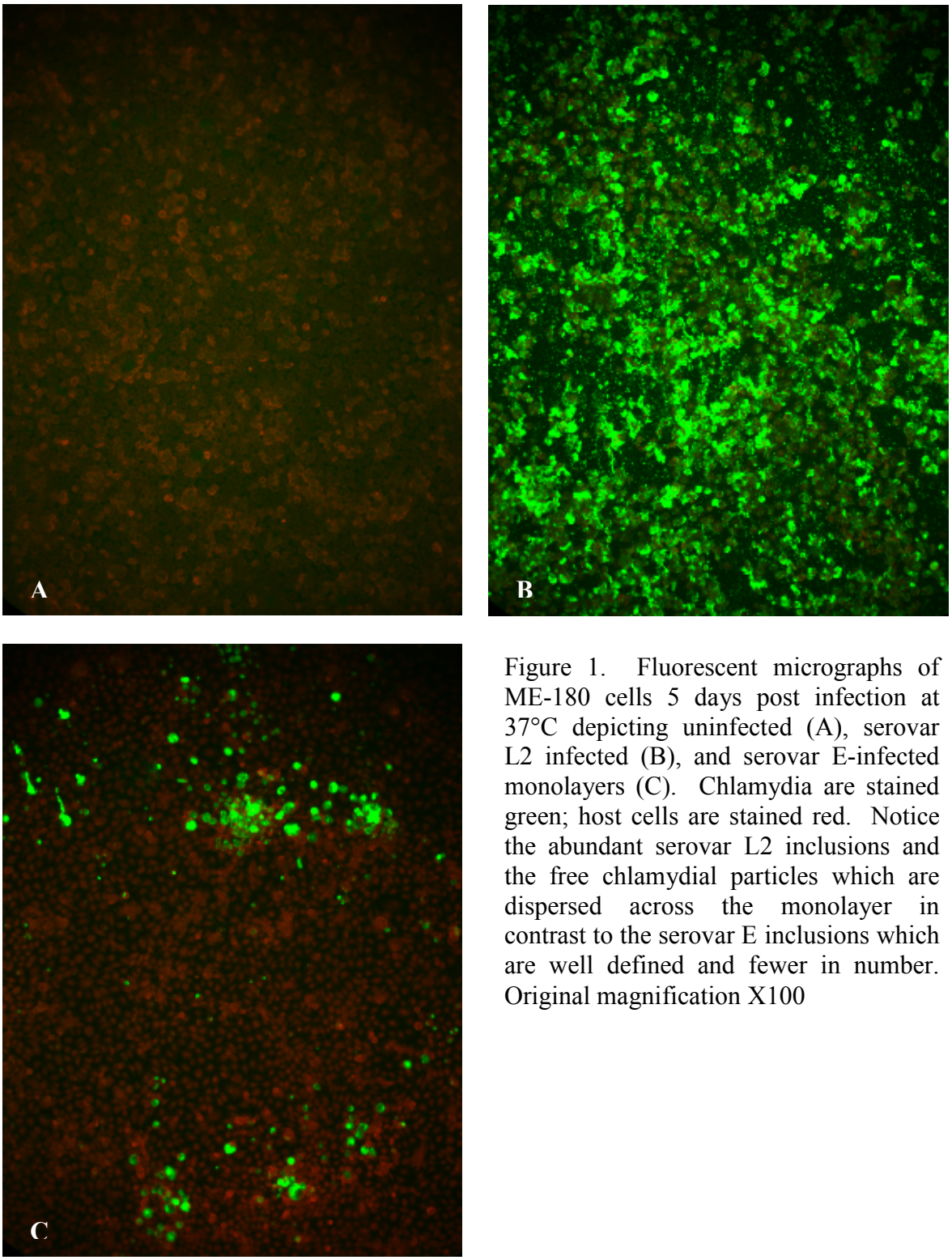

Figure 1. Fluorescent micrographs of ME-180 cells 5 days post infection at 37°C depicting uninfected (A), serovar L2 infected (B), and serovar E-infected monolayers (C). Chlamydia are stained green; host cells are stained red. Notice the abundant serovar L2 inclusions and the free chlamydial particles which are dispersed across the monolayer in contrast to the serovar E inclusions which are well defined and fewer in number. Original magnification X100

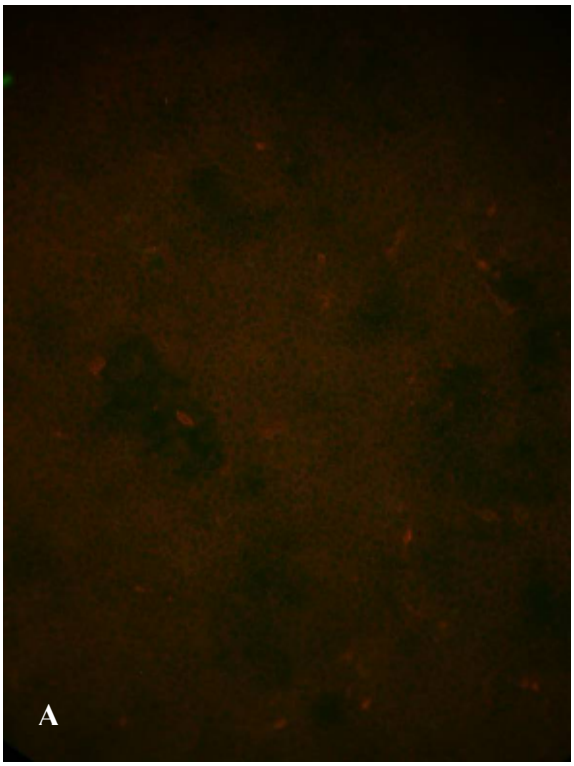

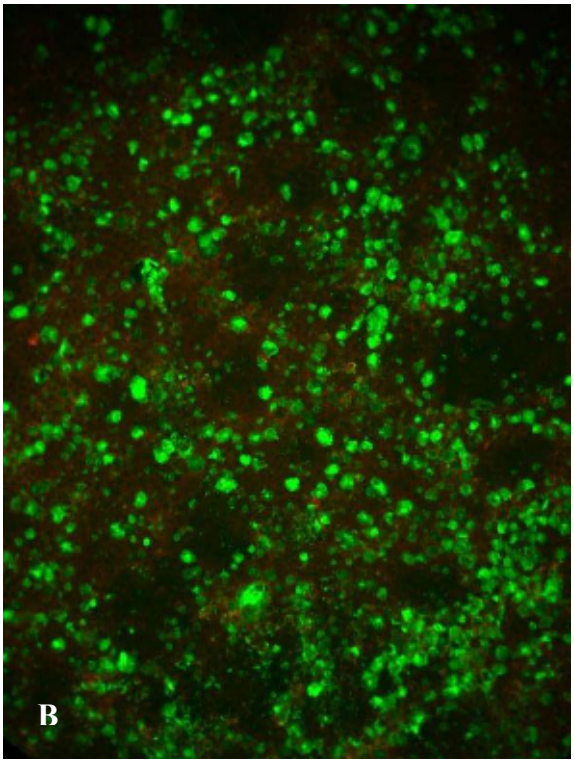

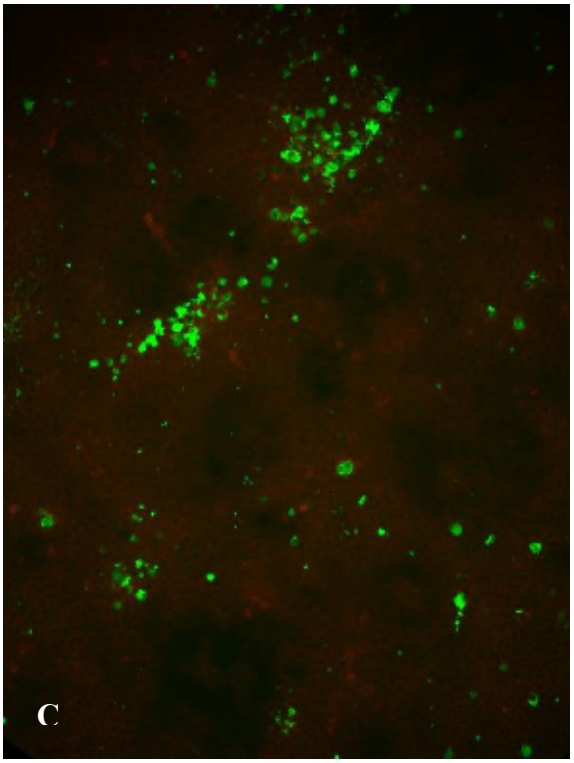

Figure 2. Fluorescent micrographs of HaCaT cells 5 days post infection at 37°C depicting uninfected (A), serovar L2 infected (B), and serovar E-infected monolayers (C). Chlamydia are stained green; host cells are stained red. Notice the abundant serovar L2 inclusions with some free chlamydial particles compared to the relatively few, well defined serovar E inclusions. Original magnification X100

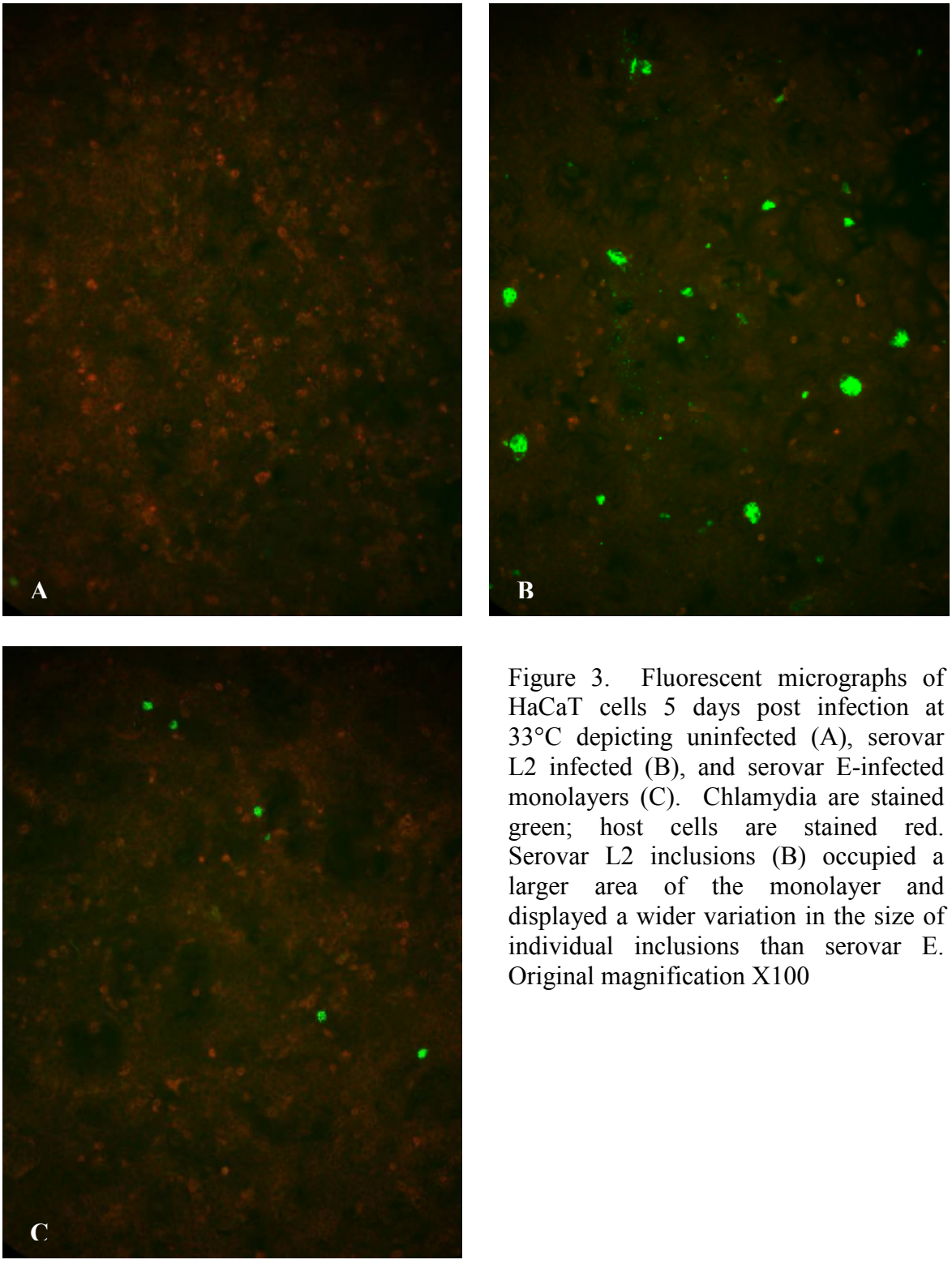

Figure 3. Fluorescent micrographs of HaCaT cells 5 days post infection at 33°C depicting uninfected (A), serovar L2 infected (B), and serovar E-infected monolayers (C). Chlamydia are stained green; host cells are stained red. Serovar L2 inclusions (B) occupied a larger area of the monolayer and displayed a wider variation in the size of individual inclusions than serovar E. Original magnification X100

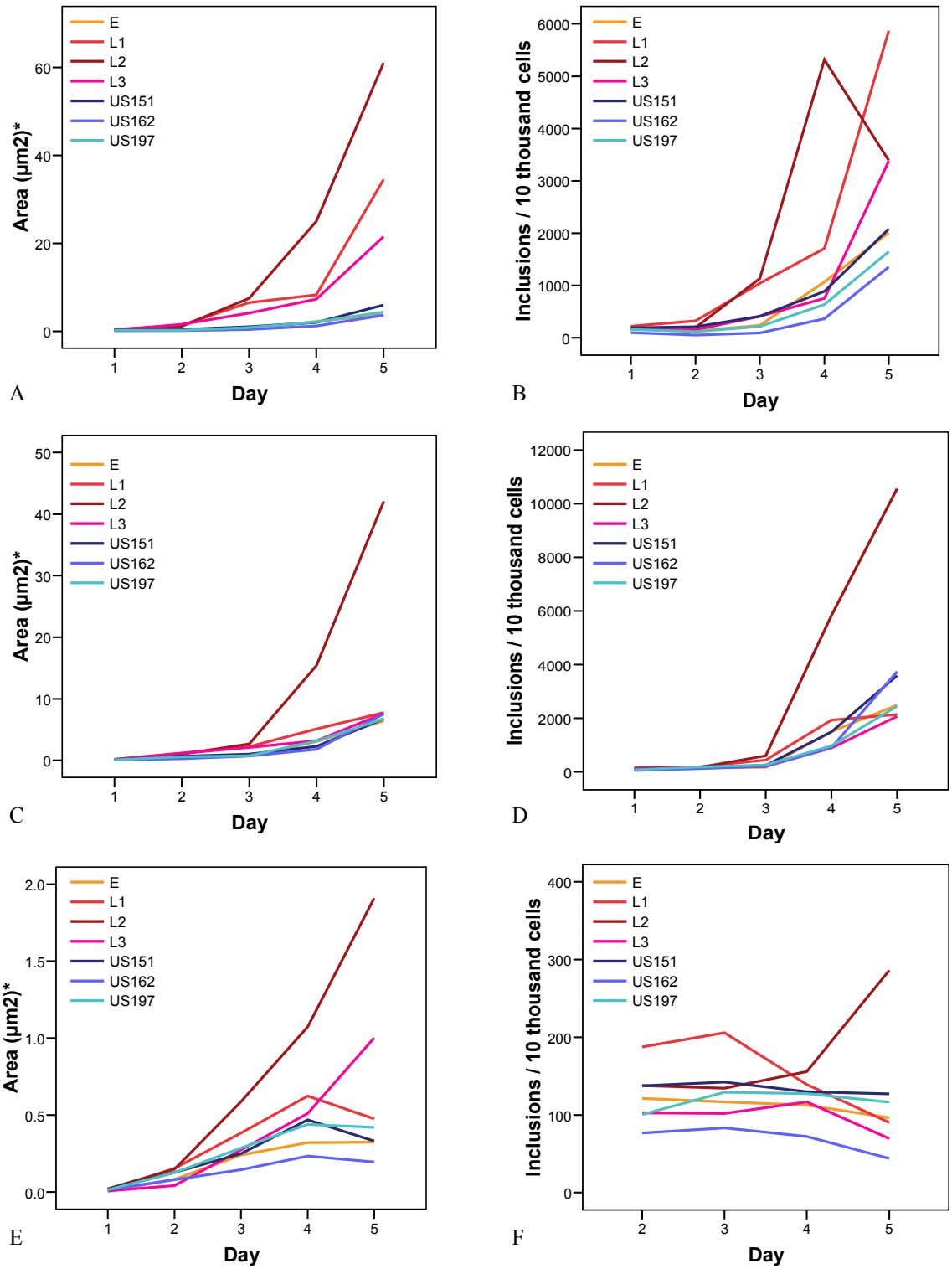

Figure 4. Chlamydial growth curves as indicated by mean area occupied by chlamydia (A, C, E), and mean number of inclusions per 10 thousand cells (B, D, F) in ME-180 cells at 37°C (A, B), HaCaT cells at 37°C (C, D), and HaCaT cells at 33°C (E, F).
* Area occupied by chlamydia per 10 thousand cells

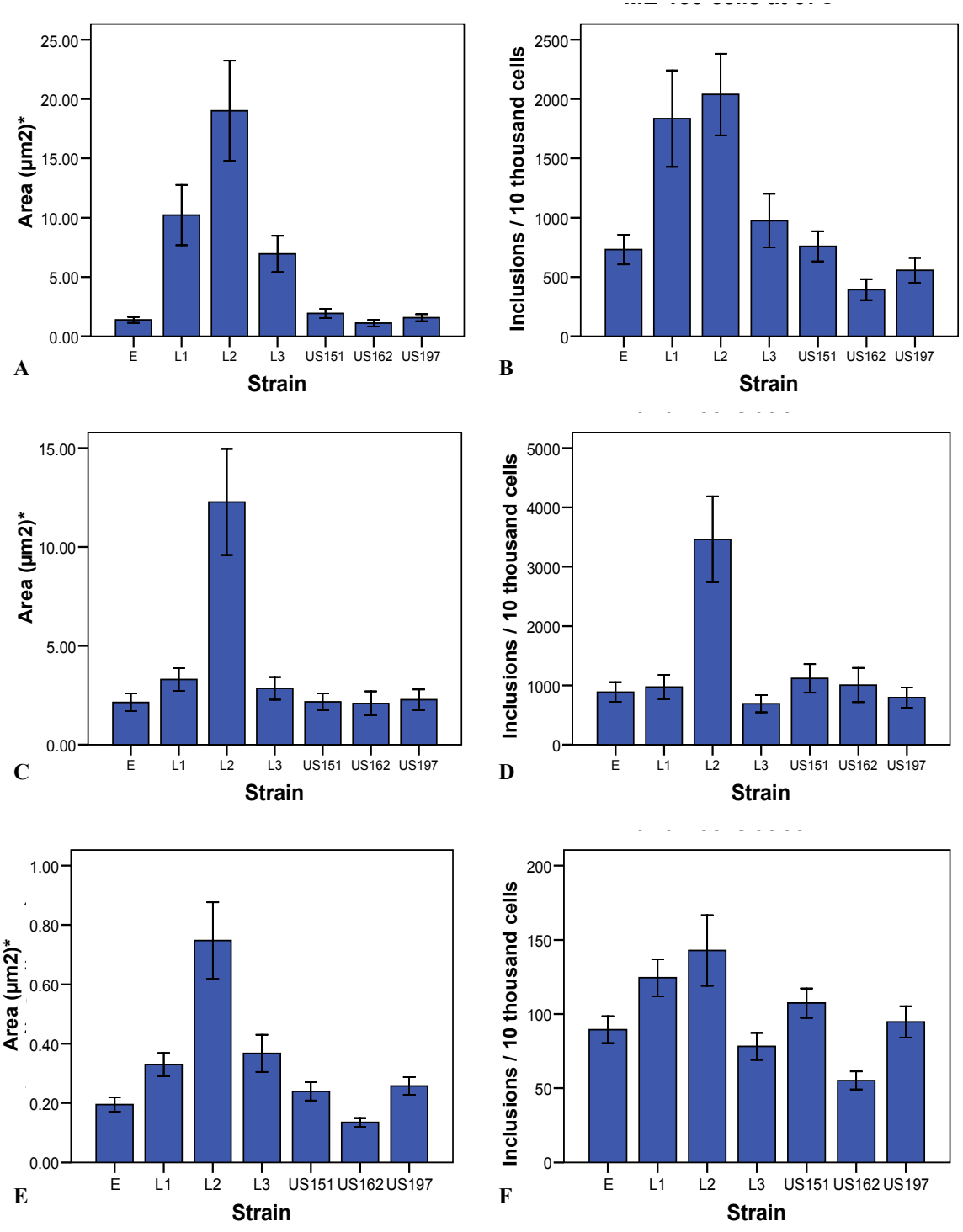

Figure 5. Overall chlamydial growth as indicated by mean area occupied by chlamydia (A, C, E) and number of inclusions per 10 thousand cells (B, D, F) in ME-180 cells at 37°C (A, B), HaCaT cells at 37°C (C, D), and HaCaT cells at 33°C (E, F). Error bars represent ± 1 standard error of the mean.

* Area occupied by chlamydia per 10 thousand cells

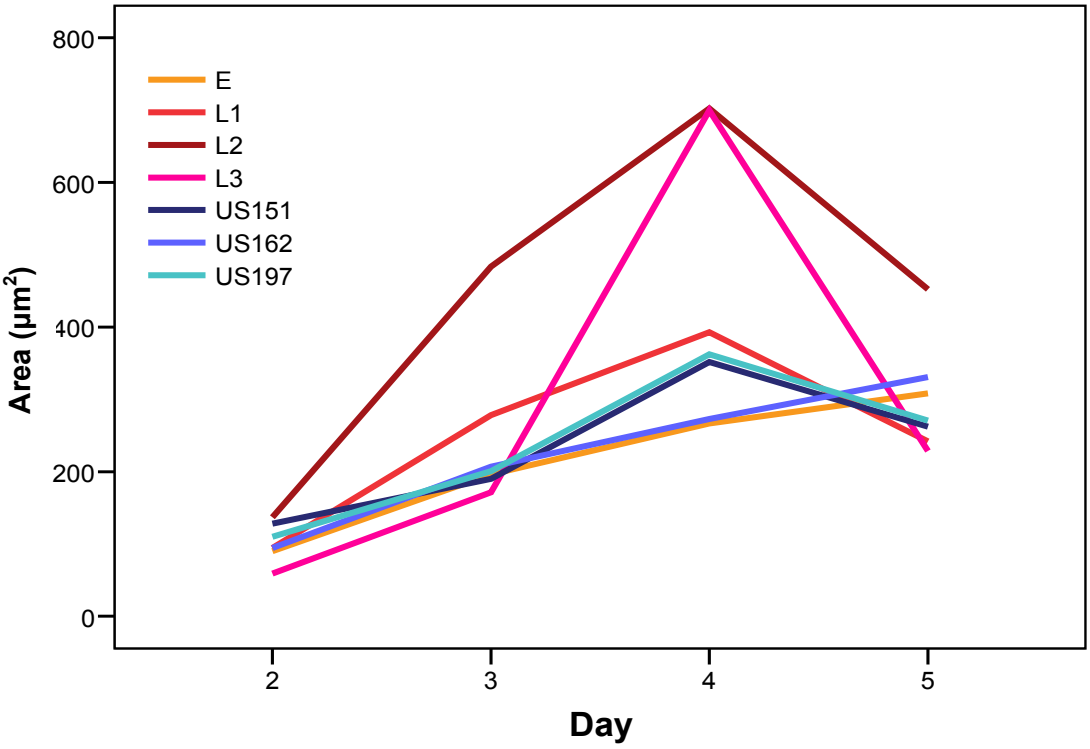

Figure 6. Median size of chlamydial inclusions in HaCaT cells at 33°C from 2 to 5 days post infection

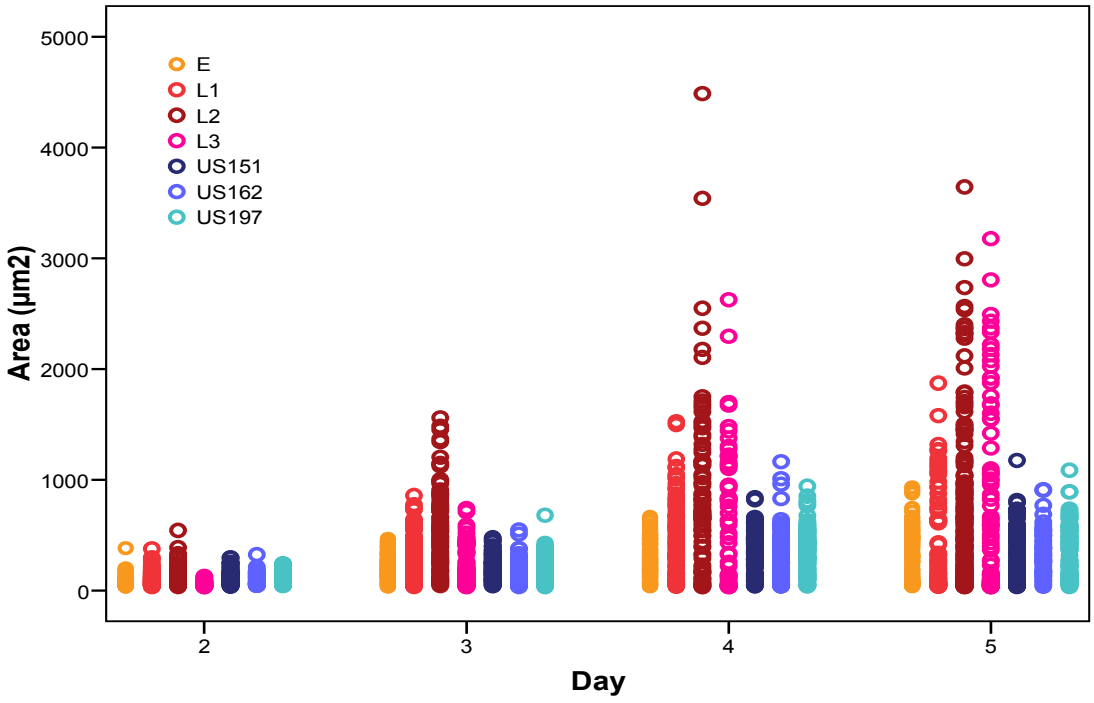

Figure 7. Size of individual chlamydial inclusions in HaCaT cells at 33°C from 2 to 5 days post infection

Table 3. Significance levels for chlamydial inclusion size in HaCaT cells at 33°C

		E	L1	L2	L3	US151	US162	US197
Overall	E		***	***	***	***	***	***
	L1	***		***	ns	***	ns	Ns
	L2	***	***		***	***	***	***
	L3	***	ns	***		***	ns	**
	US151	***	***	***	***		***	**
	US162	***	ns	***	ns	***		***
	US197	***	ns	***	**	**	***	
Day 2	E		ns	**	**	ns	ns	Ns
	L1	ns		**	***	ns	ns	Ns
	L2	**	**		***	ns	ns	Ns
	L3	**	***	***		***	**	***
	US151	ns	ns	ns	***		ns	Ns
	US162	ns	ns	ns	**	ns		Ns
	US197	ns	ns	ns	***	ns	ns	
Day 3	E		ns	***	ns	ns	ns	Ns
	L1	ns		***	ns	ns	ns	Ns
	L2	***	***		***	***	***	***
	L3	ns	ns	***		ns	ns	Ns
	US151	ns	ns	***	ns		ns	Ns
	US162	ns	ns	***	ns	ns		Ns
	US197	ns	ns	***	ns	ns	ns	
Day 4	E		*	***	***	ns	ns	Ns
	L1	*		***	ns	ns	ns	Ns
	L2	***	***		ns	***	***	***
	L3	***	ns	ns		ns	**	Ns
	US151	ns	ns	***	ns		ns	Ns
	US162	ns	ns	***	**	ns		Ns
	US197	ns	ns	***	ns	ns	ns	
Day 5	E		ns	ns	ns	ns	ns	Ns
	L1	ns		ns	ns	ns	ns	Ns
	L2	ns	ns		ns	*	ns	*
	L3	ns	ns	ns		ns	ns	Ns
	US151	ns	ns	*	ns		ns	Ns
	US162	ns	ns	ns	ns	ns		Ns
	US197	ns	ns	*	ns	ns	ns	

ns, not significant
* $P < 0.05$
** $P < 0.01$
*** $P < 0.001$

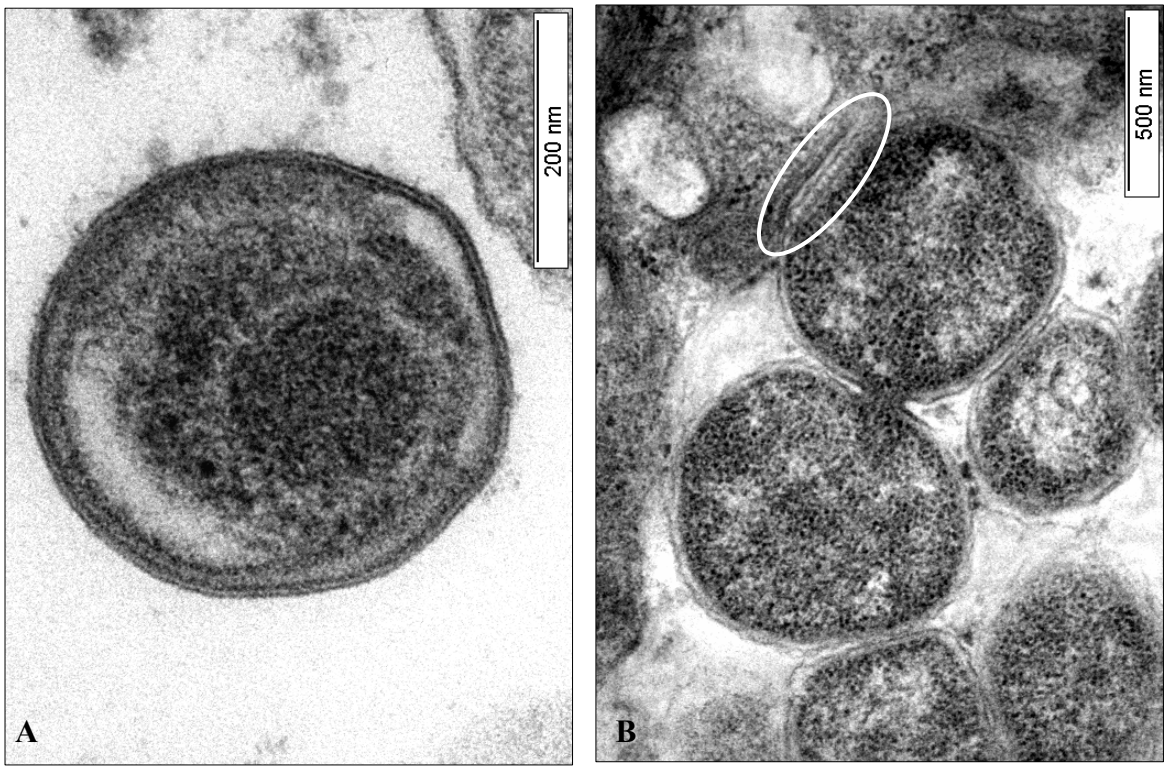

Figure 8. TEM micrographs showing the ultrastructure of a *C. trachomatis* EB (A) and a RB undergoing binary fission (B). Notice the well defined structure in the region of the RB attached to the inclusion membrane (circled)

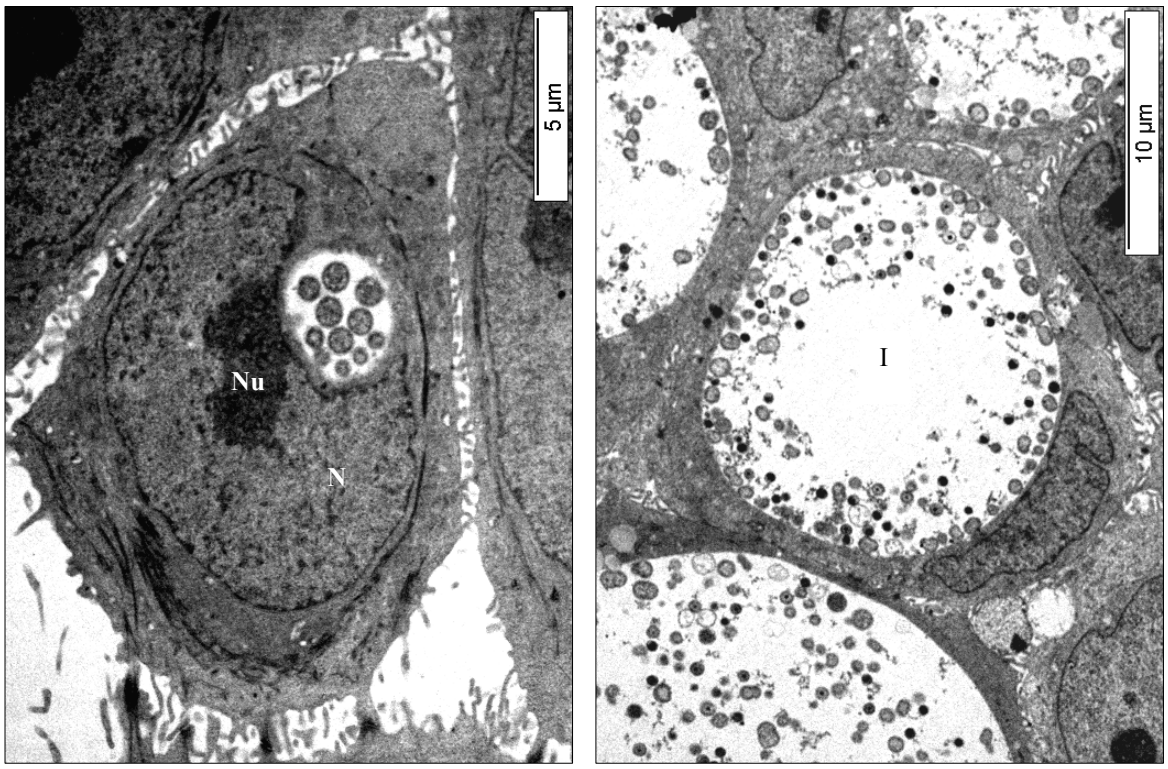

Figure 9. TEM micrographs of *C. trachomatis* infected cells at 37°C. (A) ME-180 cell 18 h after serovar E infection, and (B) HaCaT cells 36 h after serovar L2 infection. Notice the invaginated inclusion with RB undergoing binary fission in (A) compared to the inclusion containing both RB and EB has taken over the cell.
I, inclusion; N, nucleus; Nu, nucleolus

Figure 9. TEM micrographs of *C. trachomatis* infected cells at 37°C. (A) ME-180 cell 18 h after serovar E infection, and (B) HaCaT cells 36 h after serovar L2 infection.
Nu, nucleus, I, chlamydial inclusion

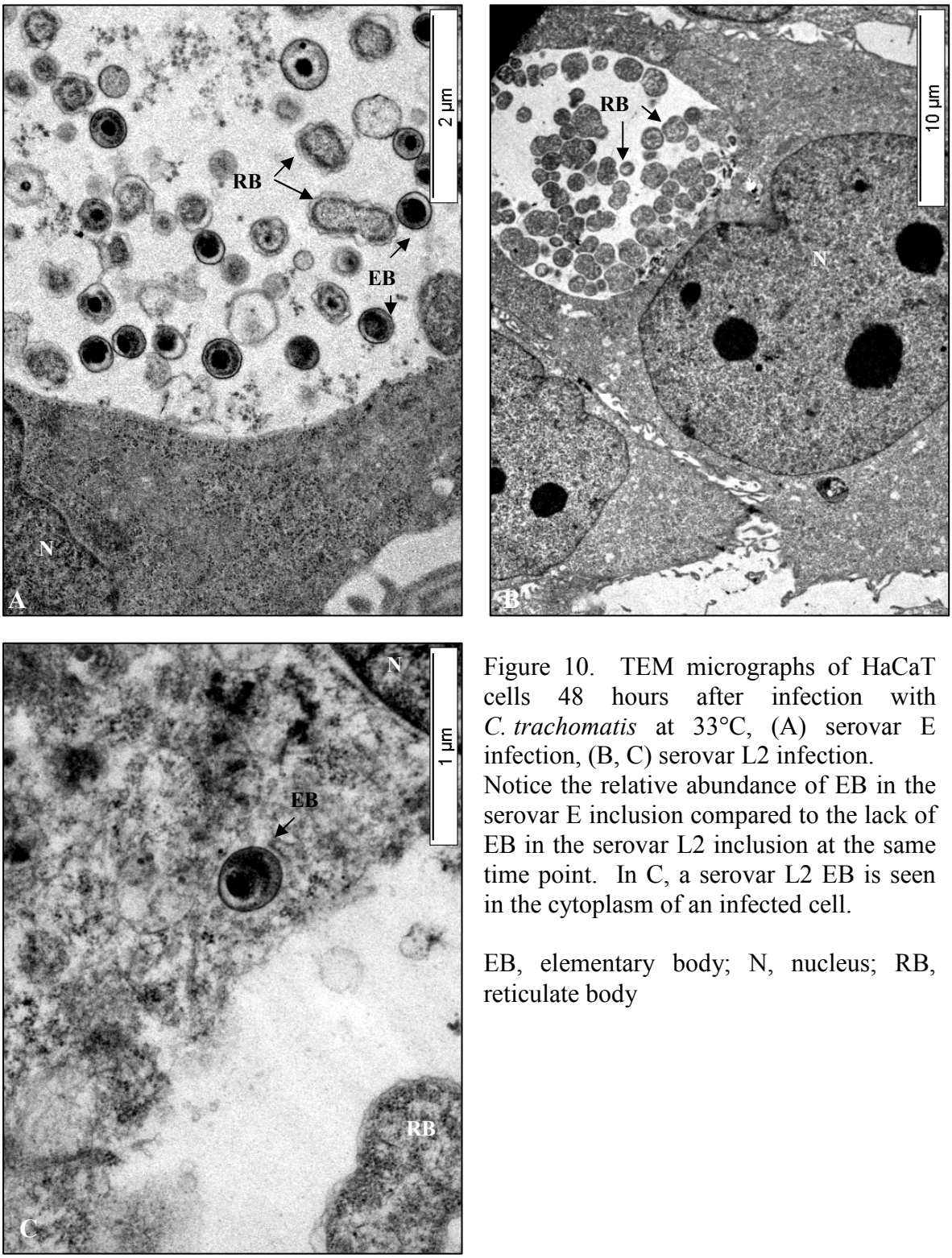

Figure 10. TEM micrographs of HaCaT cells 48 hours after infection with *C. trachomatis* at 33°C, (A) serovar E infection, (B, C) serovar L2 infection. Notice the relative abundance of EB in the serovar E inclusion compared to the lack of EB in the serovar L2 inclusion at the same time point. In C, a serovar L2 EB is seen in the cytoplasm of an infected cell.

EB, elementary body; N, nucleus; RB, reticulate body

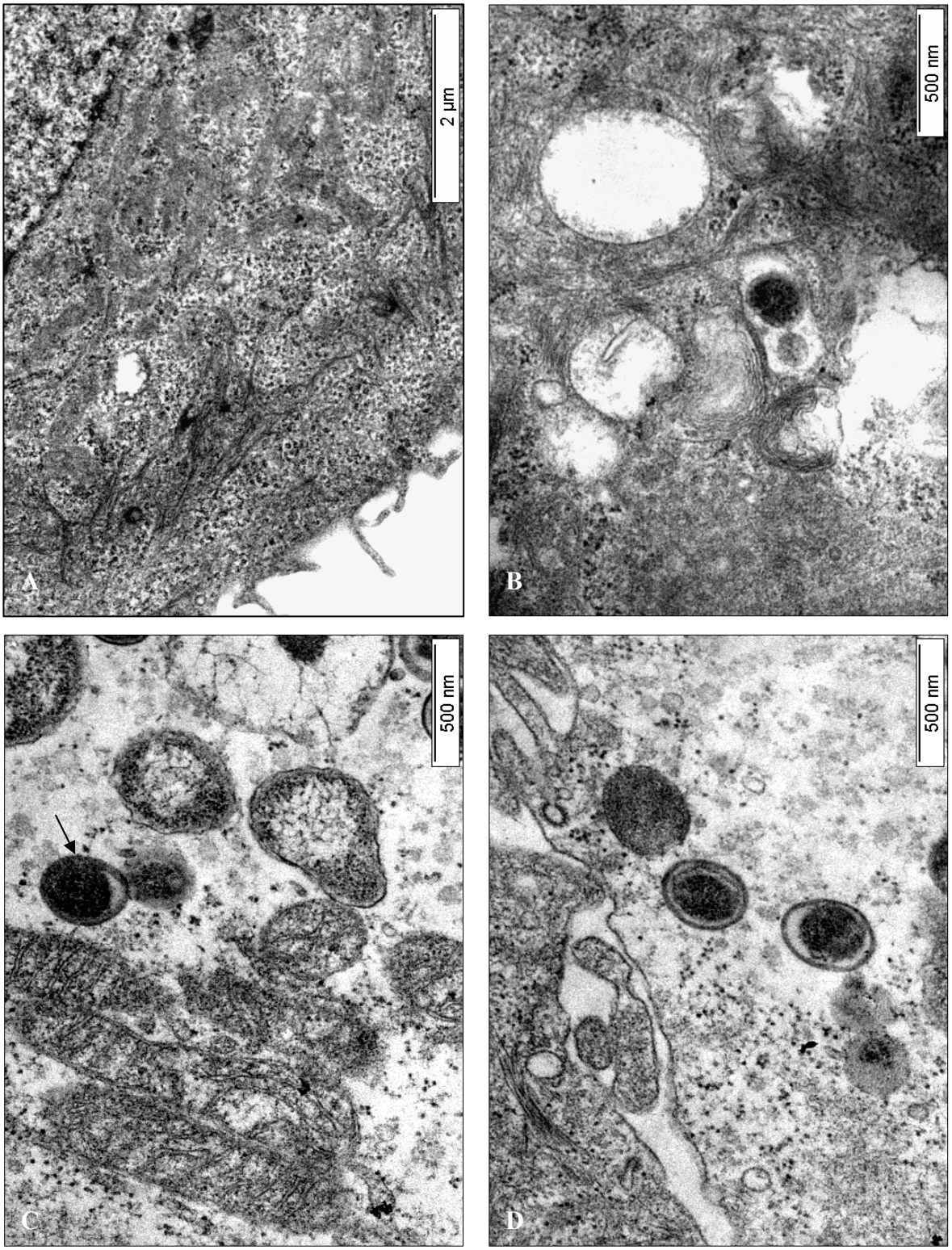

Figure 11. TEM micrographs of ME-180 cells at 37°C illustrating the cytoplasm of an uninfected cell (A) and *C. trachomatis* serovar E infected cells at 1 hour (B) and 36 hours (C, D) post infection.
Notice the cytopathic changes in the cytoplasm of cells at 1 h post infection (B) compared to the uninfected cells (A). In C and D, *C. trachomatis* exists in a non-membrane bound state. In C, the EB and RB are in close proximity to numerous intact mitochondria (M). In D, 2 EB appear to migrate through the cytoplasm towards the plasmalemma of their host cell. EB, elementary body; CL, cytoplasmic lysis, My, myelin figure, N, nucleus; RB, reticulate body

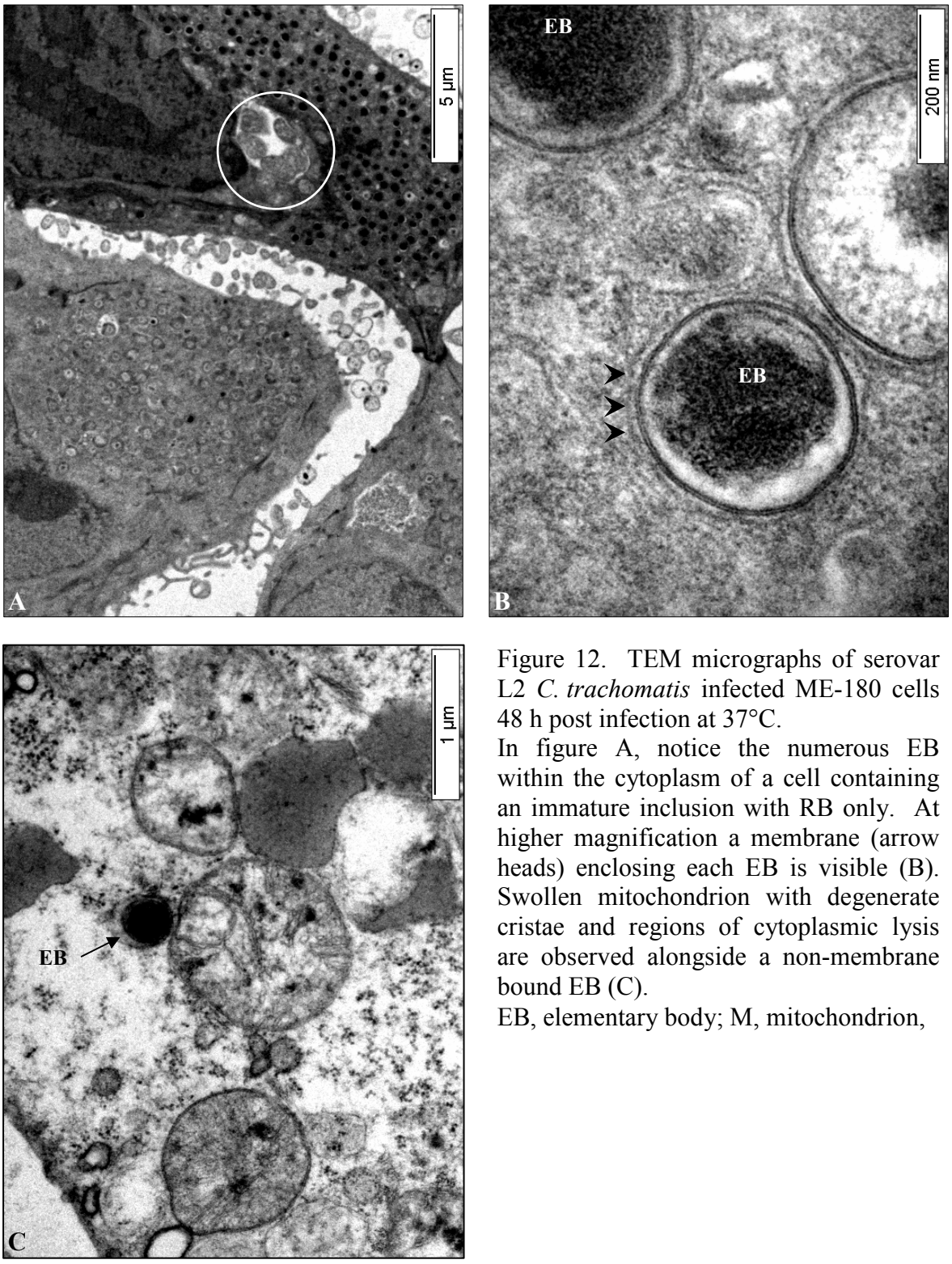

Figure 12. TEM micrographs of serovar L2 *C. trachomatis* infected ME-180 cells 48 h post infection at 37°C.
In figure A, notice the numerous EB within the cytoplasm of a cell containing an immature inclusion with RB only. At higher magnification a membrane (arrow heads) enclosing each EB is visible (B). Swollen mitochondrion with degenerate cristae and regions of cytoplasmic lysis are observed alongside a non-membrane bound EB (C).
EB, elementary body; M, mitochondrion,

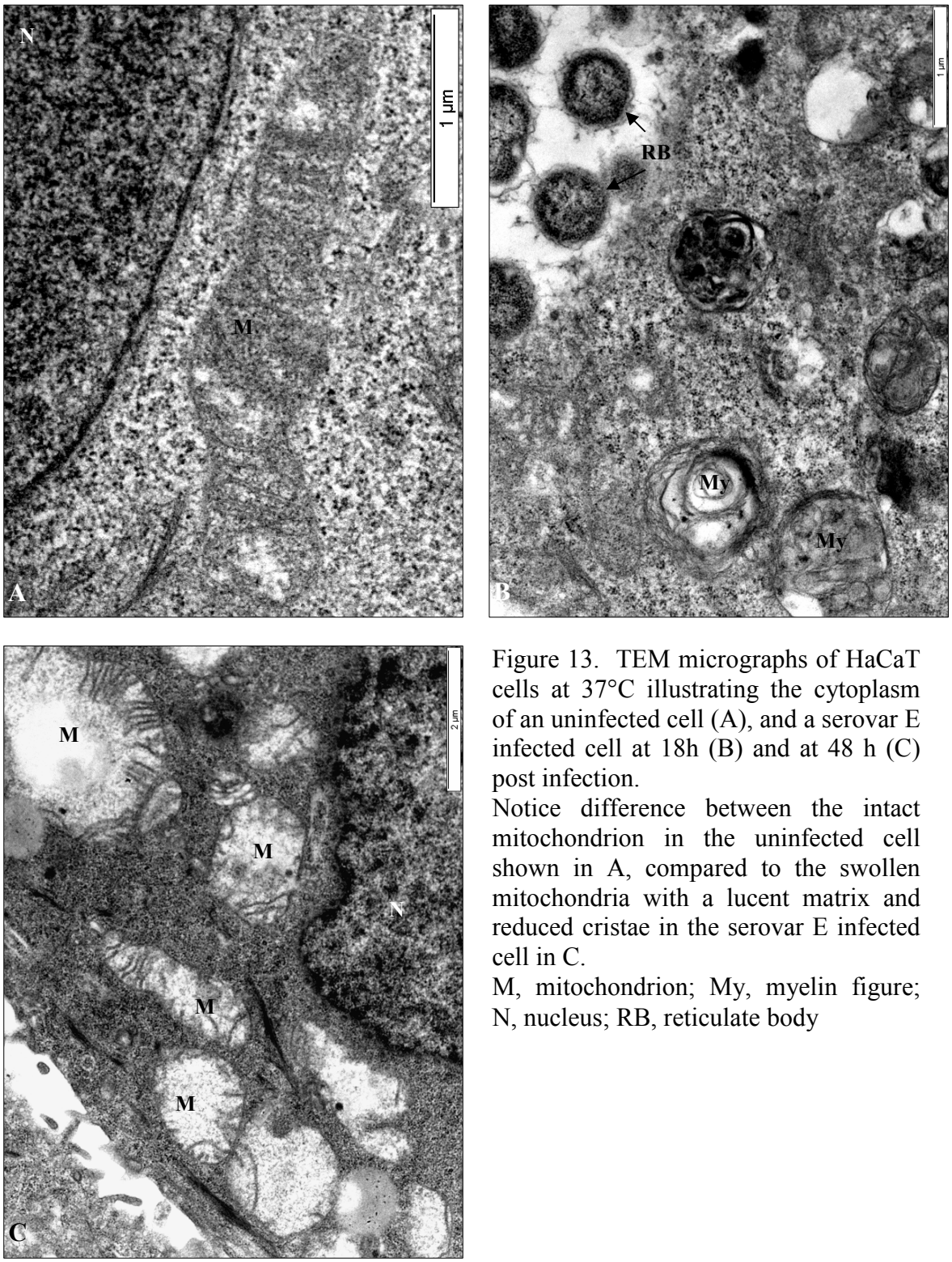

Figure 13. TEM micrographs of HaCaT cells at 37°C illustrating the cytoplasm of an uninfected cell (A), and a serovar E infected cell at 18h (B) and at 48 h (C) post infection.
Notice difference between the intact mitochondrion in the uninfected cell shown in A, compared to the swollen mitochondria with a lucent matrix and reduced cristae in the serovar E infected cell in C.
M, mitochondrion; My, myelin figure; N, nucleus; RB, reticulate body

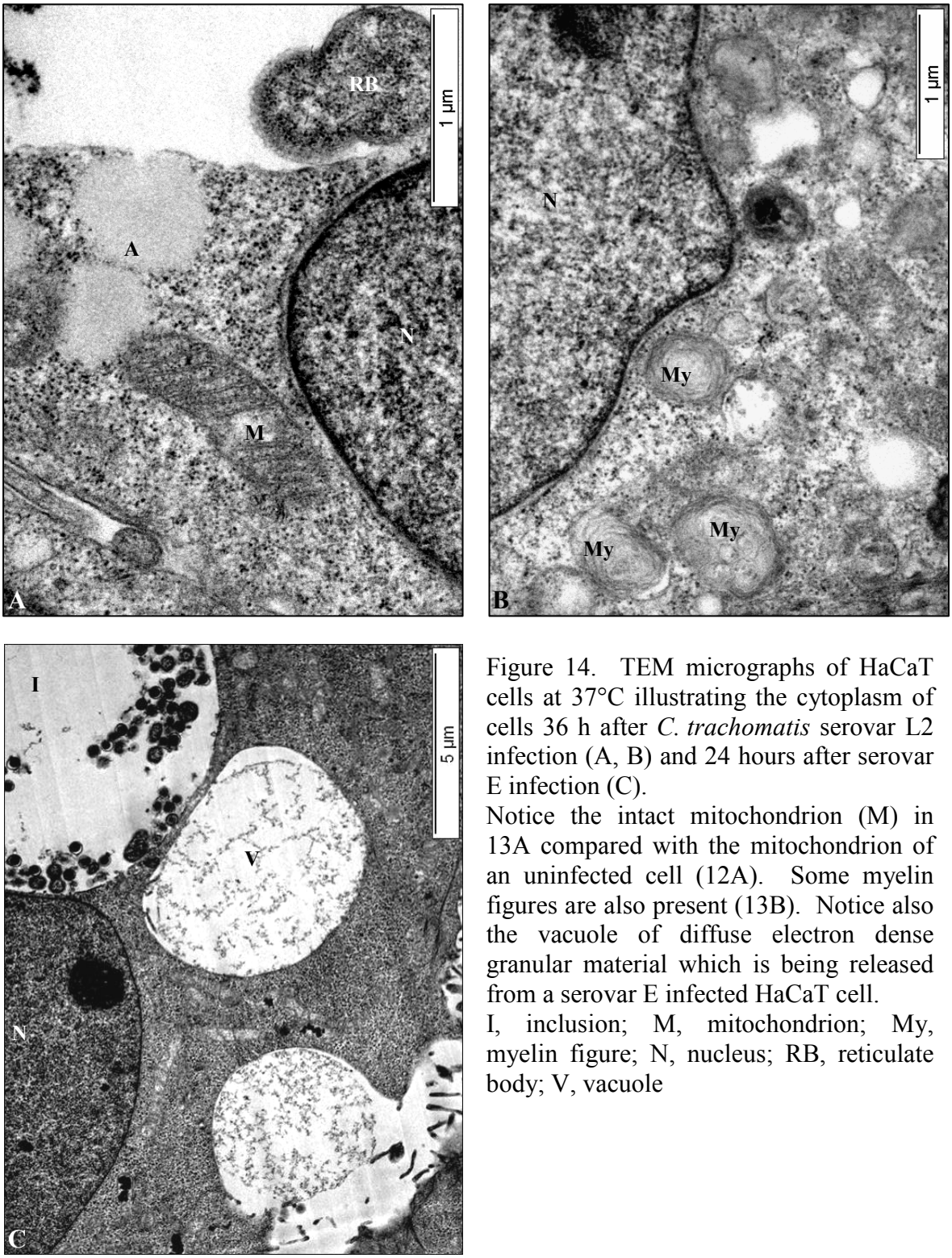

Figure 14. TEM micrographs of HaCaT cells at 37°C illustrating the cytoplasm of cells 36 h after *C. trachomatis* serovar L2 infection (A, B) and 24 hours after serovar E infection (C).
Notice the intact mitochondrion (M) in 13A compared with the mitochondrion of an uninfected cell (12A). Some myelin figures are also present (13B). Notice also the vacuole of diffuse electron dense granular material which is being released from a serovar E infected HaCaT cell.
I, inclusion; M, mitochondrion; My, myelin figure; N, nucleus; RB, reticulate body; V, vacuole

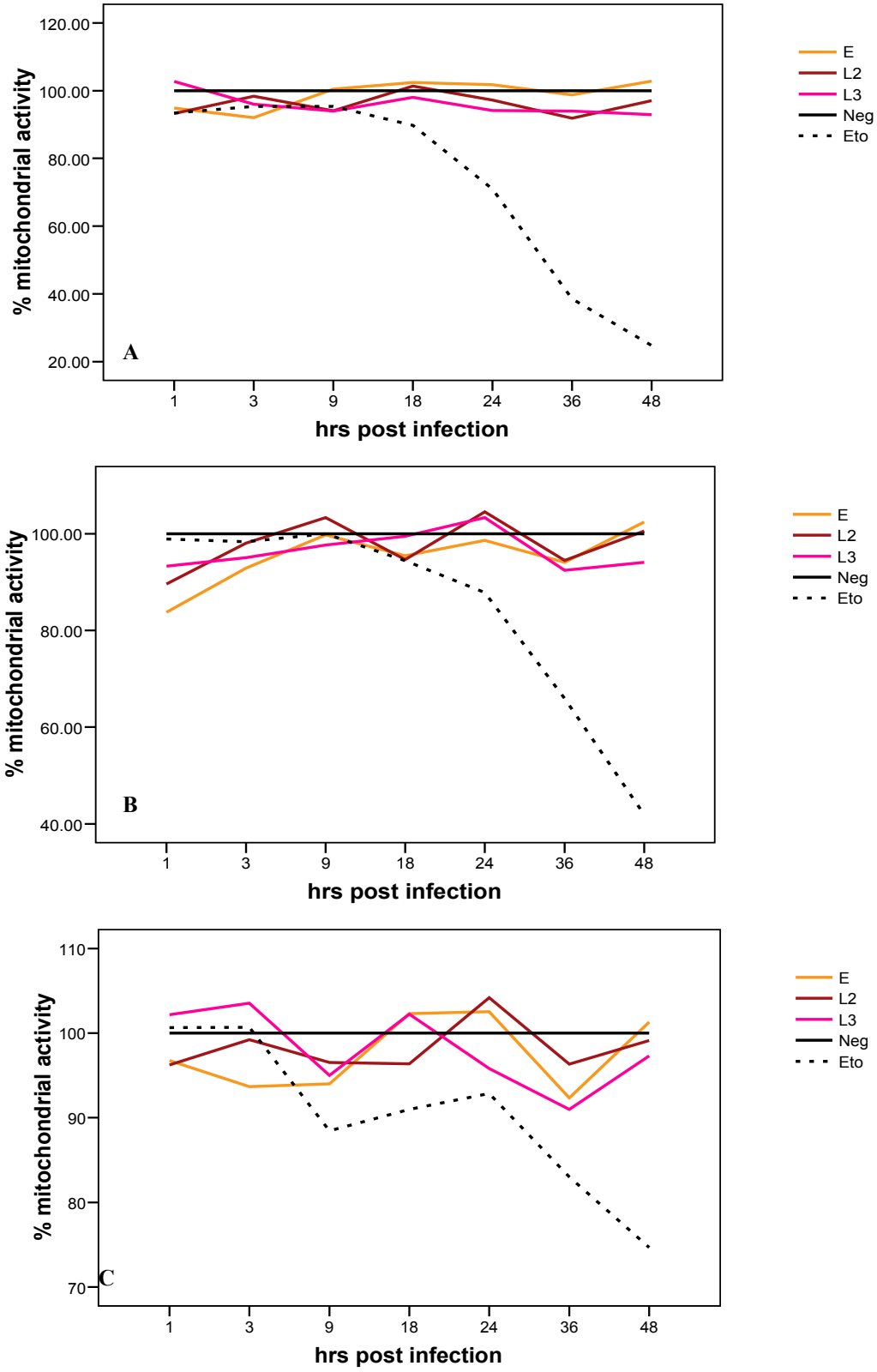

Figure 15. Relative percentage of mitochondrial activity in ME-180 cells at 37°C (A), HaCaT cells at 37°C (B), and HaCaT cells at 33°C (C) taken at various time points during the first 48 hours after chlamydial infection. Mitochondrial activity was quantified using the MTT assay and expressed as a percentage of the mitochondrial activity of uninfected monolayers.

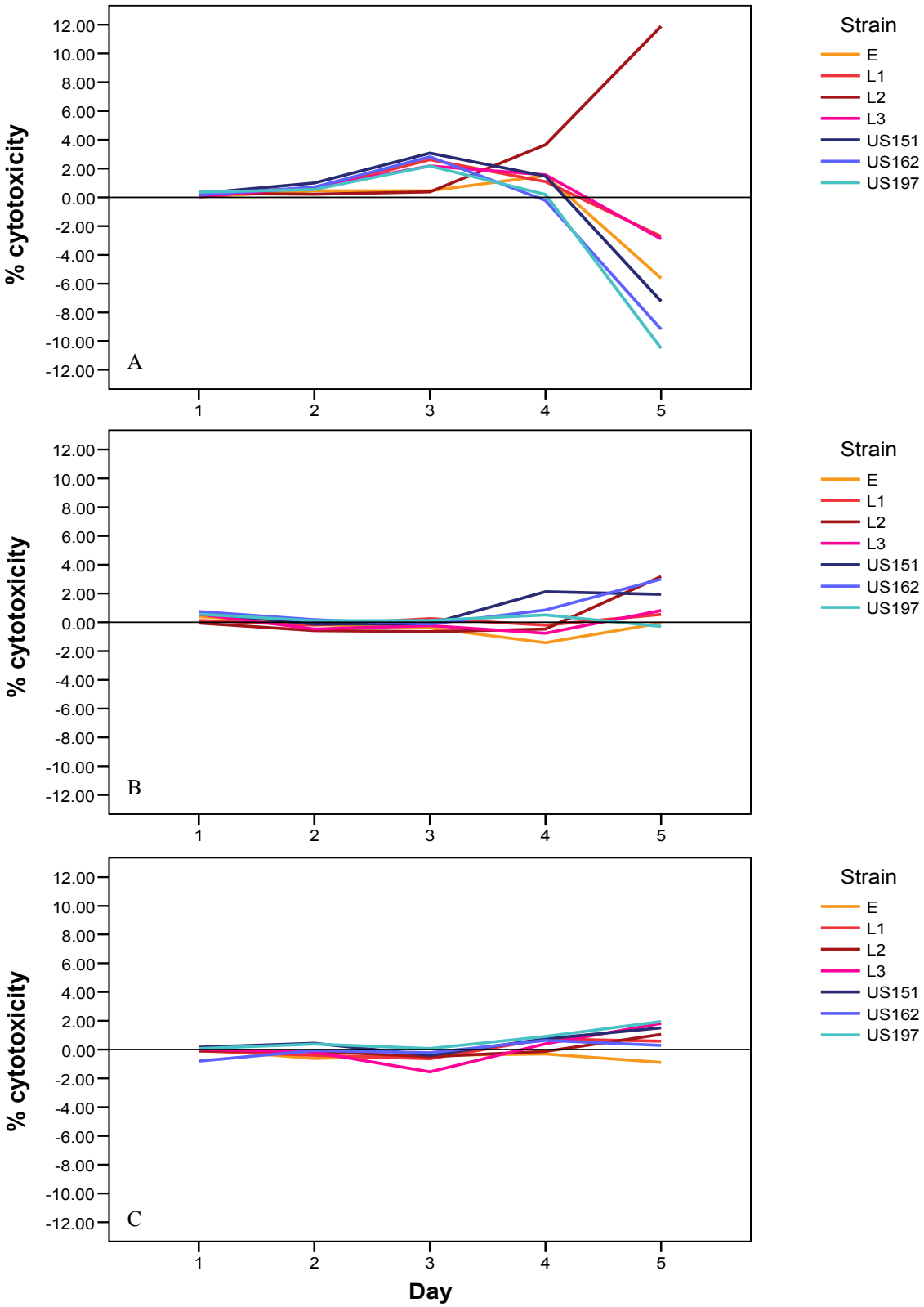

Figure 16. Median percentage *C. trachomatis*-induced cytotoxicity for 5 days post-infection in (A) ME-180 cells at 37°C, (B) HaCaT cells at 37°C, and (C) HaCaT cells at 33°C

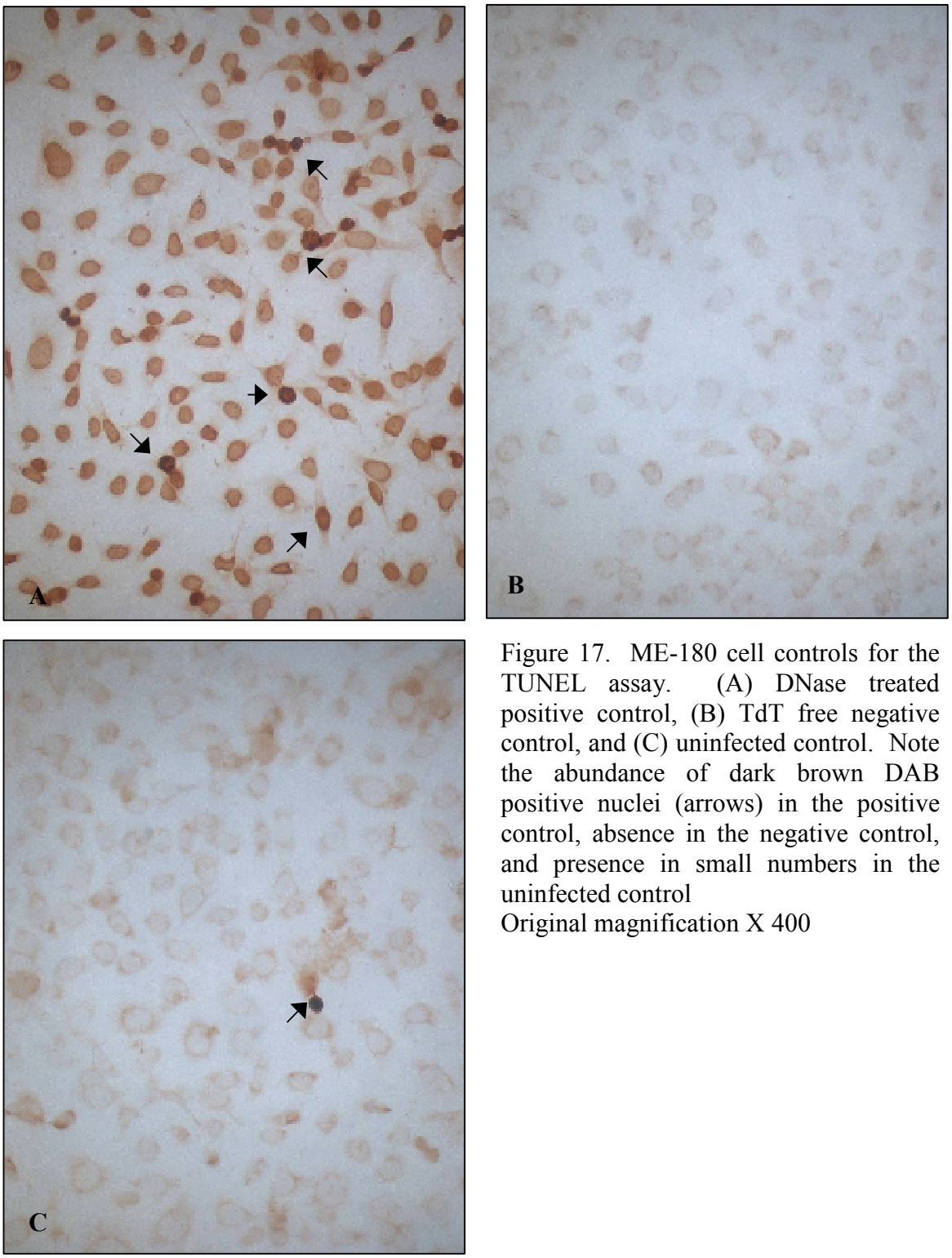

Figure 17. ME-180 cell controls for the TUNEL assay. (A) DNase treated positive control, (B) TdT free negative control, and (C) uninfected control. Note the abundance of dark brown DAB positive nuclei (arrows) in the positive control, absence in the negative control, and presence in small numbers in the uninfected control
Original magnification X 400

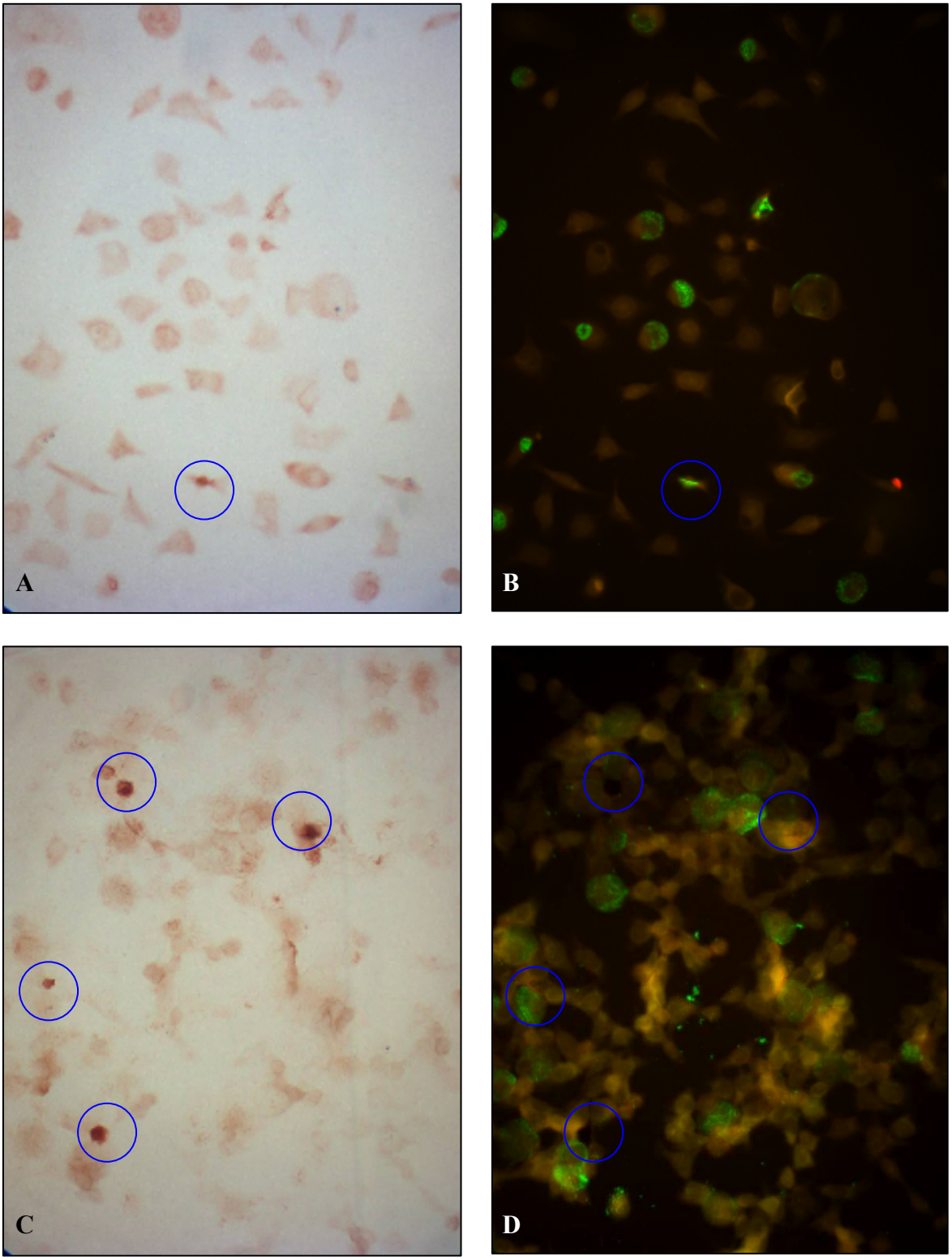

Figure 18. ME-180 cells 2 days post-infection with *C. trachomatis* serovar E (A, B) or L2 (C, D). The TUNEL stained bright field micrographs on the left represent the same field of view as the fluorescent micrographs on the right. Note the spatial relationship between the DAB positive nuclei and chlamydial inclusions in the L2 infected monolayer (indicated by blue circles).
Original magnification X 400

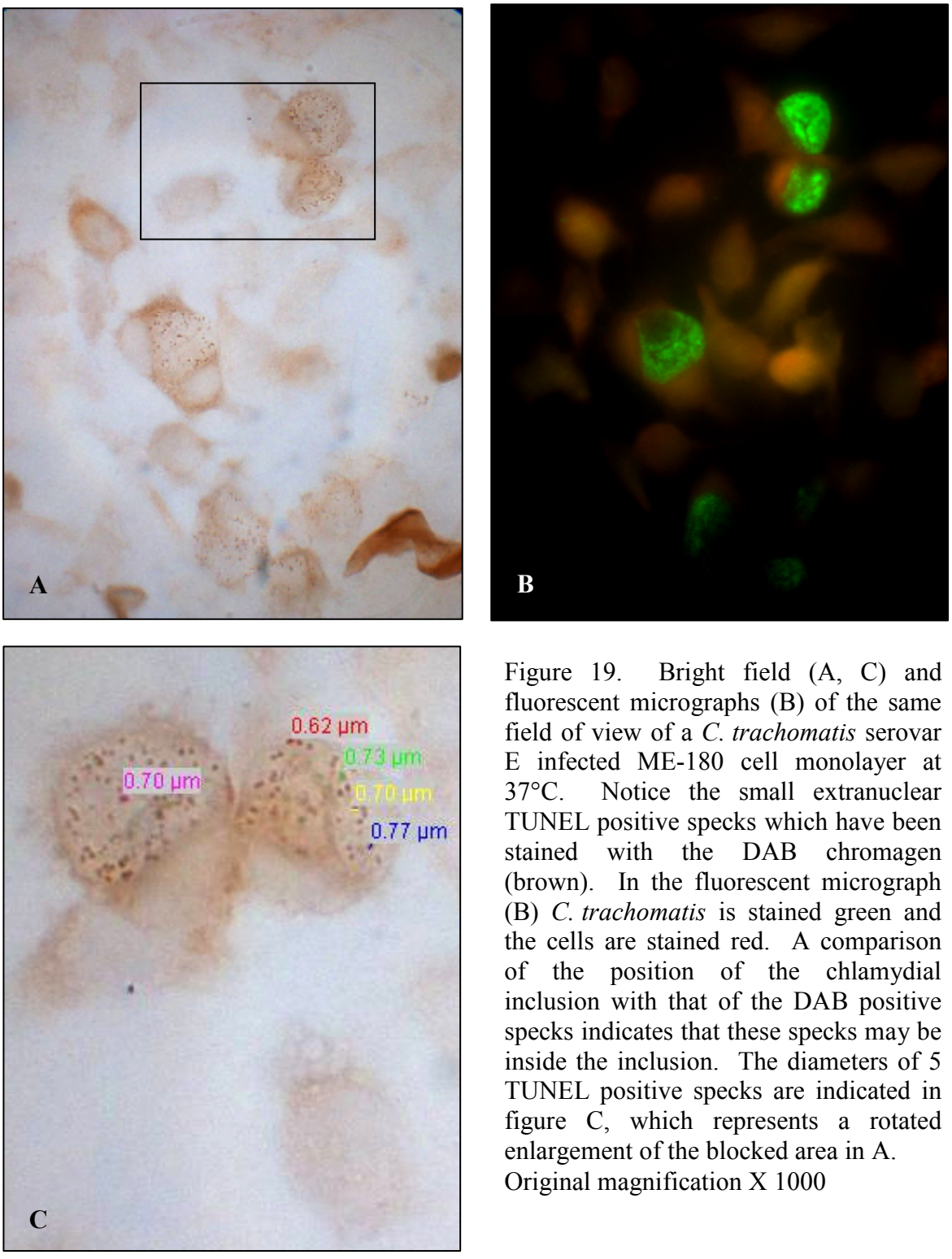

Figure 19. Bright field (A, C) and fluorescent micrographs (B) of the same field of view of a *C. trachomatis* serovar E infected ME-180 cell monolayer at 37°C. Notice the small extranuclear TUNEL positive specks which have been stained with the DAB chromagen (brown). In the fluorescent micrograph (B) *C. trachomatis* is stained green and the cells are stained red. A comparison of the position of the chlamydial inclusion with that of the DAB positive specks indicates that these specks may be inside the inclusion. The diameters of 5 TUNEL positive specks are indicated in figure C, which represents a rotated enlargement of the blocked area in A. Original magnification X 1000

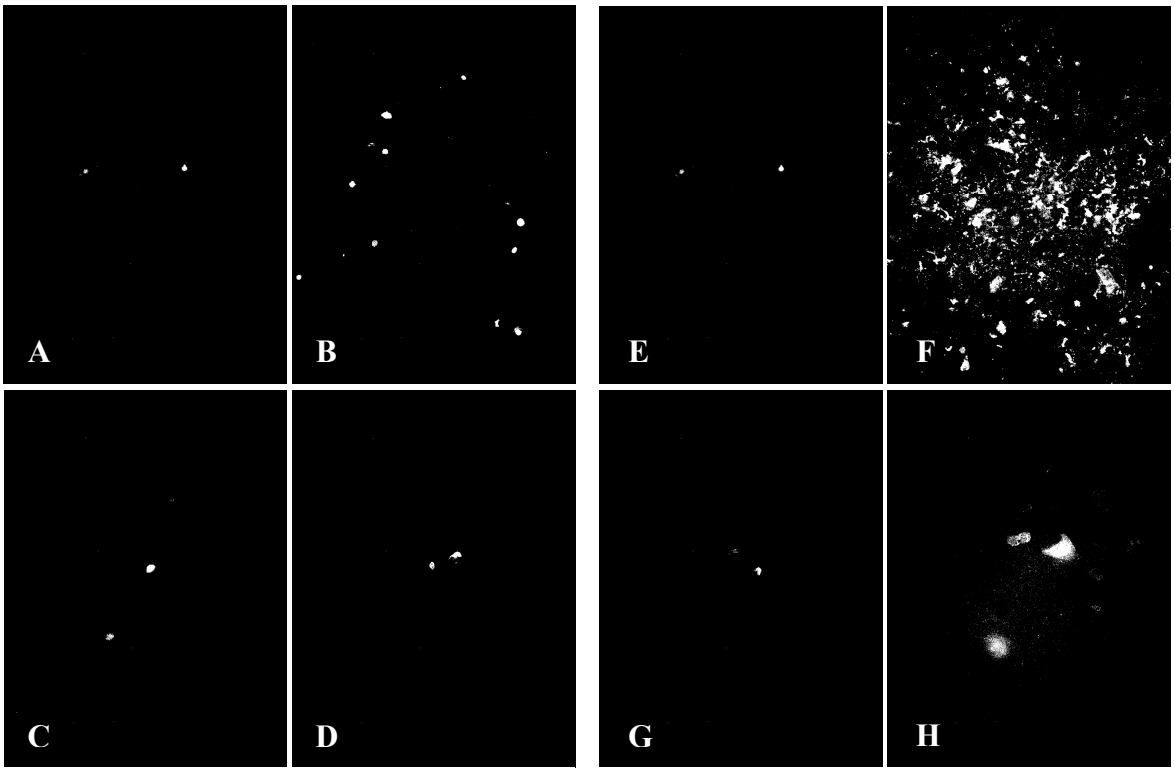

ME-180 cells at 37°C

HaCaT cells at 37°C

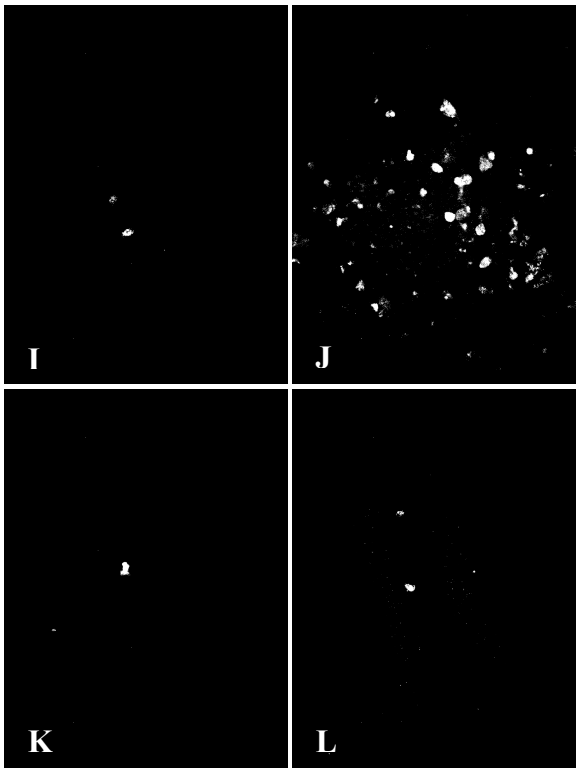

HaCaT cells at 33°C

Figure 20. Micrographs of caspase positive cells in uninfected ME-180 and HaCaT cell monolayers after exposure to uninfected cells (A, E, I), 20 μM etoposide (B, F, J), serovar E infected cells (C, G, K) or serovar L2 infected cells (D, H, L) for 16 hours. Only the caspase positive apoptotic cells are shown. The green component of the fluorescent micrographs was selected and the images binarized.
Original magnification X 200

CHAPTER 5 – DISCUSSION

Despite more than 99.6% genetic identity between *C. trachomatis* serovars (Carlson *et al* 2004) there are marked differences in virulence, growth rates, tissue tropism and disease profile. Serovars D-K of the OG biovar cause discharge disease (urethritis or cervicitis) which may progress to epididymitis and prostatitis or pelvic inflammatory disease in males and females respectively; strains of the LGV biovar cause LGV which is characterised by genital ulcers and lymphadenopathy (Ward 2002) or proctitis in gay men (Nieuwenhuis *et al* 2004). Numerous differences in *in vitro* culture requirements (Lee 1981) have been reported, as well as a difference in the length of the replication cycle (Miyairi *et al* 2006). More recently molecular analyses have revealed small genetic differences which reflect the tissue tropism and disease profile of these organisms (Carlson *et al* 2004, Caldwell *et al* 2003, Fehlner-Gardiner *et al* 2002).

We aimed to further characterise the behavioural differences between strains of the OG and LGV biovar, and compare LGV reference strains with fresh clinical isolates from our setting.

Previous studies have utilized cells which were not the native host cell, conditions which did not resemble those at the initial site of infection and reference strains rather than fresh clinical isolates. In this study we utilized conditions which more closely resemble the initial site of infection for each biovar. Because the first target of infection for the LGV organisms is skin, keratinocytes were used, while cervical cells are one of the primary targets of the OG strain. Both cell lines were infected with both biovars for comparison purposes. Both the HaCaT keratinocytes and the ME-180 cervical cells have retained the

typical characteristics of their wild-type counterparts (Boukamp 1988, Sykes 1970). The ME-180 cell line was used instead of the HeLa cell line since the ME-180 cell line is newer and thought to approximate the behaviour of native cervical cells more closely than HeLa cells. Cycloheximide or other substances which alter the host cell metabolism were not used in order to ascertain the effect of the organism on host cells under conditions which resemble the *in vitro* situation as closely as possible. But centrifugation was used to infect the cells. A low MOI was used to ensure the availability of uninfected cells for the progeny organisms to infect. This study is also unique in that there are no published reports on *C. trachomatis* infection of keratinocytes, despite the fact that skin is the first site of infection for the LGV organisms. The 3 LGV clinical isolates were passaged no more than five times in our laboratory and this was done in McCoy cells using the method described in 3.2. This was necessary to produce suffient numbers of the organism for use in experiments. Chicken eggs where not used. The reference strains we received had been stored in the yolk sac of chicken eggs and had been passaged as follows: serovar L1 (strain 440L), 25 times; serovar L2 (strain 434B), 10 times and serovar L3 (strain 404L) 26 times. Subsequent to this these strains were passage 6 to 8 times in our laboratory in McCoy cells using the method described in 3.2.

In the chlamydial growth curve experiments the three LGV reference strains grew more rapidly than the OG strain or the fresh clinical isolates in ME-180 cells at 37°C. This is indicated by both area occupied by chlamydia and inclusions per 10 thousand cells. There was a decline in the mean number of L2 reference strain inclusions per 10 thousand cells from day 4 to 5 post infection with a steady increase in area occupied by chlamydia during the same time frame. This is explained by the rupture of inclusions under these conditions resulting in decreased inclusion counts. Immunofluorescence at this time point indicated

numerous free chlamydial particles scattered over the now disrupted monolayer. These organisms were included in the area occupied by chlamydia measurement but not the inclusion counts. In summary, the LGV reference strains showed a different growth pattern than the clinical isolates and the OG strain which was also a clinical isolate from a patient with urethritis. These differences might relate to the higher number of in-vitro passages of the reference strains or to the fact that the clinical isolates, including the OG strain were never grown in chick embryos.

All strains of chlamydia tested entered, and replicated in HaCaT cells at both 37 and 33°C to produce visible inclusions. At 37°C, replication of the L2 reference strain was significantly more rapid than any other strain, including the L1 and L3 reference strains and the fresh LGV clinical isolates which were categorized as serovar L2. This dramatic difference in behaviour between the L2 reference strain and fresh L2 clinical isolates indicates a need for fresh clinical isolates for use in pathogenesis studies.

Chlamydial replication in HaCaT cells was significantly slower for all strains tested at 33°C despite the fact that 33°C is the temperature of human skin which is the first target of infection for the LGV organisms. At 1 day post infection inclusions in monolayers incubated at 33°C were smaller than those in monolayers incubated at 37°C and too small to visualize and enumerate at low magnification. Both van Ooij *et al* (1998) and Fields *et al* (2002) reported a smaller inclusion size when infected cells were incubated at a lower temperature. In both studies HeLa cells were infected with *C. trachomatis* serovar L2 at 37°C for 1 hour, and then incubated at 32 or 37°C for at least 24 hours. Inclusions were smaller when incubated at 32°C than at 37°C. *Haemophilus ducreyi*, one of the other causes of genital ulcer disease, shows optimal growth at 33°C (Sturm and Zanen, 1984). It

has been postulated that this is responsible for the difference in prevalence of chancroid between male and female. Such a difference does not exist for other genial ulcers. This is in keeping with the optimal growth of *C. trachomatis* biovar LGV at 37°C. LGV infection in the male patient might induce a more intense inflammatory response as compared to *H. ducreyi* infection, increasing the local temperature from surface to core level.

Growth curves plotted for chlamydial growth in HaCaT cells at 33°C were different when area occupied by chlamydia and inclusions per 10 thousand cells were used as an indicator of growth. Inclusions per 10 thousand cells only takes the number of inclusions into account, whereas mean area occupied by chlamydia takes into account both the number of inclusions present and the size of the inclusions. This is a more accurate reflection of the actual number of organisms because in general, the larger the inclusion, the more organisms present.

The growth curve produced using inclusions per 10 thousand cells showed an increase in the number of serovar L2 reference strain inclusions. This indicates that the progeny EB for this strain were infectious when grown in HaCaT cells at 33°C. This is in agreement with the results obtained by Fields *et al* (2002) using the same strain. The number of inclusions produced in monolayers infected with other strains was either stable throughout the times tested, or declined. Since the serovar L2 reference strain was shown to replicate more rapidly than any other strain at 37°C, and the dramatic increase in inclusions per 10 thousand cells at 33°C only occurred between days 4 and 5 post infection, it is possible that an incubation period of 5 days is too short for the same effect to be observed with the other strains tested. The decline in inclusions per 10 thousand cells observed with serovar L1

and L3 may be due to the rupture of mature inclusions. The resulting inclusions produced by progeny EB could be too small to be detected at this time point.

In contrast, mean area occupied by chlamydia indicated an increase in the number of organisms from day 1 to day 5 for all strains tested. Again the L2 reference strain replicated more rapidly than any other strain tested. This likely indicates that the L2 reference strain is better adapted to in vitro growth than the others.

Visual inspection of the stained monolayers indicated a difference in the maximum inclusion size attained by different strains of *C. trachomatis* grown in HaCaT cells at 33°C. These observations were quantified by measuring the size of individual inclusions using image analysis software. While the maximum size of inclusions for the clinical isolates and serovar E reached little more than 1000 μm^2, the maximum inclusion size for the L1, L2 and L3 reference strains was 1873, 4489 and 3178 μm^2 respectively. Of particular interest is the fact that the fresh clinical isolates were also shown to be serovar L2. This again indicates a difference in the behaviour of the reference strains compared to the fresh clinical isolates. Either the reference strains have been modified by decades of culture under conditions different to those *in vivo*, or the strains present in our setting are different to the reference strains. Either way, fresh clinical isolates are imperative for pathogenesis studies of LGV in our setting.

The chlamydial replication cycle of an LGV and an OG strain was compared in ME-180 and HaCaT cells at 37°C, and in HaCaT cells at 33°C using TEM.

Both EB and RB exhibited the same morphology that has been described in the literature.

EB were spherical with a 350 nm diameter with an electron dense core of tightly packed DNA. This core was enclosed by a trilaminar cytoplasmic membrane and outer envelope. These structures were previously described and measured by Ward (1983) who reported similar measurements to those reported in this study. In addition, we report that the electron dense core was not centrally located yielding a periplasmic space which varied from 8 to 17 nm. The tiny projections present on the external surface of the outer envelope (figure 8A) have been described by Matsumoto *et al* (1976) and Stokes (1978) in *C. psitacci* EB. These structures span the outer envelope terminating in small round protrusions on the inner surface of the outer envelope. The authors propose that these structures may have a role in EB uptake by cells, resistance of the organism to lysosomal enzymes or other functions.

The RBs were larger at almost 1µm in diameter and demonstrated a more irregular shape. The outer envelope has been described to exhibit a "ruffled-ballerina-skirt" appearance (Peterson and de la Maza 1988). This may be due to a loss of the rigid polypeptide structure of the EB cell wall (Matsumoto and Manire 1970) and the absence of sulphur containing amino acids which allow sulphur bridging between polypeptide chains and confer stability (Tamura and Manire 1967). RBs lack the electron dense core present in EB. During this stage the DNA is unravelled to allow transcription and translational. This is the metabolically active life form which replicates by binary fission (Ward 1983). RBs undergoing binary fission were often intimately associated with the inclusion membrane and some exhibited an apparently rigid region of well-defined double trilaminar cell envelope. The periplasmic space was bridged by electron-dense structures perpendicular to the two membranes to create a septated appearance. This was previously observed by

Peterson and de la Maza (1988) in HeLa cells infected with *C. trachomatis* (L2), *C. psittaci* and the TWAR-183 strain. Wyrick (2000) explains these structures as the same projections present on the EB. They are hollow and extend from the RB, through the inclusion membrane to the host cell cytoplasm. This may allow the exchange of energy and nutrients from the host cell to the replicating RB, or alternately, these structures may function as a TTSS.

Together these results indicate that RB structure is the same regardless of the host cells in which they are grown.

The typical biphasic replication cycle that has been extensively described (Ward 1983) was observed for both strains when grown in ME-180 or HaCaT cells at 37°C.

In the HaCaT cells at 33°C the replication cycle was the same for the OG strain, albeit slightly slower. With the L2 reference strain, a few intermediate bodies were observed at 36 h post infection. At 48 hours post infection, L2 inclusions still comprised replicating RB and no detectable EB. This is contrasted by the presence of numerous EB present in serovar E inclusions 48 hours after infection at 33°C. Since no electron microscopy was done using an L2 clinical isolate, these differences can either be the result of differences between OG and LGV biovars or between clinical isolates (OG) and laboratory adapted reference strains. Although no EB were observed inside L2 inclusions at 48 hours post infection, EB were detected in a non membrane bound state in the cytoplasm of cells containing an inclusion of RB (figure 10C). In HaCaT keratinocytes at 33°C a state of persistent infection may be established. Serovar L2 *C. trachomatis* may escape the

chlamydial inclusion and migrate through the cytoplasm of the host cell towards the underlying layers of the skin without rupture of the original host cell.

When viewed in light of the giant inclusions observed in the immunofluorescence growth curve experiment, it is possible that the L2 reference strain does not exit the host cell via cell lysis when grown in keratinocytes at 33°C. Instead an inclusion with continuously replicating RB is maintained. As EB develop, they escape from the inclusion, and migrate through the cytoplasm to infect the underlying layers of skin. Ward (1983) has suggested the possibility of small numbers of EB being released from persistently infected cells via budding of the host cell membrane in a manner similar to that of *Rickettsia prowazeki*. Unlike the persistent state of infection described in the literature, the RBs observed in this study were not markedly swollen with aberrant morphology (Beatty *et al* 1994b). Schramm and Wyrick (1995) investigated the host cell cytoskeletal requirements of *C. trachomatis* serovar E versus L2. In the model of infection proposed by the authors, serovar E is said to be released from the apical surface of infected polarized cells, in contrast to serovar L2, which is released from the basolateral surface to infect the underlying tissues. This model, together with our observation of free L2 EB migrating through the cytoplasm explains the classical presentation of the disease – inguinal lymphadenopathy which frequently occurs without history of a genital ulcer, and when a genital ulcer is present it is transient and painless (Schachter and Osoba 1983).

The difference in the clinical presentation of LGV – absence of an ulcer versus painful ulcer – may be determined by the level of inflammation at the site of infection. An inflammatory response at the site infection would cause a local increase in the temperature of skin. The organism would replicate more rapidly resulting in tissue damage and the

presence of an ulcer. In the absence of an inflammatory response the temperature of skin would remain at 33°C. The organism may establish a persistent state of infection without lysis of the host cell. Instead infectious EB will be continuously shed to infect the underlying tissues and ultimately migrate to the inguinal lymph nodes without the formation of an ulcer.

In our setting patients usually present in the primary stage, and the ulcer is painful, rather than the painless ulcers described in the literature (Sturm *et al* 2005). The difference in clinical presentation may also be attributed to a difference in the physiology of the organisms isolated. All 3 reference strains were isolated from bubonic aspirates in a group of military servicemen or seamen who had recently returned to the USA from Asia (Schachter *et al* 1969). Only 4 of the 11 patients in the group had primary lesions, and 2 of these hadn't even noticed the primary lesion which was detected on examination. The fresh clinical isolates used in this study were isolated from genital ulcers before inguinal lymphadenopathy occurred. Other climatic and patient demographic factors may also affect the clinical presentation of the disease.

Either way, skin cells (and cervical cells) do not escape unaffected. The organism does enter and undergo its typical lifecycle. Like other studies (Fields *et al.* 2002, Campbell *et al* 1989), intracytoplasmic inclusions form in the perinuclear region for both biovars under all conditions tested. As the inclusion grows it pushes the nucleus aside. Mitochondria are intimately associated with the inclusion like in the studies of Friis (1972) and Peterson and de la Maza (1988). This is expected since chlamydiae require ATP from their host cells and RB have been shown to transport ATP and ADP via an ATP-ADP exchange mechanism but EB cannot (Hatch *et al* 1982). RBs also tend to be located at the periphery

of the inclusion. This was described previously (Peterson and de la Maza, 1988, Phillips *et al,* 1984) Together these results indicate that the overall effect of LGV and OG *C. trachomatis* on HaCaT keratinocytes and ME-180 cervical cells is not unlike that observed with other chlamydiae like *C. psittacii* on other cell lines.

Because the aim of this study was to investigate potential pathological differences between the LGV and OG organisms, the cytoplasm of infected cells was examined.

In the ME-180 cells organelle and cytoplasm degeneration was noted at 1, 3 and 9 hours post infection for both biovars indicating that LGV and OG strains of *C. trachomatis* have a similar ultrastructural effect on this cell line. In some inclusions at the later stages of infection there was no membrane separating the organism from the host cytoplasm. In the microcinematographic study by Campbell *et al* (1989) inclusions of the trachoma organism were seen to burst while still inside their host cell. LGV organisms were not included in the study, but in the current study some inclusions without any distinct membrane were observed for both biovars allowing RB and mitochondria to exist side by side (figure 11C). EB were also captured in a nonmembrane bound state migrating through the cytoplasm (figure 10C, 11D, 12C). The absence of an inclusion membrane at the later stages of infection and non membrane bound organisms were also described by Todd and Caldwell (1985). This suggests that host cell lysis and exocytosis is not the only way these organisms are released from host cells.

At 48 hours after infection mitochondrial pathological changes were observed in monolayers infected with the LGV organism but not the OG organism. Swollen mitochondria with fragmented cristae and electron dense deposits in the mitochondrial

matrix were observed. These degenerate mitochondria looked different to the "disrupted" mitochondria observed by Friis (1972) in his study on *C. psittaci* on L-929 cells.

In HaCaT cells at 37°C, the mitochondrion was the main organelle to exhibit pathological changes. Because swollen degenerate mitochondria in serovar E infected cells occur early in the infectious cycle, and not in L2 infected cells, it is unlikely to be caused by "over-worked" mitochondria. Instead it may be due to a preformed EB cytotoxin such as that described by Belland and co-workers in 2001. This preformed cytotoxin was produced by an OG isolate but not serovar L2, and was shown to induce cell rounding and cytoskeletal collapse when host cells were infected at a high multiplicity of infection. It is also possible that this early pathological effect could be due to chlamydial endotoxin or the lipid A component of the chlamydial endotoxin and warrants further investigation.

Because myelin figures were present with both biovars throughout infection it is likely that this is a result of another pathogenic mechanism other than a preformed toxin. Myelin figures, also known as myeloid bodies, are membrane bound aggregates of smooth membranes arranged in a concentric or reticular fashion (Hruban *et al* 1972). They are part of the lysosome family. Although they may be present in normal cells, myeloid figures tend to accumulate in cells treated with a variety of drugs and disappear after removal of the drug. The absence of myelin figures in the uninfected control cells in our study, indicates that the presence of these structures was chlamydia-induced, and not due to the treatment of the cells during the infection process.

The large secretory vesicle voiding its material to the extracellular space (figure 14C) housed sparse flocculent and particulate matter in an electron lucent matrix. This resembles

the matrix of chlamydial inclusions, as well as the lysosomes containing partially degraded mucopolysaccharide observed in a liver biopsy of a patient with Hurler's disease (Ghadially 1982). This same cell with the secretory vesicle housed an inclusion with a morphologically similar matrix. Giles et al (2006) report the presence of numerous vesicles emanating from the chlamydial inclusion of serovar E infected polarised HEC-1B cells. The vesicle matrix featured in our study looks identical to those in the electron micrographs reported in this paper. Giles *et al* (2006) demonstrated the presence of the inclusion membrane proteins IncA, IncF and IncG in the vesicle membrane as well as chlamydial heat shock proteins copies 2 and 3. We demonstrate the fusion of a morphologically identical vesicle with the host cell plasmalemma.

In the HaCaT cells at 33°C, there were no noticeable ultrastructural pathological changes observed other than the typical features of *C. trachomatis* infection in other cells, including the presence of some myelin bodies. Both strains produced the same effect on their host cells.

Mitotic cells were observed under all conditions tested regardless of the cell line, temperature, the infecting organism or time post infection. Crocker *et al* (1965) reported no delay in the HeLa cell cycle when cells were infected at a low MOI such as that used in this study. The cell cycle was delayed when L cells or HeLa cells were infected with *C. psittaci* or *C. trachomatis* respectively at a high MOI (Horoschak and Moulder 1978, Bose and Liebhaber 1979).

Although dead and degenerate cells were visualised with TEM, one cannot accurately compare the relative quantity of these cells, because in cell culture monolayers, dead cells are sloughed off into the culture medium and are thus unavailable for TEM assessment.

The MTT assay was employed to quantify the mitochondrial pathology observed in the TEM studies. This assay is based on the cleavage of tetrazolium salts by dehydrogenase enzymes present in active mitochondria (Mosmann 1983). The assay is not usually used to investigate the cytotoxicity of bacteria on eukaryotic cells due to the ability of bacterial metabolic enzymes to also cleave the tetrazolium salt (Grare *et al,* 2008). We used this assay because *C. trachomatis* is an obligate intracellular pathogen which relies on ATP generated by its host cell's mitochondria (Hatch *et al,* 1982). The first published report of MTT assay use in a study on *C. pneumoniae* was by Kartikasari *et al* in 2006. These authors used the test to measure cell viability.

In the current study, no significant differences in the level of mitochondrial activity was detected at any time point in ME-180 cells at 37°C or HaCaT cells at 33°C. This is in keeping with the lack of significant ultrastructural mitochondrial pathology observed under these conditions.

In the HaCaT cells at 37°C, there was an extremely significant decrease in the level of mitochondrial activity in serovar E infected monolayers and a significant decrease in the level of mitochondrial activity in serovar L2 infected monolayers when compared to the uninfected control at 1 hour post infection. This indicates that the numerous swollen mitochondria with a lucent matrix and reduced cristae observed at this time point do have a significant effect on host cell metabolism in these monolayers. The restoration of

measured mitochondrial activity from 3 hours post infection supports the fact that these pathological mitochondria were not observed from 3 to 24 hours post infection. Markedly swollen mitochondria were visualized again at 36 and 48 hours post infection. This corresponded with a decline in the level of mitochondrial activity at 36 hours post infection, but did not reach significance. This may be due the fact that these swollen mitochondria were not observed in all cells within the monolayer. Other cells in the monolayer may have been actively metabolizing to compensate for the damage caused by chlamydial infection. Because the MTT assay measures mitochondrial activity in a population of cells, not at the single cell level, the results reflect the overall level of mitochondrial activity. A reduction of mitochondrial activity in a subset of cells would thus be diluted out by all the actively metabolizing neighbouring cells.

The LDH assay was used to investigate cytotoxic activity in cell monolayers infected with several strains of *C. trachomatis* at low MOI for 5 days. No significant difference in the level of cytotoxic activity was measured amongst any strains grown in HaCaT cells at 37 or 33°C. In ME-180 cells at 37°C, there was no significant difference in cytotoxicity amongst strains from day 1 to 4 post infection. At day 5 the serovar L2 reference strain exhibited a median cytotoxic effect of almost 12%, in contrast to all other strains which had a protective effect on the monolayer at this time point. Significance was reached between the L2 reference strain and the L2 clinical isolates. This again points to the need for fresh clinical isolates to be used in pathogenesis studies.

Despite that lack of measured cytotoxic activity with the LDH assay, this does not mean that *C. trachomatis* does not cause cytotoxic effects on HaCaT cells. The LDH assay has been reported to under estimate cytotoxicity in cases where the cytotoxic agent only affects

intracellular activity (Weyermann *et al* 2005). Because Todd and Caldwell (1985) observed host cell lysis as the only mechanism of EB release from host cells, one would have expected higher cytotoxicity values measured by the LDH assay. These results suggest that HaCaT keratinocytes are more resistant to LGV chlamydia induced cell lysis than the HeLa cells used in Todd and Caldwell's study, and that EBs are consequently released from HaCaT cells via a mechanism other than cell lysis. The increase in inclusion counts from 1 to 5 days post infection unequivocally shows that the organism does exit its initial host cell to infect other neighbouring cells. The lack of detectable cytotoxicity at 2 days post infection after one completed chlamydial lifecycle, implies that the organism exits the initial cell to infect a new one via a mechanism other than host cell lysis. If suffient numbers of the initial host cells lysed upon release of the EB, LDH would be released into the culture media, and a cytotoxic effect would have been detected.

The TUNEL assay was used to determine the spatial relationship between *C. trachomatis* infected cells, and cells undergoing cell death. This assay has been criticised for false positives in apoptosis detection, due to inadequate discrimination between the different types of cell death (Jarvis *et al*. 2002). It is used in this study due to the ability to counter stain for *C. trachomatis* and identify a spatial relationship between infected cells, and cells with fragmented nuclear DNA (Schöier 2001) indicative of cell death, regardless of the biochemical mechanism by which cell death was caused.

In both cell lines at 37°C more TUNEL positive cells were observed with both the LGV reference strains and the LGV clinical isolates than with serovar E. This indicates that the LGV strains exert a greater cytotoxic effect on both cell lines than serovar E at 37°C. The fact that TUNEL positive cells were frequently located immediately adjacent to an infected

cell indicates that this occurs either by cell-to-cell interaction or a secreted molecule which acts over a short distance. Although some infected cells had a TUNEL positive nucleus, the majority did not. A study by Schöier *et al* (2001) reports an increase in the number of TUNEL positive uninfected cells in a *C. trachomatis* infected McCoy cell monolayer compared to an uninfected monolayer. They do not report a difference between the number of TUNEL positive cells in the serovar L2 versus the serovar E infected monolayers. The same authors reported that 96% of apoptotic cells did not contain a chlamydial inclusion in the serovar L2 infected monolayer compared to 99% in serovar E infected monolayers.

In the HaCaT cells at 33°C, there was no elevation in the number of TUNEL positive cells in infected versus uninfected cells at 2 or 5 days post infection, except a slight increase in TUNEL positive cells in the L3 infected monolayer and a slight decrease in TUNEL positive cells in the serovar E infected monolayer at 5 days post infection. This indicates that *C. trachomatis* is more cytotoxic to HaCaT cells at 37°C than at 33°C.

At high magnification small non-nuclear TUNEL positive particles were observed in both cell lines at 37°C but not 33°C (figure 19). These were located in the same region as the inclusion and appeared to be inside the chlamydial inclusion. These particles could either be DNA fragments which had been transported into the chlamydial inclusion for use by the organism, or the organism itself. Because these particles were round and uniform in size, resembled the morphology of replicating RB (many particles were clustered in pairs), and had a diameter of about 0.7 μm, it is likely that these TUNEL positive particles were RB. If so, these results indicate the presence of large amounts of double-stranded DNA with

available 3'hydroxyl overhangs present in RB for the TdT enzyme to bind causing TUNEL positivity (Didenko and Hornsby, 1996).

The caspase assay coupled with Transwell® permeable inserts served two functions. It determined whether chlamydia induced cytotoxicity was apoptotic and whether or not chlamydia-induced cytotoxicity was mediated via a secreted molecule.

In both cell lines at 37°C serovar E exposed monolayers and serovar L2 exposed monolayers demonstrated almost double and almost triple the number of caspase positive cells respectively compared to the monolayer exposed to uninfected cells. Because apoptosis is defined as "caspase-mediated cell death with associated apoptotic morphology" (Samali *et al* 1999), caspase positivity indicates that cell death is occurring via apoptosis. Infected cells were separated from uninfected cell monolayers by Transwell® permeable inserts. The permeable polyester membrane allowed continuity between the CCM in the upper and lower chambers enabling secreted molecules from the infected monolayer to affect the uninfected monolayer. The presence of elevated numbers of caspase positive cells in the uninfected monolayers exposed to infected monolayers, indicates that *C. trachomatis* induces the secretion of a molecule which diffuses through the permeable membrane to induce apoptosis in uninfected cells at 37°C.

At 33°C there was no difference in the number of caspase positive cells in the monolayers exposed to infected cells versus the monolayers exposed to uninfected cells. This indicates that no apoptosis inducing molecule is secreted by HaCaT cells infected with *C. trachomatis* at 33°C during the time period tested.

These results confirm those of the TUNEL assay – at 37°C *C. trachomatis*, most notably the LGV organisms, cause an increase in the level of cytotoxicity in uninfected cells. This would be advantageous to the organism. Death of neighbouring uninfected cells would cause erosion of the skin and ulcer formation which would enable the organism to penetrate the skin and migrate to the lymph nodes faster. Conversely, the preservation of neighbouring uninfected cells at 33°C would allow the organism to migrate to the lymph nodes and establish a site of infection in the lymph nodes before the patient becomes aware that he or she is infected.

In ME-180 cells at 37°C all strains tested grew. Area occupied by chlamydia indicated a difference between the three reference strains compared to serovar E and the fresh clinical isolates, but the number of inclusions per 10 thousand cells did not. The decline in the number of serovar L2 inclusions from day 4 to 5 with an increase in the area occupied by chlamydia during the same time period was associated with rupture of the inclusions. This leaves free chlamydial particles dispersed across the monolayer which contribute towards the area occupied by chlamydia but not inclusions per 10 thousand cells. This observation was verified by the elevated level of LDH in the supernatant of L2 infected monolayers at 5 days post infection. LDH is a cytosolic enzyme. Its presence in the cell culture media indicates lysis of the host cells as would normally occur during the release of LGV chlamydial organisms from their host cells (Sepp *et al* 1996).

On ultrastructural analysis both strains exhibited the normal biphasic replication cycle when grown in ME-180 cells at 37°C. Pathological changes in the host cell cytoplasm were noted, but these were similar for both L2 and E. In some infected cells the inclusion membrane was absent, and EB were seen to migrate through the cytoplasm in a non-

membrane bound state and possibly be released by a mechanism other than host cell lysis. However, our LDH and fluorescent microscopy studies indicate that cell lysis is a major mechanism of L2 EB release from host cells when cells are infected in larger numbers. Although some mitochondrial pathology was noted in L2 infected monolayers at 48 hours post infection, this did not reach significance in the MTT assay.

The increased numbers of TUNEL positive cells in biovar LGV infected monolayers but not the biovar OG infected monolayer, indicates that under the conditions tested the LGV strains induce a cytotoxic effect on neighbouring uninfected cells. The elevated numbers of caspase positive cells in monolayers exposed but not infected with the LGV strains indicates that this cytotoxic effect occurs via apoptosis and is mediated by a secreted molecule.

In the HaCaT cells at 37°C, all strains tested replicated, but the L2 reference strain replicated far more rapidly than any other strain. Unlike the ME-180 cell line, high values for area occupied by chlamydia were not accompanied by increased cytotoxicity as indicated by LDH activity.

Ultrastructural analysis indicated that replication occurred via the previously described biphasic replication cycle in HaCaT cells at 37°C. In this cell line cytopathic changes involving the mitochondrion were noted as early as 1 hour post infection. Swollen degenerate mitochondria occurred in the serovar E infected monolayer at 1, 36 and 48 hours post infection. Because this occurred at the times when EB were initiating infection, it is likely that this cytotoxic effect is due to a preformed EB cytotoxin such as that described by Belland *et al* (2001). The significance of this observation was confirmed by a

reduction in the level of mitochondrial activity in serovar E infected monolayers at these time points, although statistical significance was only reached at 1 hour post infection.

Increased numbers of TUNEL positive cells in biovar LGV infected monolayers but not the biovar OG infected monolayer, indicates that organisms of the LGV biovar induce a cytotoxic effect on neighbouring uninfected cells. The elevated numbers of caspase positive cells in monolayers exposed but not infected with the LGV strains indicates that this cytotoxic effect occurs via apoptosis and is mediated by a secreted molecule.

In HaCaT cells at 33°C all strains tested replicated as indicated by the presence of visible inclusions and an increase in the area occupied by chlamydia. But only the L2 reference strain produced a substantial increase in the number of inclusions per 10 thousand cells. This indicates that at 33°C the L2 reference strain was able to produce infectious progeny which were released from the primary host cell to infect another cell. Because the L2 reference strain replicated far more rapidly than the other strains, it is possible that the time period investigated was too short too allow completion of the replication cycle and subsequent production of inclusions which were large enough to visualize at a low magnification. The dramatic difference in the growth curve produced by area occupied by chlamydia compared to inclusions per 10 thousand cells, coupled with the subjective observation that the LGV reference strains produced larger inclusions prompted a comparison of chlamydial inclusion size. The LGV reference strains, especially serovar L2 did produce inclusions which were significantly larger than those produced by the OG strain or the fresh clinical isolates.

Ultrastructural analysis of the chlamydial developmental cycle indicated that the serovar E strain replicated via the typical biphasic developmental cycle, albeit at a slower rate, while the L2 reference strain did not. At 48 hours post infection serovar L2 inclusions did not contain EB, only replicating RBs. This is contrasted by the serovar E strain, and chlamydial growth at 37°C – 48 hour old inclusions housed mostly EB under these conditions. Two EB were detected in a non membrane bound state within the cytoplasm of two infected cells. This indicates that at 33°C infection with the L2 reference strain may enter a persistent state of infection where an inclusion of continuously replicating RB is maintained. As EBs, develop they exit the chlamydial inclusion and migrate through the cytoplasm where they are released from the host cell to infect neighbouring cells.

Elevated levels of cytotoxicity compared to uninfected monolayers were not detected with the LDH assay, the MTT assay, the TUNEL assay or the caspase assay in HaCaT cells at 33°C. This indicates that these EB are released from the persistently infected host cell via a mechanism which does not involve death of the host cell. Since both the TUNEL assay and the caspase assay with Transwell® permeable inserts did not indicate an elevated level of cytotoxic activity, *C. trachomatis* of either biovar does not induce apoptosis in neighbouring cells when grown at 33°C in HaCaT cell monolayers.

The observed differences in chlamydial behaviour of the LGV biovar at 33 versus 37°C may explain may explain the differences in clinical presentation. The classical presentation of LGV describes inguinal lymphadenopathy which may or may not be preceded by a painless genital (Schachter and Osoba 1983). In our setting patients usually present in the primary stage before development of inguinal lymphadenopathy and the ulcer is usually painful (Sturm *et al* 2005). Because inflammation causes a local increase

in temperature, the presence or absence of an inflammatory response at the site of infection may determine whether or not ulceration occurs. In the absence of an inflammatory response, the temperature remains at 33°C causing infected cells to enter into a state of persistent infection. Under these conditions a few EB are released at a time via a mechanism such as budding, which does not cause lysis of the host cell or cytotoxicity of neighbouring uninfected cells. No ulcer is formed. The presence of an inflammatory response at the site of infection may cause a local increase in temperature causing the organism to replicate rapidly. The organism does not enter into a persistent state of infection. Instead, numerous EB are released from the host cell at the end of the first round of replication to infect neighbouring cells. This may or may not result in lysis of the host cell, but a secreted molecule induces apoptotic cell death of neighbouring uninfected cells. This aggressive pathogenic mechanism erodes the keratinocyte layer of skin and causes an ulcer.

There was a significant difference in the behaviour of the serovar L2 reference strain and the fresh clinical isolates in the following investigations:

- growth rate under all conditions tested
- inclusion size in HaCaT cells at 33°C

Although the reference strain behaved similarly to the clinical isolates in the TUNEL assay, the above observations of the difference between the L2 reference strain and the fresh clinical isolates throws some doubt on all studies, including ours, which draw conclusions from this strain.

CHAPTER 6 - CONCLUSIONS

C. trachomatis of both biovars enters and multiplies in HaCaT and ME-180 cells at 37°C. In HaCaT cells at 33°C the number of organisms increase, but the L2 reference strain is the only strain to demonstrate its ability to produce infectious progeny at 33°C. This was indicated by an increase in the number of inclusions from 2 to 5 days post infection.

The serovar L2 reference strain replicates more rapidly than the other strains tested, including the fresh clinical isolates which were also serovar L2.

In HaCaT cells at 33°C the inclusions produced by the reference strains reach a much larger maximum size than those produced by the stored clinical OG isolate or the fresh L2 clinical isolates.

These behavioural differences between the L2 reference strain and the fresh clinical isolates unequivocally demonstrate a need for fresh clinical isolates when performing LGV pathogenesis studies. This is likely the case for all *C.trachomatis* serovars.

At an ultrastructural level there is no difference in the interaction of chlamydia and its host cell when grown in cervical cells or keratinocytes at 37°C compared to the published literature. This holds true for the OG strain at 33°C but not the LGV strain at 33°C. L2 infected keratinocytes at 33°C enter a state of continuous infection allowing a few EB to be released from the host cell at a time.

Because of the difference in behaviour of the LGV organism at 37 versus 33°C, the temperature at the site of infection may determine whether or not an ulcer is formed. If the temperature is raised due to inflammation, the organism replicates rapidly to form an ulcer. In the absence of inflammation, the temperature at the site of infection remains low, enabling the organism to enter a state of continuous infection whereby EB are continuously shed. This would enable the organism to pass through skin and migrate to the lymph nodes without ulcer formation.

Chlamydial infection of HaCaT and ME-180 cells at 37°C causes organelle damage within infected host cells. Infection of HaCaT cells with the OG biovar but not the LGV biovar at 37°C results in significant mitochondrial damage early in the infectious cycle. This is likely due to the previously described preformed EB cytotoxin which is present in organisms of the OG biovar but not the LGV biovar.

LGV organisms induce apoptosis of neighbouring uninfected cells via a secreted molecule when grown at 37°C but not 33°C. Apoptosis of uninfected cells exposed to cells infected with an OG strain also occurs, but at a much lower level. This is different to the preformed EB cytotoxin since it occurs later in the developmental cycle.

The observed difference between the L2 reference strain and the fresh L2 clinical isolates throws some doubt on all studies, including ours, which draw conclusions from this strain.

REFERENCES

Aarnaes SL, Peterson EM and de la Maza LM. 1984. The Effect of Media and Temperature on the Storage of *Chlamydia trachomatis*. *Am J Clin Pathol* **81**(2): 237-9

Al-Younes HM, Rudel T, Brinkmann V, Szczepek AJ and Meyer TF. 2001. Low iron availability modulates the course of *Chlamydia pneumoniae* infection. *Cell Microbiol* **3**:427-37

Arends MJ, Morris RG and Wyllie AH. 1990. Apoptosis, The Role of the Endonuclease. *Am J Pathol* **136**(3):593-608

Ashkenazi A and Dixit VM. 1998. Death receptors: signalling and modulation. *Science* **281**:1305-8

Bannantine JP, Griffiths RS, Viratyosin W, Brown WJ, Rockey DD. 2000. A secondary structure motif predictive of protein localization to the chlamydial inclusion membrane. *Cell Microbiol* **2**:35–47

Barbour AG, Amano K-I, Hackstadt T, Perry L and Caldwell HD. 1982. *Chlamydia trachomatis* Has Penicillin-Binding Proteins but Not Detectable Muramic Acid. *J Bacteriol* **151**(1):420-8

Bavoil P, Ohlin A and Schachter J. 1984. Role of Disulfide Bonding in Outer Membrane Structure and Permeability in *Chlamydia trachomatis*. *Infect Immun* **44**(2):479-85

Bavoil PM, Hsia R-C and Ojcius DM. 2000. Closing in on *Chlamydia* and its intracellular bag of tricks. *Microbiology* **146**:2723-31

Beatty WL, Byrne GI and Morrison RP. 1993. Morphologic and antigenic characterization of interferon gamma mediated persistent *Chlamydia trachomatis* infection *in vitro*. *Proc Natl Acad Sci USA* **90**:3998-4002

Beatty WL, Belanger TA, Desai AA, Morrison RP and Byrne GI. 1994a. Tryptophan depletion as a mechanism of gamma interferon-mediated chlamydial persistence. *Infect Immun* **62**(9):3705-11

Beatty WL, Morrison RP and Byrne GI. 1994b. Persistent Chlamydiae: from Cell Culture to a Paradigm for Chlamydial Pathogenesis. *Microbiol Rev* **58**(4):686-99

Behets FMT, Andriamiadana J, Randrianasolo D, Randriamanga R, Rasamilalao D, Chen C-Y *et al*. 1999. Chancroid, primary syphilis, genital herpes, and lymphogranuloma venereum in Antananarivo, Madagascar. *J Infect Dis* **180**:1382-5

Belland RJ, Scidmore MA, Crane DD, Hogan DM, Whitmire W, McClarty G *et al*. 2001. *Chlamydia trachomatis* cytotoxicity associated with complete and partial cytotoxin genes. *Proc Natl Acad Sci USA* **98**(24):13984-9

Birkelund S, Johnsen H and Christiansen G. 1994. *Chlamydia trachomatis* serovar L2 induces protein tyrosine phosphorylation during uptake by HeLa cells. *Infect Immun* **62**:4900-8

Black CM. 1997. Current Methods of Laboratory Diagnosis of *Chlamydia trachomatis* Infections. *Clin Microbiol Rev* **10**(1): 160-184

Boatright KM and Salvesen GS. 2003. Mechanisms of caspase activation. *Cur Opin Cell Biol* **15**:725-31

Bortner CD, Oldenburg NBE and Cidlowski JA. 1995. The role of DNA fragmentation in apoptosis. *Trends Cell Biol* **5**:21-6

Bose SK and Liebhaber H. 1979. Deoxyribonucleic Acid Synthesis, Cell Cycle Progression, and Division of Chlamydia-Infected HeLa 229 Cells. *Infect Immun* **24**(3):953-7

Boukamp P, Petrussevska RT, Breitkreutz D, Hornung J, Markham A and Fusenig NE. 1988. Normal keratinisation in a spontaneously immortalised aneuploid human keratinocyte cell line. *J Cell Biol* **106**:761-71

Boukamp P, Breitkreutz D, Hülsen A, Tomakidi P and Fusenig NE. 1994. *In vitro* transformation and tumor progression: a multistep model for skin carcinogenesis. In: *The Keratinocyte Handbook* by Leigh I, Lane B and Watt F (editors), Cambridge University Press, UK, pp. 485-499

Brade L, Numinen M, Makela H and Brade H. 1985. Antigenic Properties of Chlamydia trachomatis Lipopolysaccharide. *Infect Immun* **48**(2):569-72

Brade H, Brade L and Nano FE. 1987. Chemical and serological investigations on the genus-specific lipopolysaccharide epitope of Chlamydia. *Proc Natl Acad Sci USA* **84**:2508-12

Busch C, Hofmann F, Gerhard R and Aktories K. 2000. Involvement of a conserved tryptophan residue in the UDP-glucose binding of large clostridial cytotoxin. *J Biol Chem.* **275**:13228-34

Byrd TF and Horwitz MA. 1993. Regulation of transferrin receptor expression and ferritin content in human mononuclear phagocytes. Coordinate upregulation by iron transferrin and downregulation by interferon gamma. *J Clin Invest* **91:** 969-76

Byrne GI, Lehmann LK and Landry GJ. 1986. Induction of tryptophan catabolism is the mechanism for gamma-interferon-mediated inhibition of intracellular *Chlamydia psittaci* replication inT24 cells. *Infect Immun* **53**(2):347-51

Caldwell HD, Wood H, Crane D, Bailey R, Jones RB, Mabey D, Maclean I, Mohammed Z, *et al*. 2003. Polymorphisms in *Chlamydia trachomatis* tryptophan synthase genes differentiate between genital and ocular isolates. *J Clin Invest* **111**:1757-69

Campbell S, Richmond SJ and Yates PS. 1989. The effect of *Chlamydia trachomatis* infection on the host cell cytoskeleton and membrane components. *J Gen Microbiol* **135**:2379-86

Carabeo RA, Mead DJ and Hackstadt T. 2003. Golgi-dependent transport of cholesterol to the *Chlamydia trachomatis* inclusion. *Proc Natl Acad Sci USA* **100**(11):6771-6

Carlson JH, Hughes S, Hogan D, Cieplak G, Sturdevant DE, McClarty G, Caldwell HD and Belland RJ. 2004. Polymorphisms in the *Chlamydia trachomatis* Cytotoxin Locus Associated with Ocular and Genital Isolates. *Infect Immun* **72**(12):7063-72

Chaturvedi V, Qin J-Z, Denning MF, Choubey D, Diaz MO and Nickoloff BJ. 1999. Apoptosis in Proliferating, Senescent, and Immortalized Keratinocytes. *J Biol Chem* **274**(33):23358-67

Clausen JD, Christiansen G, Holst HU and Birkelund S. 1997. *Chlamydia trachomatis* utilizes the host cell microtubule network during early events of infection. *Mol Microbiol* **25**:441-9

Cotran RS, Kumar V and Collins T. 1999. Cellular pathology I: Cell injury and cell death. In: *Robbins Pathologic Basis of Disease* by Cotran RS, Kumar V and Collins T (editors) (6th edition), W.B. Saunders Company, Pennsylvannia, USA, pp18-25

Cresswell P, Ackerman AL, Giodini A, Peaper DR and Wearsch PA. 2005. Mechanisms of MHC class I-restricted antigen processing and cross-presentation. *Immunol Rev* **207:**145-57

Crocker TT, Pelc SR, Nielson BI, Eastwood JM and Banks J. 1965. Population dynamics and deoxyribonucleic acid synthesis in HeLa cells infected with an ornithosis agent. *J Infect Dis* **115**:105-22

Darville T, O'Neill JM, Andrews CW Jr, Nagarajan UM, Stahl L and Ojcius DM. 2003. Toll-like receptor-2, but not Toll-like receptor-4, is essential for development of oviduct pathology in chlamydial genital tract infection. *J Immunol* **171:** 6187-97

Dessus-Babus S, Darville TL, Cuozzo FP, Ferguson K. and Wyrick PB. 2002. Differences in innate immune responses (*in vitro*) to HeLa cells infected with nondisseminating serovar E and disseminating serovar L2 of *Chlamydia trachomatis*. *Infect Immun* **70:** 3234-48

Didenko VV and Hornsby PJ. 1996. Presence of Double-strand Breaks with Single-base 3' Overhangs in Cells Undergoing Apoptosis but Not Necrosis. *J Cell Biol* **135**:1369-76

Dong F, Pirbhai M, Xiao Y, Zhong Y, Wu Y and Zhong G. 2005. Degradation of the proapoptotic proteins Bik, Puma, and Bim with Bcl-2 domain 3 homology in *Chlamydia trachomatis*-infected cells. *Infect Immun* **73**(3):1861-4

Dumrese C, Maurus CF, Gygi D, Schneider MKJ, Walch M, Groscurth P and Ziegler U. 2005. *Chlamydia pneumoniae* induces aponecrosis in human aortic smooth muscle cells. *BMC Microbiology* **5**:2

Elela SA and Nazar RN. 1997. Role of the 5.8S rRNA in ribosome translocation. *Nucleic Acids Res* **25**(9):1788-94

Eley A, Hosseinzadeh S, Hakimi H, Geary I and Pacey AA. 2005. Apoptosis of ejaculated human sperm is induced by co-incubation with *Chlamydia trachomatis* lipopolysaccharide. *Human Reproduction* **20**(9):2601-7

Enari M, Sakahira H, Yokoyama H, Okawa K, Iwamatsu A and Nagata S. 1998. A caspase-activated DNase that degrades DNA during apoptosis, and its inhibitor ICAD. *Nature* **391:**43-50

Fan T, Lu H, Hu H, Shi L, McClarty GA, Nance DM *et al*. 1998. Inhibition of Apoptosis in Chlamydia-infected Cells: Blockade of Mitochondrial Cytochrome c Release and Caspase Activation. *J Exp Med* **187**(4):487-96

Fawaz FS, van Ooij C, Homola E, Mutka SC and Engel JN. 1997. Infection with *Chlamydia trachomatis* alters the tyrosine phosphorylation and/or localization of several host cell proteins including cortactin. *Infect Immun* **65**:5301-8

Fehlner-Gardiner C, Roshick C, Carlson JH, Hughes S, Belland RJ, Caldwell HD *et al*. 2002. Molecular basis defining human *Chlamydia trachomatis* tissue tropism. *J Biol Chem* **277**(30):26893-903

Fields KA, Hackstadt T. 2000. Evidence for the secretion of *Chlamydia trachomatis* CopN by a type III secretion mechanism. *Mol Microbiol* **38**:1048-60

Fields KA, Fischer E and Hackstadt T. 2002. Inhibition of Fusion of *Chlamydia trachomatis* Inclusions at 32°C Correlates with Restricted Export of IncA. *Infect Immun* **70**(7):3816-23

Fink SL and Cookson BT. 2005. Apoptosis, Pyroptosis, and Necrosis: Mechanistic Description of Dead and Dying Eukaryotic Cells. *Infect Immun* **73**(4):1907-6

Fischer SL, Vier J, Kirschnek S, Klos A, Hess S, Ying S and Häcker G. 2004a. *Chlamydia* Inhibit Host Cell Apoptosis by Degradation of Proapoptotic BH3-only Proteins. *J Exp Med* **200**(7):905-16

Fischer SK, Harlander T, Vier J and Häcker G. 2004b. Protection against CD95-Induced Apoptosis by Chlamydial Infection at a Mitochondrial Step. *Infect Immun* **72**(2):1107-15

Fling SP, Sutherland RA, Steele LN, Hess B, D'Orazio SE, *et al*. 2001. $CD8^+$ T cells recognize an inclusion membrane-associated protein from the vacuolar pathogen *Chlamydia trachomatis*. *Proc Natl Acad Sci USA* **98**:1160–65

Freidank HM, Billing H, Wiedmann-Al-Ahmad M. 2001. Influence of iron restriction on *Chlamydia pneumoniae* and *C. trachomatis*. *J Med Microbiol* **50**:223-27

Friis RR. 1972. Interaction of L cells and *Chlamydia psittaci*: entry of the parasite and host responses to its development. *J Bacteriol* **110**:706-21

Garcia-Calvo M, Peterson EP, Leiting B, Ruel R, Nicholson DW and Thornberry NA. 1998. Inhibition of Human Caspases by Peptide-based and Macromolecular Inhibitors. *J Biol Chem* **273**(49):32608-13

Gavrieli Y, Sherman Y and Ben-Sasson SA. 1992. Identification of programmed cell death in situ via specific labelling of nuclear DNA fragmentation. *J Cell Biol* **119**(3):493-501

Gerard HC, Whittum-Hudson JA and Hudson AP. 1997. Genes required for assembly and function of the protein synthetic system in *Chlamydia trachomatis* are expressed early in the elementary to reticulate body transformation. *Mol Gen Genet* **255**: 637-642 (Abstract)

Ghadially FN. 1982. Ultrastructural Pathology of the Cell and Matrix (2nd edition). Butterworths, UK, pp 534-5

Ghuysen J-M and Goffin C. 1999. Lack of Cell Wall Peptidoglycan versus Penicillin Sensitivity: New Insights into the Chlamydial Anomaly. *Antimicrob Agents Chemoth* **43**(10):2339-44

Gilbert GL. 1996. Chlamydia. In: *Mackie & McCartney Practical Medical Microbiology* by Collee JG, Fraser AG, Marmion BP and Simmons A (editors), Longman Singapore Publishers (Pte) Ltd., Singapore, pp. 621-633

Giles DK, Whittimore JD, LaRue RW, Raulston JE and Wyrick PB. 2006. Ultrastructural analysis of chlamydial antigen-containing vesicles everting from the Chlamydia trachomatis inclusion. *Microbes and Infect* **8**:1579-91

Giles DK and Wyrick PB. 2008. Trafficking of chlamydial antigens to the endoplasmic reticulum of infected epithelial cells. *Microb Infect*, doi:10.1016/j.micinf.2008.09.001 (article in press)

Goth SR and Stephens RS. 2001. Rapid, Transient Phosphatidylserine Externalization Induced in Host Cells by Infection with *Chlamydia* spp. *Infect Immun* **69**(2):1109-19

Grare M, Fontanay S, Cornil C, Finance C and Duval RE. 2008. Tetrazolium salts for MIC determination in microplates: Why? Which salt to select? How? *J Microbiol Methods* **75**:156-9

Green DR and Reed JC. 1998. Mitochondria and apoptosis. *Science* **281**:1309-12

Greene W, Xiao Y, Huang Y, McClarty G and Zhong G. 2004. Chlamydia-Infected Cells Continue To Undergo Mitosis and Resist Induction of Apoptosis. *Infect Immun* **72**(1):451-60

Grieshaber S, Swanson JA and Hackstadt T. 2002. Determination of the physical environment within the *Chlamydia trachomatis* inclusion using ion-selective ratiometric probes. *Cell Microbiol* **4**:273-84

Hackstadt T, Baehr W and Ying Y. 1991. *Chlamydia trachomatis* developmentally regulated protein is homologous to eukaryotic histone H1. *Proc Natl Acad Sci* **88**:3937-41

Hackstadt T, Scidmore MA, Rockey DD. 1995. Lipid metabolism in *Chlamydia trachomatis* infected cells: directed trafficking of Golgi-derived sphingolipids to the chlamydial inclusion. *Proc Natl Acad Sci USA* **92**:4877–81

Hackstadt T, Scidmore-Carlson M, Shaw E, Fischer E. 1999. The *Chlamydia trachomatis* IncA protein is required for homotypic vesicle fusion. *Cell Microbiol* **1**:119–30

Hakimi H, Geary I, Pacey A and Eley A. 2006. Spermicidal Activity of Bacterial Lipopolysaccharide Is Only Partly Due to Lipid A. *J Androl* **27**:774-9

Hansen SH, Sandvig K and van Deurs B. 1993. Molecules internalized by clathrin-independent endocytosis are delivered to endosomes containing transferrin receptors. *J Cell Biol* **123:**89–97

Hanelt M, Gareis M and Kollarczik B. 1994. Cytotoxicity of mycotoxins evaluated by the MTT-cell culture assay. *Mycopathologia* 1994; **128**:167-74

Hatch TP. 1975. Utilization of L-Cell Nucleoside Triphosphates by *Chlamydia psittaci* for Ribonucleic Acid Synthesis. *J Bacteriol* **122**:393-400

Hatch TP, Al-Hossainy E and Silverman JA. 1982. Adenine Nucleotide and Lysine Transport in *Chlamydia psittaci*. *J Bacteriol* **150**(2):662-70

Hatch TP, Allan I and Pearce JH. 1984. Structural and Polypeptide Differences Between Envelopes of Infective and Reproductive Life Cycle Forms of Chlamydia spp. *J Bacteriol* **157**(1):12-20

Hatch GM and McClarty G. 1998. Cardiolipin remodeling in eukaryotic cells infected with *Chlamydia trachomatis* is linked to elevated mitochondrial metabolism. *Biochem Biophys Res Commun* **243**:356–60

Hawkins RA, Rank RG and Kelly KA. 2002. A *Chlamydia trachomatis*-specific Th2 clone does not provide protection against a genital infection and displays reduced trafficking to the infected genital mucosa. *Infect Immun* **70**(9):5132-9

Heine H, Müller-Loennies S, Brade L, Lindner B and Brade H. 2003. Endotoxic activity and chemical structure of lipopolysaccharides from *Chlamydia trachomatis* serotypes E and L2 and *Chlamydophila psittaci* 6BC. *Eur J Biochem* **270:**440-50

Heinzen RA and Hackstadt T. 1997. The *Chlamydia trachomatis* parasitophorous vacuolar membrane is not passively permeable to low-molecular-weight compounds. *Infect Immun* **65**:1088-94

Hennings H and Holbrook KA. 1983. Calcium regulation of cell-cell contact and differentiation of epidermal cells in culture. *Exp Cell Res* **143**:127-42

Hodinka RL, and Wyrick PB**.** 1986. Ultrastructural study of mode of entry of *Chlamydia psittaci* into L-929 cells. *Infect Immun* **54:**855–63

Hodinka RL, Davis CH, Choong J and Wyrick PB. 1988. Ultrastructural study of endocytosis of *Chlamydia trachomatis* by McCoy cells. *Infect Immun* **56:**1456–63

Holbrook KA. 1994. Ultrastructure of the epidermis. In: *The Keratinocyte Handbook* by Leigh I, Lane B and Watt F (editors), Cambridge University Press, UK, pp. 3-39

Hook CE, Telyatnikova N, Goodall JC, Braud VM, Carmichael AJ, Wills MR *et al*. 2004. Effects of *Chlamydia trachomatis* infection on the expression of natural killer (NK) cell ligands and susceptibility to NK cell lysis. *Clin Exp Immunol* **138:**54-60

Horoschak K and Moulder JW. 1978. Division of Single Host Cells after Infection with Chlamydiae. *Infect Immun* **19**(1):281-6

Hruban Z, Sleser A and Hopkins E. 1972. Drug-induced and naturally occurring myeloid bodies. *Lab Invest* **27**:62-70

Hybiske K and Stephens RS. 2007. Mechanisms of host cell exit by the intracellular bacterium chlamydia. *Proc Natl Acad Sci USA* **104**(27):11430-5

Igietseme JU, Uriri IM, Chow M, Abe E and Rank RG. 1997. Inhibition of intracellular meultiplication of human strains of *Chlamydia trachomatis* by nitric oxide. *Biochem Biophys Res Commun* **232**:595-601

Iliffe-Lee ER, McClarty G. 1999. Glucose metabolism in *Chlamydia trachomatis*: the 'energy parasite' hypothesis revisited. *Mol Microbiol* **33**:177-87

Ingalls RR, Rice PA, Qureshi N, Takayama K, Lin JS and Golenbock DT. 1995. The inflammatory cytokine response to *Chlamydia trachomatis* infection is endotoxin mediated. *Infect Immun* **63**:3125-30

Jarvis M, Schulz U, Dickinson AM, Sviland L, Jackson G, Konur A *et al*. 2002. The detection of apoptosis in a human in vitro skin explant assay for graft versus host reactions. *J Clin Pathol* **55**:127-32

Jendro MC, Fingerle F, Deutsch T, Liese A, Köhler L, Kuipers JG *et al*. 2004. *Chlamydia trachomatis*-infected macrophages induce apoptosis of activated T cells by secretion of tumor necrosis factor-α in vitro. *Med Microbiol Immunol* **193**: 45-52

Johnson LF, Coetzee DJ and Dorrington RE. 2005. Sentinel surveillance of sexually transmitted infections in South Africa: a review. *Sex Transm Infect* **81**:287-93

Jungas T, Verbeke P, Darville T and Ojcius DM. 2004. Cell death, BAX activation, and HMGB1 release during infection with *Chlamydia*. *Microbes Infect* **6**:1145-55

Kartikasari AER, Georgiou NA, de Geest M, van Kats-Renaud JH, BouwmanJJM, van AsbeckBS *et al*. 2006. Iron enhances endothelial cell activation in response to Cytomegalovirus or *Chlamydia pneumoniae* infection. *Eur J Clin Invest* **36:**743-2

Kitajima Y. 2002. Mechanisms of desmosome assembly and disassembly. *Clin Exp Dermatol* **27**:684-90

Kubori T, Matsushima Y, Nakamura D, Uralil J, Lara-Tejero M, Sukhan A *et al*. 1998. Supramolecular Structure of the Salmonella typhimuriumType III Protein Secretion System. *Science* **280**:602-5

Kuo CC. 1978. Immediate cytotoxicity of *Chlamydia trachomatis* for mouse peritoneal macrophages. *Infect Immun* **20**:613-18

Lee CK. 1981. Interaction between a Trachoma Strain of *Chlamydia trachomatis* and Mouse Fibroblasts (McCoy Cells) in the Absence of Centrifugation. *Infect Immun* **31**(2): 584-91

Lee E-R, Kang Y-J, Kim J-H, Lee HT and Cho S-G. 2005. Modulation of apoptosis in HaCaT keratinocytes via differential regulation of ERK signalling pathway by flavonoids. *J Biol Chem* **280**(36):31496-507

Los M, Wesselborg S and Schulze-OsthoffK. 1999. The Role of Caspases in Development, Immunity, and Apoptotic Signal Transduction: Lessons from Knockout Mice. *Immunity* **10**:629-39

Maas-Szabowski N, Stärker A and Fusenig NE. 2003. Epidermal tissue regeneration and stromal interaction in HaCaT cells is initiated by TGF-α. *J Cell Sci* **116**:2937-48

Majno G and Joris I. 1995. Apoptosis, Oncosis, and Necrosis: An Overview of Cell Death. *Am J Pathol* **146**:3-15

Majeed M, Ernst JD, Magnusson KE, Kihlstrom E and Stendahl O. 1994. Selective translocation of annexins during intracellular redistribution of *Chlamydia trachomatis* in HeLa and McCoy cells. *Infect Immun* **62**:126–34

Makakole SC and Sturm AW. 1999. Pathogenesis of chancroid: the effect of cell polarization and temperature on the interaction of *Haemophilus ducreyi* with human epithelial cells. MMedSc dissertation, University of Natal Medical School, Department of Medical Microbiology, Durban, South Africa (unpublished)

Maleka DM, Hoosen AA, Sturm AW and Kiepiela P. 1996. The Laboratory Diagnosis of Lymphogranuloma venereum (LGV). MMedSc dissertation, University of Natal Medical School, Department of Medical Microbiology, Durban, South Africa. (unpublished)

Martin SJ, Reutelingsperger CEM, McGahon AJ, Rader JA, van Schie RCAA, LaFace DM *et al*. 1995. Early Redistribution of Plasma Membrane Phosphatidylserine Is a General Feature of Apoptosis Regardless of the Initiating Stimulus: Inhibition by Overexpression of Bcl-2 and Abl. *J Exp Med* **182**:1545-56

Matsumoto A and Manire GP. 1970. Electron Microscopic Observations on the Fine Structure of Cell Walls of *Chlamydia psittaci*. *J Bacteriol* **104**(3):1332-7

Matsumoto A, Fujiwara E and Higashi N. 1976. Observations of the Surface Projections of Infectious Small Cell of *Chlamydia psittaci* in Thin Sections. *J Electron Microsc* **25**:169-70

Misaghi S, Balsara ZR, Catic A, Spooner E, Ploegh HL and Starnbach MN. 2006. *Chlamydia trachomatis*-derived deubiquitinating enzymes in mammalian cells during infection. *Molec Microbiol* **61**(1):142-50

Miyairi I and Byrne GI. 2006. *Chlamydia* and programmed cell death. *Current Opin Microbiol* **9**:102-8

Miyairi I, Mahdi OS, Ouellette SP, Belland RJ and Byrne GI. 2006. Different growth rates of *Chlamydia trachomatis* biovars reflect pathotype. *J Infect Dis* **194**:350-7

Moodley P, Sturm PDJ, Vanmali T, Wilkinson D, Connolly C and Sturm AW. 2003. Association Between HIV-1 Infection, the Etiology of Genital Ulcer Disease, and Response to Syndromic Management. *Sex Transm Dis* **30**(3):241-5

Morrison RP. 2000. Differential sensitivities of *Chlamydia trachomatis* strains to inhibitory effects of gamma interferon. *Infect Immun* **68**(10):6038-40

Mosmann T. 1983. Rapid colorimetric assay for cellular growth and survival: application to proliferation and cytotoxicity assays. *J Immunol Methods* **65**:55-63

Moulder JW. 1966. The relation of the psittacosis group (Chlamydiae) to bacteria and viruses. *Annu Rev Microbiol* **20**:107-30

Moulder JW, Hatch TP, Byrne GI and Kellogg KR. 1976. Immediate toxicity of high multiplicities of *Chlamydia psittaci* for mouse fibroblasts (L cells). *Infect Immun* **14**:277-89

Nelson DE, Virok DP, Wood H, Roshick C, Johnson RM, Whitmire WM, Crane DD, Steele-Mortimer O, *et al.* 2005. Chlamydial IFN-γ immune evasion is linked to host infection tropism. *Proc Natl Acad Sci USA* **102**(30):10658-63

Newhall WJ and Jones RB. 1983. Disulfide-Linked Oligomers of the Major Outer Membrane Protein of Chlamydiae. *J Bacteriol* **154**(2):998-1001

Nieuwenhuis RF, Ossewaarde JM, Gotz HM, *et al*. 2004. Resurgence of lymphogranuloma venereum in Western Europe: an outbreak of *Chlamydia trachomatis* serovar L2 proctitis in The Netherlands among men who have sex with men. *Clin Infect Dis* **39**:996-1003

Núnez MT, Gaete V, Watkins JA and Glass J. 1990. Mobilization of iron from endocytic vesicles: the effects of acidification and reduction. *J Biol Chem* **265:**6688-92

Nurminen M, Rietschel ET and Brade H. 1985. Chemical characterization of *Chlamydia trachomatis* lipopolysaccharide. *Infect Immun* **48**(5):573-5

O'Farrell N, Morison L, Moodley P, Pillay K, Vanmali T, Quigley M *et al*. 2008. Genital ulcers and concomitant complaints in men attending a sexually transmitted infections clinic: implications for sexually transmitted infections management. *Sex Transm Dis* **35**(6):545-50

Perfettini J-L, Hospital V, Stahl L, Jungas T, Verbeke P and Ojcius DM. 2003a. Cell death and inflammation during infection with the obligate intracellular pathogen, *Chlamydia*. *Biochimie* **85**:763-9

Perfettini J-L, Ojcius DM, Andrews CW, Jr., Korsmeyer SJ, Rank RG and Darville T. 2003b. Role of Proapoptotic BAX in Propagation of *Chlamydia muridarum* (the Mouse Pneumonitis Strain of *Chlamydia trachomatis*) and the Host Inflammatory Response. *J Biol Chem* **278**(11):9496-502

Perry LL, Feilzer K and Caldwell HD. 1997. Immunity to *Chlamydia trachomatis* is mediated by T helper 1 cells through IFN-γ-dependent and –independent pathways. *J Immunol* **158**:3344-52

Peterson EM and de la Maza FM. 1988. Chlamydia Parasitism: Ultrastructural Characterization of the Interaction between the Chlamydial Cell Envelope and the Host Cell. *J Bacteriol* **170**(3):1389-92

Petrucci RH and Harwood WS. 1997. General Chemistry (7th edition). Prentice Hall, inc. USA. p. 868

Phillips, D. M., C. E. Swenson, and J. Schachter. 1984. Ultrastructure of *Chlamydia trachomatis* infection of the mouse oviduct. *J Ultrastruct Res* **88**:244-256

Quayle AJ. 2002. The innate and early immune response to pathogen challenge in the female genital tract and the pivotal role of epithelial cells **57**:61-70

Qureshi N, Kaltashovi I, Walkeri K, Doroshenkoi V, Cotteri RJ, Takayama K *et* al. 1997. Structure of the Monophosphoryl Lipid A Moiety Obtained from the Lipopolysaccharide of *Chlamydia trachomatis*. *J Biol Chem*. **272**(16):10594-600

Rake G and Jones HP. 1944. Studies on lymphogranuloma venereum. II. The association of specific toxins with agents of the lymphogranuloma-psittacosis group. *J Exp Med* **79**:463-85

Rasmussen SJ, Eckmann L, Quayle AJ, Shen L, Zhang Y-X, Anderson DJ *et al*. 1997. Secretion of Proinflammatory Cytokines by Epithelial Cells in Response to Chlamydia Infection Suggests a Central Role for Epithelial Cells in Chlamydial Pathogenesis. *J Clin Invest* **99**:77-87

Raulston JE. 1997. Response of *Chlamydia trachomatis* serovar E to iron restriction *in vitro* and evidence for iron-regulated chlamydial proteins. *Infect Immun* **65**:4539-47

Read TD, Brunham RC, Shen C, Gill SR, Heidelberg JF, *et al*. 2000. Genome sequence of *Chlamydia trachomatis* MoPn and *Chlamydia pneumoniae* AR39. *Nucleic Acids Res.* **28**:1397-406

Reynolds ES. 1963. The use of lead citrate at high pH as an electron opaque stain in electron microscopy. *J Cell Biol* **17**:208-12

Roan NR and Starnbach MN. 2006. Antigen-specific CD8+ T cells respond to *Chlamydia trachomatis* in the genital mucosa. *J Immunol* **177:** 7974-9

Roan NR, Gierahn TM, Higgins DE and Starnbach MN. 2006. Monitoring the T cell response to genital tract infection. *Proc Natl Acad Sci USA* **103:**12069-74

Roan NR and Starnbach MN. 2008. Immune-mediated control of *Chlamydia* infection. *Cell Microbiol* **10**(1): 9-19

Rund S, Lindner B, Brade H, Holst O. 1999. Structural analysis of the lipopolysaccharide from *Chlamydia trachomatis* serotype L2. *J Biol Chem*. **274**:16819-4

Samali A, Zhivotovsky B, Jones D, Nagata S and Orrenius S. 1999. Apoptosis: cell death defined by caspase activation. *Cell Death Differ* **6**:495-6

Schachter J, Smith DE, Dawson CR, Anderson WR, Deller JJ Jr., Hoke AW *et al*. 1969. Lymphogranuloma Venereum. I. Comparison of the Frei test, Complement Fixation test, and Isolation of the Agent. *J Infect Dis* **120**(3):372-5

Schachter J and Osoba AO. 1983. Lymphogranuloma venereum. *Br Med Bull* **39**(2):151-4

Schöier J, Öllinger K, Kvarnström M, Söderlund G and Kihlström E. 2001. *Chlamydia trachomatis*-induced apoptosis occurs in uninfected McCoy cells late in the developmental cycle and is regulated by the intracellular redox state. *Microb Pathog* **31**:173-84

Schramm N and Wyrick PB. 1995. Cytoskeletal Requirements in C*hlamydia trachomatis* Infection of Host Cells. *Infect Immun* **63**(1):324-32

Scidmore MA, Rockey DD, Fischer ER, Heinzen RA, Hackstadt T. 1996. Vesicular interactions of the *Chlamydia trachomatis* inclusion are determined by chlamydial early protein synthesis rather than route of entry. *Infect Immun* **64**:5366-72

Scidmore-Carlson MA, Shaw EI, Dooley CA, Fischer ER and Hackstadt T. 1999. Identification and characterization of a *Chlamydia trachomatis* early operon encoding four novel inclusion membrane proteins. *Mol Microbiol* **33**:753–65

Scidmore MA, Hackstadt T. 2001. Mammalian 14-3-3beta associates with the *Chlamydia trachomatis* inclusion membrane via its interaction with IncG. *Mol Microbiol* **39**:1638–50

Sepp A, Binns RM and Lechler. 1996. Improved protocol for calorimetric detection of complement-mediated cytotoxicity based on the measurement of cytoplasmic lactate dehydrogenase activity. *J Immunol Methods* **196**:175-80

Shaffer MF, Jones H, Grace AW, Hamre DM and Rake G. 1944. Use of the yolk sac of the developing chicken embryo in the isolation of the agent of lymphogranuloma venereum. *J Infect Dis* **75**:109-12

Shaw EI, Dooley CA, Fischer ER, Scidmore MA, Fields KA and Hackstadt T. 2000. Three temporal classes of gene expression during the *Chlamydia trachomatis* developmental cycle. *Mol Microbiol* **37**:913-25

Starnbach MN, Bevan MJ and Lampe MF. 1994. Protective cytotoxic T lymphocytes are induced during murine infection with *Chlamydia trachomatis*. *J Immunol* **153:**5183-9

Steele LN, Balsara ZR and Starnbach MN. 2004. Hematopoietic cells are required to initiate a *Chlamydia trachomatis*-specific CD8+ T cell response. *J Immunol* **173:**6327-37

Stenner-Liewen F, Liewen H, Zapata JM, Pawlowski K, Godzik A and Reed JC. 2002. CADD, a *Chlamydia* Protein That Interacts with Death Receptors. *J Biol Chem* **277**(12):9633-6

Stephens RS, Kuo C-C and Tam MR. 1982. Sensitivity of Immunofluorescence with Monoclonal Antibodies for Detection of *Chlamydia trachomatis* Inclusions in Cell Culture. *J Clin Microbiol* **16**(1): 4-7

Stephens RS, Kalman S, Lammel C, Fan J, Marathe R, *et al*. 1998. Genome sequence of an obligate intracellular pathogen of humans: *Chlamydia trachomatis*. *Science* **282**:754–59

Stephens RS, Wagar EA and Schoolnik GK. 1988. High-resolution mapping of serovar-specific and common antigenic determinants of the major outer membrane protein of *Chlamydia trachomatis*. *J Exp Med* **167**:817-31

Stokes GV. 1978. Surface Projections and Internal Structure of *Chlamydia psittaci*. *J Bacteriol* **133**:1514-6

Stothard DR, Boguslawski G and Jones RB. 1998. Phylogenetic Analysis of the *Chlamydia trachomatis* Major Outer Membrane Protein and Examination of Potential Pathogenic Determinants. *Infect Immun* **66**(8):3618-3625

Sturm AW and Zanen HC. 1984. Characteristics of *Haemophilus ducreyi* in culture. *J Clin Micro* **19**(5):672-4

Sturm PDJ, Moodley P, Khan N, Ebrahim S, Govender K, Connolly C *et al*. 2004. Aetiology of male urethritis in patients recruited from a population with a high HIV prevalence. *Int J Antimicrob Agents* **24S**:S8-14

Sturm PDJ, Moodley P, Govender K, Bohlken L, Vanmali T and Sturm AW. 2005. Molecular Diagnosis of Lymphogranuloma Venereum in Patients with Genital Ulcer Disease. *J Clin Microbiol* **43**(6):2973-5

Sturm-Ramirez K, Brumblay H, Diop K, Guèye-Ndiaye A, Sankalé J-L, Thior T *et al*. 2000. Molecular Epidemiology of Genital *Chlamydia trachomatis* Infection in High-Risk Women in Senegal, West Africa. *J Clin Micro* **38**(1):138-45

Su H and Caldwell HD. 1995. CD4+ T cells play a significant role in adoptive immunity to *Chlamydia trachomatis* infection of the mouse genital tract. *Infect Immun* **63:**3302-8

Su H, Feilzer K, Caldwell HD and Morrison RP. 1997. *Chlamydia trachomatis* genital tract infection of antibody deficient gene knockout mice. *Infect Immun* **65:**1993-9

Sykes JA, Whitescarver J, Jernstrom P, Nolan JF and Byatt P. 1970. Some Properties of a New Epithelial Cell Line of Human Origin. *J Nat Cancer Inst* **45**: 107-122

Tamura A and Manire GP. 1967. Preparation and Chemical Composition of the Cell Membranes of Developmental Reticulate Forms of Meningopneumonitis Organisms. *J Bacteriol* **94**:1184-8

Tanaka T, Bai T, and Yukawa K and Umesaki N. 2006. Optical combination chemotherapy and chemoradiotherapy with etoposide for advance cervical squamous cancer cells *in vitro*. *Oncol Rep* **15**:939-47

Tao S, Kaul R and Wenman WM. 1991. Identification and Nucleotide Sequence of a Developmentally Regulated Gene Encoding a Eukaryotic Histone H1-Like Protein from *Chlamydia trachomatis*. *J Bacteriol* **173**(9):2818-2822

Taub DD, Anver M, Oppenheim JJ, Longo DL and Murphy WJ. 1996. T Lymphocyte Recruitment by Interleukin-8 (IL-8). *J Clin Invest* **97**:1931-41

Taylor MW and Feng G. 1991. Relationship between interferon-γ, indoleamine 2,3-dioxygenase, and tryptophan catabolism. *FASEB J* **5**:2516-22

Tseng C-TK and Rank RG. 1998. Role of NK Cells in Early Host Response to Chlamydial Genital Infection. *Infect Immun* **66**(12):5867-75

Todd WJ and Caldwell HD. 1985. The interaction of *Chlamydia trachomatis* with host cells: ultrastructural studies of the mechanism of release of a biovar II strain from HeLa 229 cells. *J Infect Dis* **151**:1037-44

van Ooij C, Apodaca G and Engel J. 1997. Characterization of the *Chlamydia trachomatis* vacuole and its interaction with the host endocytic pathway in HeLa cells. *Infect Immun* **65:**758-66

van Ooij C, Homola E, Kincaid E and Engel J. 1998. Fusion of *Chlamydia trachomatis*-Containing Inclusions Is Inhibited at Low Temperatures and Requires Bacterial Protein Synthesis. *Infect Immun* **66**(11):5364-71

Velculescu VE and El-Deiry WS. 1996. Biological and clinical importance of the p53 tumor suppressor gene. *Clin Chem* **42**:858-68

von Eichel-Streiber C, Boquet P, Sauerborn M. and Thelestam M. 1996. Large clostridial cytotoxins – a family of glycosyltransferases modifying small GTP-binding proteins. *Trends Microbiol.* **4**:375-82

Wagar EA and Stephens RS. 1988. Developmental-Form-Specific DNA-Binding Proteins in *Chlamydia spp*. *Infect Immun* **56**(7):1678-84

Wang S-P, Kuo C-C and Grayston JT. 1973. A Simplified Method for Immunological Typing of Trachoma-Inclusion Conjunctivitis-Lymphogranuloma Venereum Organisms. *Infect Immun* **7**(3):356-60

Wang S-P and Grayston JT. 1991. Three new serovars of *Chlamydia trachomatis*: Da, Ia, and L_2a. *J Infect Dis* **163**:403-5

Wang S-P, Kuo CC, Burnes RC, Stephens RS and Grayston JT. 1985. Immunotyping of *Chlamydia trachomatis* with monoclonal antibodies. *J Infect Dis* **152**:791-800

Ward ME. 1983. Chlamydial classification, development and structure. *Br Med Bull* **39**(2):109-15

Ward ME. 2002. Chlamydia. In: *Medical Microbiology* (16th edition) by Greenwood D, Slack RCB and Peutherer JF (editors), Elsevier Science Ltd., UK pp. 358-68

Watson MW, Lambden PR and Clarke N. 1991. Genetic Diversity and Identification of Human Infection by Amplification of the Chlamydial 60-Kilodalton Cysteine-Rich Outer Membrane Protein. *J Clin Microbiol* **29**(6):1188-93

Weiss E and Wilson NN. 1969. Role of Exogenous Adenosine Triphosphate in Catabolic and Synthetic Activities of *Chiamydia psittaci*. *J Bacteriol* **97**:719-24

Weisburg WG, Hatch TP and Woese CR. 1986. Eubacterial Origin of Chlamydiae. *J Bacteriol* **167**(2): 570-574

Weyermann J, Lochmann D and Zimmer A. 2005. A practical note on the use of cytotoxicity assays. *Int J Pharm* **288**:369-76

Williams DM, Grubbs BG, Pack E, Kelly K and Rank RG. 1997. Humoral and cellular immunity in secondary infection due to murine *Chlamydia trachomatis*. *Infect Immun* **65:**2876-82

Workowski A and Berman SM. 2007. Centers for Disease Control and Prevention Sexually Transmitted Diseases Treatment Guidelines. *Clin Infect Dis* **44**:S73-6

Wylie JL, Hatch GM, McClarty G. 1997. Host cell phospholipids are trafficked to and then modified by *Chlamydia trachomatis*. *J Bacteriol* **179**:7233-42

Wyrick PB, Choong J, Davis CH, Knight ST, Royal MO, Maslow AS *et al*. 1989. Entry of *Chlamydia trachomatis* into polarized human epithelial cells. *Infect Immun* **57:**2378-89

Wyrick PB. 2000. Intracellular survival by *Chlamydia*. *Cell Microbiol* **2**(4):275-82

Xia M, Bumgarner RE, Lampe MF and Stamm WE. 2003. *Chlamydia trachomatis* Infection Alters Host Cell Transcription in Diverse Cellular Pathways. *J Infect Dis* **187**:424-34

Young B and Heath JW (editors). 2000. *Wheater's Functional Histology* (4th edition). Harcourt Publishers Limited, Edinburgh, UK pp.157-171

Zhong G and de la Maza LM. 1988. Activation of Mouse Peritoneal Macrophages In Vitro or In Vivo by Recombinant Murine Gamma Interferon Inhibits the Growth of Chlamydia trachomatis Serovar L1. Infect Immun **56**(12):3322-5

Zhong G, Fan T, Liu L. 1999. *Chlamydia* inhibits interferon γ-inducible major histocompatibility complex class II expression by degradation of upstream stimulatory factor 1. *J Exp Med* **189**:1931-8

Zhong G, Liu L, Fan T, Fan P, Ji H. 2000. Degradation of transcription factor RFX5 during the inhibition of both constitutive and interferon γ-inducible major histocompatibility complex class I expression in chlamydia infected cells. *J Exp Med* **191**:1525-34

Zhong G, Fan P, Ji H, Dong F, Huang Y. 2001. Identification of a chlamydial protease-like activity factor responsible for the degradation of host transcription factors. *J Exp Med* **193**:935-42

Zou H, Li Y, Liu X and Wang X. 1999. An APAF-1-cytochrome *c* multimeric complex is a functional apoptosome that activates procaspase-9. *J Biol Chem* **274**(17):11549-56

APPENDIX A – REAGENTS AND MEDIA

Phosphate buffered saline (PBS) (Dulbecco A)

5 PBS tablets (Oxoid)

500ml distilled water

Five PBS tablets were dissolved in 500ml autoclaved distilled water. The PBS was autoclaved at 121°C for 10 minutes, then decanted into 20ml aliquots and refrigerated until use.

0.05% EDTA

0.05g EDTA

1 PBS tablet

100ml distilled water

One PBS tablet and 0.05g EDTA was dissolved in approximately in 80ml autoclaved distilled water. The pH was adjusted to approximately 7.4 using 7.5% sodium bicarbonate and the volume brought up to 100ml. The solution was autoclaved at 121°C for 10 minutes, pipetted into 1ml aliquots and refrigerated until use.

McCoy cell freezing fluid

30ml EMEM with EBSS, NEAA, sodium pyruvate, L-glutamine and HEPES

10ml dimethyl sulphoxide (DMSO) (Fluka, Steinheim, Germany)

10ml FBS

Ten millilitres of DMSO and 10ml of FBS were added to 30ml of EMEM and the solution filter-sterilized through a 0.22µm filter into a sterile container.

HaCaT cell freezing fluid

30ml RPMI-1640 with L-glutamine and HEPES

10ml glycerol (BDH Laboratory supplies, Poole, England)

10ml FBS

Ten millilitres of glycerol and 10ml of FBS were added to 30ml of RPMI-1640 and the solution filter-sterilized through a 0.22µm filter into a sterile container.

ME-180 cell freezing fluid

40 ml McCoy 5a medium

5 ml DMSO

5 ml FCS

Five millilitres of DMSO and 5 ml of FBS were added to 40ml McCoy 5a medium and the solution filter-sterilized through a 0.22µm filter into a sterile container.

Sucrose-Phosphate-Glutamate Buffer (SPG)

sucrose

KH_2PO_4

$Na_2HPO_4.7H_2O$

glutamic acid

Distilled water

The sucrose, KH_2PO_4, $Na_2HPO_4.7H_2O$ and glutamic acid were dissolved in approximately in 400ml autoclaved distilled water, the pH was adjusted to approximately 7.4 using 7.5% sodium bicarbonate and the volume brought up to 500ml. The solution was filter sterilised through a 0.22µm filter, then aliquoted and stored at -20°C until use.

MicroTrak® *C. trachomatis* Reagent

MicroTrak® *C. trachomatis* Culture Confirmation Test (8H019UL):

***C. trachomatis* reagent** – fluorescein-labelled mouse monoclonal antibodies specified to *C. trachomatis*; protein-stabilized phosphate buffer; Evans Blue counter-stain; 0.01% sodium azide

Reconstitution diluent – deionized water; 0.1% sodium azide

The metal seal and rubber stoppers were removed from the *C. trachomatis* reagent vial and the reconstitution diluent vial. The lyophilized *C. trachomatis* reagent was reconstituted by the addition of 3.0ml reconstitution diluent. The vial was gently swirled to dissolve the contents and the reconstitution date recorded on the vial. The reagent was allowed to reach

room temperature of 20-25°C for 15 minutes before use and stored at 2-8°C for 12 weeks from the date of reconstitution.

2% Gluteraldehyde Solution

8 ml 25% gluteraldehyde

96ml EMEM

Add gluteraldehyde to EMEM and mix thoroughly.

Spurr Resin

10.0g Vinylcyclophene dioxide (VCD) (TAAB®)

6.0g Diglycidyl ether of polypropylene glycol (DER 736) (TAAB®)

26.0g Nonenyl succinic anhydride (NSA) (TAAB®)

0.4g Dimethylaminoethanol (DMAE) (Sigma®)

The 4 components were added to a beaker, covered and stirred with a magnetic stirrer until thoroughly mixed.

Uranyl acetate

A saturated solution of uranyl acetate (421.15 g/ml) was prepared in 50% ethanol:water and the solution allowed to settle for 4 hours. It was refrigerated until required and centrifuged for 15 minutes prior to use in order to pellet any particles.

Lead citrate

2.66 g Lead nitrate

3.52 g Sodium citrate

60 ml Distilled water

16 ml 1N Sodium hydroxide

Lead citrate was dissolved in 60 ml distilled water. On the addition of sodium citrate, a precipitate formed and was left to stand at room temperature for 30 minutes. After 30 minutes 1 N sodium hydroxide was added which dissolved the precipitate causing the solution became clear. This stain was filtered and refrigerated until use.

APPENDIX B – CALCULATIONS

Calculation of objective lens conversion factors

In order to calculate the conversion factor, the field area and hence the field diameter of each objective lens must be known.

The field diameter is calculated by dividing the eyepiece field of view number by the objective magnification and the tube factor. Then the radius (r), which is half the diameter, is used to calculate the area of the field of view. The objective lens conversion factor is then equal to the area of the well divided by the field area for a particular objective lens.

E.g. 40x objective

Objective field diameter = eyepiece field of view number ÷ objective magnification ÷ tube factor
= 20 ÷ 40 ÷ 1
= 0.5 mm

Radius = diameter ÷ 2
= 0.5 ÷ 2
= 0.25 mm

Objective field area $= \pi r^2$
$= (22 \div 7) \times 0.25^2$
$= 0.196\ mm^2$

Area of well $= \pi r^2$
$= (22 \div 7) \times 8^2$
$= 201\ mm^2$

Objective conversion factor = area of well ÷ objective field area
= 201 ÷ 0.196
= 1024

Table. Objective lens conversion factors

		Diameter (mm)	Radius (mm)	Field area (mm^2)	Conversion factor
Objective magnification	10x	2	1	3.143	64
	40x	0.5	0.25	0.196	1024
	50x	0.4	0.2	0.126	1600
	100x	0.2	0.1	0.031	6400
Well		16	8	201.1	1

APPENDIX C – RAW DATA

Chlamydial growth curve – inclusions per 10 thousand cells

ME-180 cells at 37°C

Day	Strain	Inclusions per 10 thousand cells									Mean
1	E	140	347	177	192	174	200	220	182	206	204
1	L1	175	163	233	183	156	218	289	258	342	224
1	L2	128	128	209	261	69	165	182	130	175	161
1	L3	151	163	325	227	35	26	244	198	160	170
1	US151	151	198	151	279	183	227	190	190	137	189
1	US162	70	58	116	35	139	200	38	99	114	97
1	US197	93	175	186	183	96	270	190	92	175	162
2	E	258	200	163	61	148	113	152	92	30	135
2	L1	378	416	384	270	374	366	266	258	198	323
2	L2	169	175	256	252	165	131	235	320	53	195
2	L3	148	189	215	261	174	105	106	152	23	153
2	US151	189	160	177	200	200	244	198	244	296	212
2	US162	55	75	70	69	18	69	38	38	46	53
2	US197	163	184	131	122	96	156	84	61	92	121
3	E	229	163	163	78	209	96	137	190	882	239
3	L1	405	774	1115	218	235	131	1551	2472	2480	1042
3	L2	436	934	235	244	113	592	2380	2601	2684	1136
3	L3	495	221	1449	69	122	156	342	578	289	413

3	US151	157	451	256	52	96	322	342	943	1095	413
3	US162	70	111	82	200	61	113	38	99	68	94
3	US197	165	160	294	183	122	113	228	396	296	217
4	E	1529	1233	945	662	1254	435	1225	1087	1225	1066
4	L1	892	1455	1315	453	827	244	2692	3156	4343	1708
4	L2	4608	4841	7656	3405	6827	4380	3544	6601	5978	5316
4	L3	722	454	1362	383	174	627	472	1217	1399	757
4	US151	1042	672	620	1724	235	1315	624	684	1080	888
4	US162	58	82	70	348	401	113	1301	791	114	364
4	US197	788	1038	335	1306	618	940	160	198	358	638
5	E	1706	938	2740	1350	3109	1767	2251	3072	1163	2011
5	L1	7285	11544	7447	1306	1776	1384	6069	9598	6434	5872
5	L2	4887	6400	5469	2647	2473	1602	2406	1853	2752	3388
5	L3	7656	4282	4631	2282	1785	1193	2890	3377	2327	3380
5	US151	2013	2385	1850	1541	2055	1602	4313	2031	958	2083
5	US162	896	1885	315	827	1446	1306	2327	1149	2023	1353
5	US197	3154	2467	989	862	1524	801	1141	1521	2342	1645

HaCaT cells at 37°C

Day	Strain	Inclusions per 10 thousand cells									Mean
1	E	134	124	147	90	90	202	141	125	110	129
1	L1	223	214	195	202	225	180	31	78	47	155
1	L2	121	147	140	202	157	225	63	78	78	135

1	L3	198	163	230	135	202	112	78	31	78	136
1	US151	179	163	112	157	67	67	31	47	47	97
1	US162	57	51	70	112	45	22	16	78	78	59
1	US197	150	108	102	157	22	90	63	78	31	89
2	E	179	121	89	112	157	45	266	172	157	144
2	L1	220	239	258	225	225	225	125	110	110	193
2	L2	144	191	188	157	157	135	282	219	125	178
2	L3	201	214	191	135	135	157	110	110	172	158
2	US151	115	150	226	67	90	67	282	251	251	167
2	US162	41	70	51	45	22	67	219	235	329	120
2	US197	172	92	179	112	202	67	251	251	329	184
3	E	102	182	166	129	168	118	63	219	392	171
3	L1	434	440	810	196	247	264	1144	360	141	448
3	L2	191	1225	182	309	820	539	564	909	689	603
3	L3	287	341	303	118	230	213	204	47	78	202
3	US151	360	421	290	124	219	101	172	157	360	245
3	US162	73	29	48	129	45	376	799	235	219	217
3	US197	453	332	440	174	140	101	251	282	251	269
4	E	1850	574	1084	1045	1644	2642	1253	1770	1692	1506
4	L1	3011	5129	2743	2135	492	584	924	1128	1222	1930
4	L2	6902	5001	4108	2504	2319	1521	10215	12753	7160	5831
4	L3	1365	2143	753	1137	292	261	846	188	1065	894
4	US151	1174	1161	1850	1183	922	1367	1911	2334	1582	1498
4	US162	179	204	204	645	1843	707	1050	1864	1410	901

4	US197	217	957	230	1306	1213	799	2381	705	924	970
5	E	1250	1123	1097	2995	3640	1905	3290	3556	3541	2489
5	L1	5920	4491	2194	461	415	492	1159	1896	2272	2144
5	L2	5307	6481	6813	8802	10399	11474	14038	13505	18236	10562
5	L3	3789	1301	2220	1751	399	507	1661	3306	3697	2070
5	US151	1263	1505	778	5422	5345	3226	5060	5687	4042	3592
5	US162	1072	89	574	5453	6405	2611	3212	8977	5248	3738
5	US197	357	510	1110	3395	2780	3210	3447	4778	2538	2458

HaCaT cells at 33°C

Day	Strain	Inclusions per 10 thousand cells									Mean
2	E	186	83	135	115	102	128	111	123	111	121
2	L1	114	135	166	204	204	217	190	211	245	187
2	L2	114	125	145	229	191	90	123	100	123	138
2	L3	73	125	104	102	77	77	134	156	78	103
2	US151	145	93	135	141	90	178	234	111	111	138
2	US162	52	93	73	64	51	90	78	134	56	77
2	US197	156	73	62	64	90	128	134	144	56	101
3	E	186	135	156	64	77	90	144	67	134	117
3	L1	166	238	197	141	153	165	256	245	290	206
3	L2	145	166	166	141	90	90	100	178	134	134
3	L3	62	114	83	128	77	77	67	167	144	102
3	US151	156	145	177	115	153	90	167	134	144	142

3	US162	83	73	104	77	77	102	111	78	44	83
3	US197	218	125	135	178	102	38	44	178	144	129
4	E	145	166	156	141	64	64	78	56	144	113
4	L1	186	114	156	77	90	128	156	190	156	139
4	L2	125	156	114	90	345	217	67	144	144	156
4	L3	41	135	62	115	204	293	56	44	100	117
4	US151	208	156	145	141	64	90	67	123	178	130
4	US162	52	166	31	26	51	90	56	123	56	72
4	US197	145	197	186	51	102	153	78	134	100	127
5	E	145	83	208	77	51	26	156	78	44	96
5	L1	156	62	114	128	77	64	44	89	78	90
5	L2	270	114	259	153	1021	357	67	123	211	286
5	L3	52	83	83	77	115	51	33	100	33	70
5	US151	177	166	156	115	204	115	78	44	89	127
5	US162	114	52	41	26	38	13	23	56	33	44
5	US197	197	104	285	153	64	102	44	44	56	117

Chlamydial growth curve – area occupied by chlamydia

ME-180 cells at 37°C

Day	Strain	Area occupied by chlamydia (μm^2)									Mean
1	E	0.1	0.1	0.1	0.3	0.1	0.3	0.4	0.4	0.4	0.2
1	L1	0.2	0.6	0.5	0.1	0.1	0.1	0.7	0.8	0.7	0.4

1	L2	0.4	0.4	0.4	0.6	0.1	0.3	0.4	0.4	0.3	0.3
1	L3	0.3	0.4	0.4	0.1	0.0	0.0	0.2	0.4	0.2	0.2
1	US151	0.3	0.2	0.2	0.1	0.3	0.2	0.5	0.2	0.3	0.3
1	US162	0.1	0.2	0.2	0.1	0.0	0.2	0.1	0.1	0.1	0.1
1	US197	0.4	0.2	0.6	0.0	0.0	0.3	0.2	0.2	0.3	0.2
2	E	0.3	0.2	0.2	0.1	0.0	0.0	0.1	0.4	0.1	0.2
2	L1	0.9	1.7	1.1	1.5	0.7	1.3	1.7	1.4	1.9	1.4
2	L2	1.1	1.3	0.9	1.1	0.6	1.5	1.7	1.2	1.0	1.1
2	L3	2.1	2.1	2.1	0.9	1.4	1.8	1.3	1.5	0.9	1.6
2	US151	0.3	0.4	0.3	0.2	0.2	0.6	0.3	0.5	0.5	0.4
2	US162	0.2	0.1	0.2	0.1	0.1	0.2	0.1	0.2	0.1	0.1
2	US197	0.2	0.3	0.3	0.1	0.2	0.5	0.4	0.1	0.1	0.2
3	E	0.5	0.6	0.4	0.2	0.2	0.2	0.8	0.6	0.5	0.4
3	L1	3.6	6.5	6.0	2.0	1.3	1.4	10.9	11.7	15.3	6.5
3	L2	6.5	3.2	3.0	1.6	2.2	3.3	19.2	15.1	13.2	7.5
3	L3	4.3	6.4	7.3	2.1	2.0	0.8	4.3	6.2	3.6	4.1
3	US151	0.7	2.0	0.5	0.3	0.2	0.5	1.0	2.8	1.3	1.0
3	US162	0.5	0.6	0.8	0.3	0.3	0.3	0.3	0.4	0.3	0.4
3	US197	0.9	0.9	1.0	0.4	0.4	0.2	1.1	0.9	1.6	0.8
4	E	3.6	0.7	1.3	0.6	2.0	1.0	2.0	4.8	4.3	2.2
4	L1	11.2	16.9	9.1	2.5	2.0	1.8	6.8	12.4	11.7	8.3
4	L2	30.4	14.2	18.3	10.5	17.5	11.9	59.8	38.6	24.0	25.0
4	L3	4.4	13.2	13.1	1.4	2.3	3.3	16.0	7.3	4.6	7.3
4	US151	2.3	1.4	2.5	3.2	0.5	3.1	1.8	1.0	2.4	2.0

4	US162	0.3	0.6	0.6	2.2	0.3	0.3	5.0	0.8	0.4	1.2
4	US197	2.5	4.6	2.3	1.3	0.8	1.2	1.4	3.3	1.7	2.1
5	E	3.2	1.7	2.7	4.0	4.3	2.0	5.4	3.8	6.8	3.8
5	L1	40.4	46.5	39.1	2.0	3.5	1.9	69.4	44.9	62.7	34.5
5	L2	120.4	101.5	79.3	20.0	39.5	18.5	61.8	53.3	54.5	61.0
5	L3	34.4	41.6	16.7	3.1	3.9	4.6	28.7	31.9	28.9	21.5
5	US151	7.2	8.5	9.3	1.4	2.4	2.8	10.2	6.5	5.1	5.9
5	US162	5.0	10.8	3.7	1.2	1.6	1.9	3.4	3.2	1.9	3.6
5	US197	8.7	4.6	5.0	1.3	1.7	3.2	3.4	4.7	6.9	4.4

HaCaT cells at 37°C

Day	Strain	Area occupied by chlamydia (μm^2)									Mean
1	E	0.2	0.1	0.1	0.1	0.1	0.1	0.1	0.0	0.1	0.1
1	L1	0.2	0.2	0.2	0.3	0.2	0.5	0.0	0.0	0.0	0.2
1	L2	0.2	0.2	0.1	0.2	0.3	0.3	0.0	0.0	0.0	0.1
1	L3	0.2	0.2	0.2	0.1	0.2	0.1	0.0	0.0	0.0	0.1
1	US151	0.1	0.2	0.1	0.1	0.0	0.3	0.0	0.0	0.1	0.1
1	US162	0.1	0.2	0.1	0.1	0.1	0.2	0.0	0.0	0.0	0.1
1	US197	0.1	0.1	0.1	0.3	0.1	0.1	0.0	0.0	0.0	0.1
2	E	0.3	0.4	0.4	0.2	0.2	0.2	0.2	1.0	0.3	0.4
2	L1	1.7	1.9	2.5	0.9	1.1	1.0	0.4	0.6	0.6	1.2
2	L2	1.3	1.4	1.2	0.4	1.0	0.9	0.8	1.1	1.2	1.0
2	L3	1.6	1.6	1.2	1.7	0.9	1.8	0.6	0.5	0.6	1.2

2	US151	0.7	1.4	1.2	0.3	0.2	0.2	0.5	0.6	0.7	0.7
2	US162	0.2	0.4	0.1	0.2	0.1	0.3	0.4	0.4	0.5	0.3
2	US197	0.8	0.6	0.8	0.6	0.7	0.4	0.6	0.3	0.6	0.6
3	E	0.9	0.9	0.7	0.2	0.7	0.5	1.2	0.5	1.3	0.8
3	L1	2.3	4.0	3.7	1.6	0.9	2.9	1.5	1.7	1.6	2.2
3	L2	2.7	3.0	3.5	1.3	3.2	1.7	2.8	2.1	3.8	2.7
3	L3	3.3	3.0	2.2	0.6	1.0	1.4	2.0	2.4	3.2	2.1
3	US151	1.4	1.6	1.1	0.3	0.8	0.9	1.5	0.8	0.9	1.0
3	US162	0.3	0.2	0.4	0.8	0.4	2.0	0.8	0.6	1.1	0.7
3	US197	0.8	0.7	0.6	0.2	0.6	1.4	0.7	1.1	0.7	0.8
4	E	2.1	1.4	1.5	2.8	4.4	1.5	5.6	2.1	6.4	3.1
4	L1	5.2	6.2	11.8	3.0	5.4	2.8	3.0	3.3	5.2	5.1
4	L2	25.0	16.7	15.7	12.8	14.8	6.2	8.9	15.7	23.0	15.4
4	L3	5.3	3.9	4.0	2.8	1.3	2.0	2.3	4.9	2.3	3.2
4	US151	2.2	0.9	2.4	2.2	2.2	4.5	2.0	1.4	2.7	2.3
4	US162	0.5	0.7	0.4	1.7	0.5	1.1	2.3	4.1	5.0	1.8
4	US197	0.8	2.9	3.8	3.5	2.2	1.5	4.1	1.1	8.4	3.2
5	E	2.8	2.6	4.2	5.2	8.5	8.8	5.5	13.4	6.8	6.4
5	L1	12.4	6.9	14.7	1.8	3.3	1.4	4.0	12.9	12.5	7.8
5	L2	30.4	13.5	39.8	29.7	40.0	35.0	71.1	57.0	62.0	42.1
5	L3	11.7	7.3	19.0	2.3	1.9	2.0	2.9	15.3	6.4	7.7
5	US151	3.7	3.4	3.5	11.2	10.2	8.4	6.3	10.8	3.2	6.8
5	US162	1.4	0.6	0.9	14.1	18.4	13.9	3.4	8.4	6.8	7.5
5	US197	1.0	5.3	2.5	6.5	5.2	9.5	8.3	18.0	4.6	6.8

HaCaT cells at 33°C

Day	Strain	Area occupied by chlamydia (μm^2)									Mean
1	E	0.0	0.0	0.0	0.0	0.0	0.0	0.0	0.0	0.0	0.0
1	L1	0.0	0.0	0.0	0.0	0.0	0.0	0.0	0.0	0.0	0.0
1	L2	0.1	0.0	0.0	0.0	0.0	0.0	0.0	0.0	0.0	0.0
1	L3	0.0	0.0	0.0	0.0	0.0	0.0	0.0	0.0	0.0	0.0
1	US151	0.0	0.0	0.0	0.0	0.0	0.0	0.0	0.0	0.0	0.0
1	US162	0.0	0.0	0.0	0.0	0.0	0.0	0.0	0.0	0.0	0.0
1	US197	0.0	0.0	0.0	0.0	0.0	0.0	0.0	0.0	0.0	0.0
2	E	0.1	0.0	0.0	0.1	0.1	0.1	0.1	0.1	0.1	0.1
2	L1	0.2	0.1	0.0	0.2	0.2	0.2	0.1	0.2	0.1	0.2
2	L2	0.2	0.1	0.1	0.3	0.1	0.2	0.1	0.1	0.2	0.1
2	L3	0.0	0.0	0.0	0.1	0.1	0.0	0.0	0.1	0.0	0.0
2	US151	0.1	0.0	0.0	0.2	0.2	0.2	0.1	0.1	0.2	0.1
2	US162	0.1	0.0	0.0	0.1	0.1	0.1	0.1	0.1	0.1	0.1
2	US197	0.1	0.1	0.1	0.2	0.1	0.2	0.1	0.2	0.2	0.1
3	E	0.2	0.2	0.2	0.4	0.1	0.1	0.3	0.4	0.2	0.2
3	L1	0.2	0.5	0.3	0.4	0.3	0.3	0.3	0.6	0.5	0.4
3	L2	0.2	0.5	0.8	0.6	1.2	0.4	0.5	0.5	0.5	0.6
3	L3	0.2	0.3	0.1	0.3	0.4	0.5	0.2	0.2	0.3	0.3
3	US151	0.1	0.2	0.3	0.2	0.4	0.2	0.4	0.2	0.3	0.2
3	US162	0.0	0.1	0.0	0.1	0.1	0.3	0.2	0.1	0.3	0.1
3	US197	0.3	0.1	0.3	0.2	0.4	0.1	0.3	0.4	0.5	0.3

4	E	0.4	0.4	0.4	0.2	0.3	0.4	0.3	0.2	0.3	0.3
4	L1	0.7	0.7	0.9	0.6	0.6	0.4	0.6	0.7	0.5	0.6
4	L2	0.9	1.1	0.6	0.6	1.5	2.6	0.6	0.6	1.0	1.1
4	L3	0.2	0.6	0.3	0.4	0.6	0.5	0.8	0.6	0.5	0.5
4	US151	1.0	0.7	0.7	0.3	0.5	0.2	0.1	0.5	0.3	0.5
4	US162	0.2	0.3	0.3	0.2	0.1	0.1	0.3	0.4	0.2	0.2
4	US197	0.7	0.5	0.5	0.5	0.4	0.2	0.2	0.5	0.3	0.4
5	E	0.7	0.2	0.3	0.3	0.4	0.2	0.3	0.2	0.2	0.3
5	L1	0.9	0.3	0.2	0.7	0.5	0.7	0.3	0.3	0.4	0.5
5	L2	3.3	1.8	1.3	2.0	2.6	3.2	1.3	0.6	1.0	1.9
5	L3	0.3	1.1	1.4	1.3	1.2	1.5	0.8	0.9	0.6	1.0
5	US151	0.4	0.2	0.5	0.5	0.3	0.2	0.4	0.2	0.2	0.3
5	US162	0.3	0.2	0.2	0.2	0.2	0.1	0.2	0.2	0.2	0.2
5	US197	0.4	0.5	0.6	0.3	0.5	0.6	0.2	0.3	0.3	0.4

Inclusion size in HaCaT cells at 33°C

Day	Strain	Inclusion size (μm^2)
2	E	42 85 50 82 77 74 41 87 97 90 63 37 45 46 66 95 131 186 180 123 165 76 43 37 72 202 75 188 383 89 193 54 96 75 117 98 66 147 122 89 108 154 85 59 163 131 94 121 115 148 88 127 136
2	L1	235 196 76 65 291 143 68 121 59 47 40 89 113 50 133 57 67 66 167 52 66 46 167 163 66

		165 50 119 103 178 67 218 108 112 49 89 77 75 191 182 98 214 77 113 103 265 118 163 36 132 48 123 377 94 120 297 41 95 120 76 44 57 80 99 154 106 83 62 103 80 99 128 86 93 71 146 143 101 88 109 209 153 39 133 77 43 60 129 54 66 51 179 87 93 57 69
2	L2	131 110 182 311 125 200 121 236 62 144 120 36 72 301 72 100 58 49 49 44 138 237 51 82 544 309 127 290 46 126 334 107 114 159 199 62 220 142 288 60 136 101 218 78 173 388 157 169 66 162 91 136 252 51 137 107 237 232 198 243 193 111 231 125 103 143 52 160 234 138 154 171 130 98 182
2	L3	40 76 85 51 57 46 37 36 51 85 59 60 103 50 49 36 71 128 40 73 122 65 49 75 70 41 77 59 57 57 91
2	US151	172 116 90 296 91 40 294 76 76 63 65 251 131 156 122 130 87 167 125 133 55 127 99 114 151 108 41 92 50 99 62 102 208 244 179 257 240 163 165 186 104 93 138 136 117 128 130 138 56 130 166 102 150 141 146 88 67 156 51 140 144 220 157 196 45 252 217 76 114 102 57
2	US162	60 52 105 63 80 66 80 62 80 47 62 95 49 66 159 63 122 214 91 62 167 47 186 67 115 150 324 168 63 115 141 157 47 118 124 92 60 128 142 178 172 154 144
2	US197	93 70 86 108 182 99 167 103 63 147 107 112

		67 126 86 149 65 238 108 59 124 49 50 60 177 124 70 103 54 85 201 176 170 160 73 43 153 224 158 118 54 131 169 153 107 127 174 165 140 241 106 153 91 85 50 154 79 151 107 53 242 73 126 91 193 110 165 178 137 87 143 144 72 83 136 134 146 66 131 66 106 135 89 67 80
3	E	195 131 351 129 227 178 130 144 147 133 123 241 255 289 141 66 263 122 254 338 222 100 237 66 65 149 179 214 267 331 154 158 309 136 37 402 159 194 341 74 431 209 167 44 274 234 45 181 101 72 56 387 189 196 102 69 85 127 321 110 344 235 121 319 211 342 260 195 439 198 140 121 196 159 467 281 276 394 233 190 253 279 440 408 170 287 330 38 275 378 149 196 233
3	L1	64 201 61 450 113 218 126 300 424 454 409 157 638 278 292 146 172 48 67 111 94 362 366 315 51 474 207 730 233 88 302 547 80 353 79 105 51 278 372 108 328 622 388 749 250 67 563 631 78 173 83 345 202 572 36 142 167 309 421 105 596 341 70 118 335 195 45 165 23 255 338 554 775 97 315 859 470 331 329 91 180 497 88 399 477 295 314 453 63 44 62 315 265 88 400 156 378 639
3	L2	183 285 205 289 251 180 600 60 492 447 450 395 45 580 266 747 153 1205 1127 317 581 262 117 834 721 1485 635 766 540 659 860 889 910 549 486 121 273 987 96 1454 241 76 1345 529 749 1369 102 482

		661 424 1148 231 1001 1560 131 619 249 331 866 744 338 253 988 391 98 485 70 537 966 522 72 85 774 721 1146 717 168 179 301 466 404 179 76 579 796 872 560 430 552 56 356 103
3	L3	38 483 127 132 41 40 133 469 741 357 43 519 560 107 182 411 195 712 173 92 147 133 199 199 328 261 427 45 57 50 152 157 260 117 218 436 241 198 345 420 441 55 441 72 104 157 59 395 72 71 124 56 44 41 475 83 82 423 170 36 449 186 105 204 439 345 157 414 589 449 156 415 234 133 36 198 89 70
3	US151	78 107 245 105 153 144 57 59 187 46 117 367 183 231 151 257 77 363 166 218 324 165 222 440 49 288 252 330 72 344 190 395 198 167 153 211 177 118 140 305 104 249 158 117 401 58 214 110 44 86 178 360 200 282 148 259 143 159 139 256 478 227 230 251 92 247 331 301 469 206 259 283 112 91 315 341 217 452 172 238 265 93 325 142 189 73 402 91 136 174 257 244 86
3	US162	142 64 143 154 240 207 226 289 55 173 82 96 265 123 273 182 275 60 292 241 36 194 269 191 45 141 379 152 210 156 293 72 306 312 236 59 511 375 44 303 278 276 166 547 207 334 238 98
3	US197	201 242 354 312 133 124 404 246 298 201 191 160 71 150 182 128 254 284 201 164 267 248 316 358 217 125 167 172 181 263 215 347 102 387 400 321 61 163 269 253 304 165 129 45 154 154 63 92

		79 220 37 56 372 285 258 366 253 427 261 58 141 132 681 178 220 81 330 109 243 37 83 46 147 285 57 98 229 158 65 196 129 178 186 118 66 366 372 313 318 279 209 160 220 76 200 328 276 290 355 222 82 111 323 392
4	E	188 509 256 428 183 591 211 551 335 462 131 463 188 466 520 441 351 477 193 344 288 327 159 193 249 287 101 251 582 283 625 418 272 172 205 404 430 475 143 249 354 54 54 293 117 257 179 225 297 365 665 507 459 313 67 277 225 407 156 562 256 318 144 262 82 179 38 136 66 505 198 370 481 169 120 119 82 644 133 436 497 114 420 298 370 85 75 376 43 67 228 336 214 41
4	L1	303 330 967 268 670 1048 1188 378 352 821 217 66 158 178 86 762 149 85 278 341 1118 565 89 122 460 871 1525 63 51 144 103 251 56 838 538 78 98 1118 775 48 571 646 1011 417 600 1108 1500 437 560 163 315 149 476 612 327 40 931 131 421 439 380 43 721 296 195 537 608 333 792 75 224 492 163 295 671 1020 826 679 507 225 1040 302 225 105 320 639 794 569 85 678 756 66 687 147 89 58 586 917 405 920
4	L2	1041 741 1615 322 105 36 51 707 1131 1277 118 767 79 1408 975 650 228 676 1529 721 780 1018 1049 1244 655 816 670 398 819 555 290 844 679 66 1751 655 440 1487 167 585 1133 870 36 969 163 542 67 105 2370 644 1171 48 1387 609 691 187 3542 4489 158

		658 1711 2550 1512 1149 395 329 1680 496 713 1321 1653 493 1162 40 654 173 681 827 541 639 2178 697 947 211 2106 1167 1469 875
4	L3	221 97 479 135 515 806 760 57 36 1675 927 1211 633 1159 632 38 811 335 45 70 50 2628 325 257 830 44 953 941 1482 1213 2296 47 1133 1223 1443 1699 1130 597 1104 431 699 834 1303 1377 146 838 36 133 43 1278 119
4	US151	548 617 351 440 45 422 283 608 225 486 838 352 107 322 49 429 539 475 292 355 472 577 480 411 43 468 140 492 423 535 238 821 253 284 559 476 598 130 272 370 389 487 463 273 615 660 614 475 457 528 425 474 356 438 449 78 230 626 579 225 130 325 260 284 650 159 144 109 204 214 254 249 597 354 475 507 143 96 219 290 331 150 465 330 285 126 241 450 340 409 538 101 451 643 284 48 228 625 128 89 87 284 464 150 110 83 318 155 462 337
4	US162	475 56 641 42 56 446 289 395 393 558 605 353 43 565 242 372 133 64 194 253 598 1010 419 831 425 475 253 576 109 188 63 149 94 299 183 428 460 167 608 127 264 46 146 247 245 407 356 430 273 494 213 247 83 104 1165 327 97 526 499 181 44 254 88 961 134 376 75 380 305
4	US197	98 444 138 440 790 550 414 312 547 346 541 430 600 532 42 115 537 630 188 480 557 301 270 193 243 307 461 375 147 121 377 141 366 126 502 418

		199 381 385 301 477 399 135 853 106 943 446 423 404 56 98 53 301 436 426 239 259 447 235 104 290 515 280 283 430 293 588 428 424 171 421 143 420 528 606 362 360 67 769 140 166 345 113 167 331 208 49 250 104 273 206 44 421 93 383 463 577 507 517 416 357 471 273 567 811 256 298 676 395 466 299 290 454 482 307 380 333
5	E	622 593 472 570 325 746 462 931 112 879 262 499 505 79 385 62 67 79 421 103 440 65 69 82 305 128 41 526 264 229 61 408 624 50 322 295 485 446 75 89 712 39 136 187 399 485 669 47 152 195 82 431 486 62 567 153 47 332 902 607 99 459 302 87 272 478 366 490 180 550 531 307 544 310 117 653 46 260
5	L1	41 1083 104 876 45 53 1318 169 641 821 1195 54 113 750 69 59 57 318 65 934 326 646 192 265 152 80 40 72 45 57 1873 1138 1165 632 201 126 117 1066 242 1580 108 1051 791 91 230 937 49 50 72 39 62 1273 719 270 70 53 431 150 337 49 622 1263 613 85 640 288 983 145 739 1116 417
5	L2	2327 576 212 2538 748 1493 760 982 324 174 468 48 418 382 285 99 1346 212 197 151 399 145 678 238 115 337 473 217 98 528 273 129 661 493 827 159 959 585 715 617 276 111 278 305 176 326 184 509 618 2996 933 2737 1309 2279 667 1166 954 1176 1453 1130 73 1034 662 596 785 38 40 1447 2371 879 1156 858 825 2009 898 157 47 42 44 60 67 36 2120

		865 2366 2401 756 1473 176 47 2312 57 85 39 454 1706 59 239 295 649 92 112 192 62 1788 904 314 265 169 2565 379 470 1660 99 311 396 161 973 226 366 136 460 85 124 140 492 39 212 244 404 120 446 237 662 452 630 729 458 1201 131 791 876 395 965 544 105 692 59 1743 295 658 81 421 917 486 547 544 354 180 161 117 56 530 77 79 715 1413 886 650 1454 745 724 82 88 48 1504 1050 834 331 49 95 38 36 83 524 397 1792 649 1615 112 2328 973 3645 130 611 204 1686 1033 148
5	L3	274 91 56 72 44 1552 1421 584 866 1075 1685 956 63 431 81 1675 1288 2372 472 57 269 2433 667 41 767 3178 36 47 1007 2807 91 1098 69 2076 2027 395 42 38 36 113 228 1601 76 2182 72 37 42 59 648 551 90 50 60 54 162 58 121 1546 43 67 55 151 44 80 824 2221 99 1757 83 144 2131 79 2334 37 594 62 42 44 142 143 2494 1921 1877 367 1920 51 502 38 1047 597 628 1059 992
5	US151	706 36 349 546 793 151 262 212 332 318 83 162 259 722 538 54 507 75 244 47 488 41 354 502 1176 199 598 354 567 41 56 119 557 650 813 72 436 490 731 41 46 110 115 250 263 232 704 340 451 509 594 79 85 150 673 109 305 66 148 521 448 404 59 261 266 348 390 560 200 482 64 41 550 78 200 488 93 206 69 734 83 185
5	US162	550 912 620 584 57 397 770 688 557 349 224 267 128 905 385 456 266 140 166 320 503 40 381 178

		263	502	321	133	341	161	288	380	494	83	272	165
		191	420	250	98	544	307	445	535				
5	US197	99	679	228	155	215	368	72	218	394	658	576	446
		111	235	411	575	439	203	60	539	43	685	63	221
		83	172	376	646	139	534	482	591	159	369	434	238
		647	86	95	154	76	107	524	315	480	415	432	141
		76	556	892	457	73	62	36	215	120	66	82	143	61
		62	492	392	92	175	735	107	537	137	483	60	58
		689	417	499	60	576	554	270	269	440	580	715	154
		496	80	273	892	604	382	1087	140				

MTT assay

ME-180 cells at 37°C

Hrs	Strain	% mitochondrial acitivity									Mean
1	Spont*	95	103	102	114	104	82	107	94	99	100
1	E	102	104	123	80	87	77	91	90	100	95
1	L2	97	100	115	90	87	76	103	60	112	93
1	L3	104	120	123	93	99	95	100	89	102	103
1	Eto#	110	119	86	76	72	77	88	107	106	93
3	Spont	87	115	98	107	97	96	79	102	119	100
3	E	82	116	90	106	89	95	77	85	87	92
3	L2	104	111	119	97	91	96	77	100	90	98
3	L3	102	103	110	96	98	86	79	96	94	96

3	Eto	101	102	118	84	96	103	87	94	73	95
9	Spont	101	99	99	86	103	112	126	87	87	100
9	E	106	111	113	102	113	125	74	84	77	100
9	L2	107	102	102	82	100	108	75	83	87	94
9	L3	92	98	98	79	103	109	88	104	74	94
9	Eto	94	98	109	136	81	84	82	77	97	95
18	Spont	101	102	96	110	101	89	88	101	110	100
18	E	106	102	105	103	99	109	101	98	99	102
18	L2	112	115	110	100	118	86	96	87	90	101
18	L3	109	104	97	115	102	106	70	87	92	98
18	Eto	92	91	86	101	113	79	64	89	93	90
24	Spont	109	91	100	92	98	110	100	94	106	100
24	E	95	103	103	94	99	102	87	114	120	102
24	L2	104	104	104	94	97	102	90	93	88	97
24	L3	95	93	83	98	101	99	85	93	100	94
24	Eto	75	77	70	77	72	75	69	60	64	71
36	Spont	94	98	108	107	99	93	109	94	97	100
36	E	99	110	110	128	96	88	90	83	84	99
36	L2	96	102	107	104	81	80	91	80	85	92
36	L3	96	103	101	115	103	102	73	76	77	94
36	Eto	35	42	43	45	41	56	27	27	29	39
48	Spont	104	106	89	109	96	94	90	98	112	100
48	E	108	114	108	105	105	107	90	89	99	103
48	L2	108	96	106	108	96	97	80	89	94	97

48	L3	93	95	91	108	88	94	85	84	99	93
48	Eto	14	10	14	57	45	50	12	10	12	25

* spontaneous mitochondrial activity without chlamydia

cells treated with etoposide

HaCaT cells at 37°C

Hrs	Strain	% mitochondrial acitivity									Mean
1	Spont*	85	114	101	92	112	97	89	114	97	100
1	E	89	72	90	86	84	89	83	83	78	84
1	L2	88	95	84	99	84	86	85	91	95	90
1	L3	99	97	81	100	96	97	93	87	90	93
1	Eto#	95	111	95	89	102	104	94	101	100	99
3	Spont	98	95	106	99	103	98	96	106	98	100
3	E	99	84	99	91	93	103	84	88	94	93
3	L2	106	104	114	91	99	96	83	100	90	98
3	L3	99	100	103	83	86	89	112	94	89	95
3	Eto	105	106	107	94	86	112	91	96	88	98
9	Spont	110	96	94	108	101	91	107	100	93	100
9	E	103	98	107	71	108	112	90	109	99	100
9	L2	97	99	94	99	122	115	105	103	96	103
9	L3	102	102	99	89	104	91	103	93	96	98
9	Eto	111	105	99	97	99	79	106	102	102	100
18	Spont	103	100	97	99	92	109	97	104	100	100

18	E	101	101	103	80	101	99	91	89	95	95
18	L2	92	91	96	88	103	114	93	90	86	95
18	L3	102	106	97	112	103	103	89	92	92	99
18	Eto	102	96	95	107	109	101	78	79	81	94
24	Spont	103	97	100	100	96	104	106	102	92	100
24	E	109	104	102	92	92	99	99	91	100	99
24	L2	106	126	108	109	94	100	102	95	101	105
24	L3	106	108	105	133	94	102	101	94	87	103
24	Eto	99	94	103	86	94	95	71	70	77	88
36	Spont	100	102	98	90	96	114	112	92	97	100
36	E	90	94	88	96	93	111	98	84	92	94
36	L2	84	91	96	86	104	111	103	84	92	94
36	L3	92	89	94	85	84	110	102	83	94	92
36	Eto	67	71	70	60	59	75	64	67	60	66
48	Spont	104	97	99	104	98	99	105	96	99	100
48	E	100	89	97	127	93	130	99	96	89	102
48	L2	96	91	97	111	125	127	91	87	81	101
48	L3	98	84	90	101	113	108	90	77	84	94
48	Eto	61	57	62	19	21	23	47	44	44	42

* spontaneous mitochondrial activity without chlamydia

cells treated with etoposide

HaCaT cells at 33°C

Hrs	Strain	% mitochondrial acitivity									Mean
1	Spont*	93	100	107	108	96	96	94	103	103	100
1	E	94	94	89	85	106	105	96	101	101	97
1	L2	106	103	102	96	110	84	84	94	87	96
1	L3	96	99	92	101	143	113	92	96	88	102
1	Eto#	98	104	103	104	112	105	92	91	97	101
3	Spont	98	104	98	106	98	96	109	110	81	100
3	E	74	96	95	80	122	95	94	91	96	94
3	L2	95	102	105	101	104	115	93	95	83	99
3	L3	100	102	101	99	115	119	106	91	100	104
3	Eto	91	94	100	95	107	91	107	131	89	101
9	Spont	105	96	99	89	119	92	98	106	97	100
9	E	92	99	119	105	88	100	74	81	87	94
9	L2	104	104	101	107	105	101	86	84	75	97
9	L3	106	100	97	127	88	105	65	93	75	95
9	Eto	106	101	91	86	76	79	62	105	90	88
18	Spont	104	99	97				118	85	97	100
18	E	103	102	110				90	118	90	102
18	L2	94	92	81				89	105	117	96
18	L3	109	103	109				103	104	87	102
18	Eto	96	99	90				82	102	78	91
24	Spont	88	110	102	90	110	101	110		125	104
24	E	80	95	88	95	115	118	111	106	115	103
24	L2	82	86	104	94	113	110	106	122	121	104

24	L3	78	86	102	56	101	103	123	112	102	96
24	Eto	79	97	102	90	90	96	95	78	110	93
36	Spont	103	102	95	127	73	100	103	95	101	100
36	E	81	96	86	102	91	91	95	92	97	92
36	L2	89	95	95	107	95	90	103	92	101	96
36	L3	89	85	71	96	91	91	100	93	103	91
36	Eto	81	88	82	107	81	86	76	71	75	83
48	Spont	108	100	92	98	95	107	101	98	101	100
48	E	99	90	100	111	101	112	108	99	93	101
48	L2	93	92	101	118	96	113	95	93	91	99
48	L3	96	83	93	103	120	101	96	93	90	97
48	Eto	79	90	79	61	75	79	69	71	69	75

* spontaneous mitochondrial activity without chlamydia

cells treated with etoposide

Lactate dehydrogenase assay - % cytotoxicity

ME-180 cells at 37°C

Day	Strain	% cytotoxicity									Mean
1	E	-0.3	2.4	1.7	0.0	-0.1	-0.4	0.2	0.2	-0.2	0.4
1	L1	0.5	1.1	0.8	0.4	0.3	1.6	-0.1	-0.2	0.1	0.5
1	L2	2.1	0.5	0.5	-0.7	0.4	0.3	-0.8	-0.3	-0.7	0.1
1	L3	2.1	1.0	1.3	0.0	-0.8	-0.2	0.6	-0.5	-0.4	0.3
1	US151	1.6	1.0	1.2	0.8	0.2	0.3	-0.6	-0.3	-0.1	0.4

1	US162	0.8	0.8	0.9	0.0	-0.3	0.0	-0.5	0.2	0.4	0.2
1	US197	1.5	0.1	1.5	0.8	-0.2	0.9	0.4	0.4	-0.1	0.6
2	E	1.6	2.2	0.5	-1.5	-0.9	-0.9	-0.2	0.7	0.5	0.2
2	L1	1.5	0.6	1.4	-0.3	-0.4	-0.2	1.3	1.5	0.5	0.7
2	L2	0.4	2.2	1.1	-2.7	-1.3	-0.2	1.7	0.2	0.2	0.2
2	L3	1.3	1.6	0.8	-1.1	-1.0	0.0	1.7	0.7	0.7	0.5
2	US151	1.3	1.0	0.6	-0.1	-0.3	-0.5	1.6	1.1	1.1	0.6
2	US162	1.6	0.7	0.0	-0.4	0.8	1.1	0.5	0.7	2.2	0.8
2	US197	1.3	1.1	1.3	-0.6	0.3	0.6	0.5	0.5	0.2	0.6
3	E	2.2	1.1	0.1	0.0	0.5	0.6	2.7	-1.7	0.4	0.7
3	L1	2.6	1.5	4.1	2.3	0.6	4.3	4.5	1.6	3.6	2.8
3	L2	-0.4	1.2	0.4	0.1	-0.5	-1.5	2.1	1.4	3.2	0.6
3	L3	2.3	2.4	1.6	1.1	1.3	0.3	4.0	2.5	2.2	2.0
3	US151	3.1	2.4	1.4	3.1	1.6	1.8	3.4	3.2	4.0	2.6
3	US162	3.4	2.2	3.2	1.5	1.4	1.2	3.3	2.8	3.5	2.5
3	US197	3.2	2.8	1.8	0.6	1.9	1.0	3.8	2.7	2.2	2.2
4	E	-5.3	-4.6	-7.1	2.5	2.0	3.0	1.8	1.3	1.5	-0.6
4	L1	1.1	1.2	-0.9	4.3	3.3	4.0	-0.3	-0.1	0.5	1.5
4	L2	0.0	-0.6	-2.3	3.7	5.2	3.3	10.7	8.0	7.4	3.9
4	L3	1.6	-1.0	-1.2	3.6	3.8	3.2	2.4	0.8	-0.9	1.4
4	US151	3.3	1.9	1.5	3.9	2.7	1.4	0.0	0.1	0.0	1.6
4	US162	-0.1	-0.2	-0.8	2.6	1.6	2.9	-0.3	-0.7	-0.5	0.5
4	US197	-2.6	-0.7	-1.1	3.4	2.0	2.1	0.2	1.2	-0.2	0.5
5	E	-4.6	-6.1	-7.2	0.8	-0.7	0.2	-7.9	-5.8	-5.6	-4.1

5	L1	-2.7	-6.8	-7.6	-2.0	-1.1	-1.9	-1.8	-5.4	-4.6	-3.8
5	L2	11.9	-0.9	-4.0	10.7	14.2	6.2	41.0	34.3	22.9	15.1
5	L3	-2.9	-4.6	-8.6	-1.6	-1.6	-2.0	-2.8	-7.9	-7.5	-4.4
5	US151	-6.9	-7.2	-9.4	-3.1	-2.2	-2.7	-10.8	-11.6	-11.3	-7.2
5	US162	-7.9	-9.2	-10.2	-4.2	-5.9	-6.6	-11.3	-11.1	-11.5	-8.6
5	US197	-8.3	-10.5	-11.1	-5.1	-3.3	-4.6	-11.4	-11.4	-11.4	-8.6

HaCaT cells at 37°C

Day	Strain	Values									Mean
1	E	-0.7	-0.3	-0.4	0.4	0.6	0.0	3.5	2.9	0.8	0.7
1	L1	-1.0	-0.8	-0.7	0.1	0.0	0.1	3.5	4.1	4.2	1.1
1	L2	-1.2	-1.1	-0.6	-0.2	-0.1	0.2	1.3	4.1	6.2	1.0
1	L3	-0.9	-0.9	0.0	0.8	0.6	0.1	4.5	3.5	3.3	1.2
1	US151	-0.6	-0.8	-0.9	0.7	0.7	0.7	4.3	3.5	2.8	1.1
1	US162	-1.3	-1.6	-0.5	0.7	0.6	0.8	5.2	5.7	4.7	1.6
1	US197	-0.9	-0.2	0.0	0.4	0.8	0.6	2.0	2.6	2.3	0.9
2	E	0.0	0.4	0.4	0.3	-0.5	-0.2	-0.7	-0.3	-0.8	-0.1
2	L1	0.4	-0.2	0.5	0.0	-0.6	-0.9	-0.2	-0.2	-1.0	-0.2
2	L2	0.4	-0.6	0.3	-1.0	-1.5	-0.9	-0.8	-0.3	-0.2	-0.5
2	L3	-0.4	-0.2	-0.6	0.2	-0.2	-0.6	-0.5	-0.8	-0.8	-0.4
2	US151	0.0	-0.7	-0.1	1.0	0.0	-0.3	-0.7	-0.5	-0.1	-0.1
2	US162	0.5	-0.2	-0.1	0.8	0.0	0.3	.	0.3	0.0	0.2
2	US197	0.1	0.4	0.1	1.6	0.4	1.0	-0.4	-0.3	-0.1	0.3

3	E	-0.5	-0.4	0.6	0.1	0.0	0.0	-2.7	-2.6	-2.3	-0.9
3	L1	2.5	1.5	2.3	-0.6	0.2	0.2	-2.2	0.3	-0.8	0.4
3	L2	0.0	0.4	-0.2	-0.7	-0.1	-0.9	-0.7	-1.7	-0.7	-0.5
3	L3	1.3	0.8	1.4	0.7	-0.6	-0.2	-1.4	-1.1	-1.3	0.0
3	US151	2.7	2.9	3.1	-0.5	-0.4	-0.1	0.6	-2.0	-1.7	0.5
3	US162	3.3	3.4	2.9	-1.0	-0.4	0.2	-0.8	-0.1	-1.3	0.7
3	US197	2.0	0.9	1.3	0.1	0.2	-0.4	-1.3	-0.1	-1.3	0.2
4	E	0.6	-1.7	3.0	-1.0	-1.9	-1.2	-2.9	-1.4	-2.1	-1.0
4	L1	3.0	3.9	3.6	-2.5	-0.2	-0.9	1.9	-0.4	-0.7	0.9
4	L2	-0.8	-2.1	-1.4	-0.6	-0.4	-0.5	1.2	0.3	-0.3	-0.5
4	L3	3.3	3.9	3.7	-1.5	-3.0	-0.7	-0.8	-1.9	-2.1	0.1
4	US151	4.1	5.2	3.3	3.7	1.8	2.1	-1.3	-2.3	-2.5	1.6
4	US162	4.9	6.9	6.9	0.1	0.7	4.7	0.2	0.1	0.9	2.8
4	US197	4.6	4.9	5.3	1.2	-0.1	0.5	-1.4	0.2	0.4	1.7
5	E	4.8	6.4	1.7	-0.5	-1.2	-3.5	-0.1	6.2	-0.4	1.5
5	L1	0.8	-0.1	0.5	-0.1	-0.6	2.2	0.5	0.6	0.8	0.5
5	L2	4.4	2.3	3.2	-0.3	2.5	3.0	7.1	5.9	4.9	3.6
5	L3	-0.6	-1.3	0.8	-1.7	-1.3	2.3	1.9	2.3	3.7	0.7
5	US151	5.9	3.3	2.7	3.5	0.8	2.0	0.0	0.6	-0.7	2.0
5	US162	6.1	6.7	6.3	4.1	3.0	2.7	0.3	0.7	1.5	3.5
5	US197	2.0	2.3	-1.7	-6.2	0.0	-0.3	0.4	-1.4	-1.0	-0.6

HaCaT cells at 33°C

Day	Strain	Values									Mean
1	E	0.0	0.1	0.0	0.2	0.7	0.4	-2.4	-2.2	-2.3	-0.6
1	L1	0.2	-0.1	-0.5	0.5	0.9	0.3	-2.0	-1.9	-2.3	-0.6
1	L2	-0.1	-0.3	-0.1	1.0	0.5	0.3	-2.4	-2.0	-2.3	-0.6
1	L3	0.0	0.0	0.0	-0.2	0.5	0.3	-1.9	-2.0	-2.2	-0.6
1	US151	0.2	0.8	0.1	0.4	0.7	0.4	-2.2	-1.5	-2.2	-0.4
1	US162	-1.5	0.2	-0.8	0.6	0.5	0.7	-1.8	-2.1	-2.2	-0.7
1	US197	0.6	1.0	0.1	-0.1	0.1	0.5	-2.3	-0.6	-2.2	-0.3
2	E	-0.6	-0.8	-0.7	-0.7	-0.1	-0.6	-0.3	-0.8	-0.1	-0.5
2	L1	-1.1	-0.7	-0.1	-0.6	-1.3	-0.4	1.3	1.3	0.5	-0.1
2	L2	-1.2	0.6	-0.7	-0.4	-0.1	-0.7	0.6	-0.1	0.7	-0.1
2	L3	-1.8	-0.3	-0.9	0.9	-0.1	-0.3	-0.2	-0.1	1.4	-0.2
2	US151	0.6	0.5	0.3	-0.3	0.2	-0.4	1.2	0.7	0.8	0.4
2	US162	-0.6	0.4	-0.3	-0.1	-1.0	-0.9	1.0	0.3	0.7	-0.1
2	US197	0.8	0.1	0.1	0.1	0.3	0.5	0.7	0.4	1.5	0.5
3	E	-1.3	1.0	-0.2	0.5	-0.4	0.0	-2.2	-2.0	-1.7	-0.7
3	L1	-0.6	-1.2	-0.4	0.0	0.3	-0.2	-2.2	-2.3	-1.4	-0.9
3	L2	-0.5	0.8	-0.8	0.3	0.6	0.7	-1.4	-2.4	-1.8	-0.5
3	L3	-0.4	-1.5	-1.7	0.3	0.3	0.7	-3.1	-2.8	-1.5	-1.1
3	US151	0.9	1.3	2.0	-0.8	0.9	-0.4	-1.5	-1.2	-1.8	-0.1
3	US162	-0.2	1.0	-0.2	0.0	-0.1	0.6	-0.4	-0.7	-1.0	-0.1
3	US197	0.8	1.0	0.8	0.7	0.1	-0.5	-1.3	-1.3	-1.5	-0.1
4	E	0.3	-0.4	-1.7	-1.7	-0.3	-0.7	3.4	1.4	0.9	0.1
4	L1	1.1	1.0	1.0	0.4	-0.1	-2.8	0.8	0.7	1.2	0.4

4	L2	0.6	0.9	0.8	-0.1	-1.5	-0.9	-0.5	-1.1	0.9	-0.1
4	L3	0.5	0.4	0.7	-0.8	-1.2	-1.2	1.0	0.8	-1.6	-0.2
4	US151	0.5	0.8	0.6	1.4	-0.4	-0.5	4.2	2.9	1.7	1.2
4	US162	0.6	-0.4	-0.5	1.0	0.4	1.4	0.3	1.3	2.4	0.7
4	US197	-1.6	-1.4	-1.6	1.3	0.9	0.2	1.0	1.0	2.5	0.3
5	E	-1.0	-2.1	0.2	1.9	3.5	0.6	16.8	12.7	8.7	4.6
5	L1	-1.5	0.6	-1.2	1.1	-0.6	0.4	17.2	11.1	20.4	5.3
5	L2	-1.3	1.8	1.7	2.6	1.9	-0.5	19.9	7.4	10.2	4.8
5	L3	0.1	-2.0	2.2	4.0	2.5	0.8	21.1	14.9	13.1	6.3
5	US151	1.9	-0.7	1.5	4.0	2.3	-0.9	21.2	6.0	11.1	5.2
5	US162	-1.0	-0.3	1.8	5.2	2.6	2.4	19.0	11.5	8.0	5.5
5	US197	-0.8	0.5	-1.5	3.7	4.2	3.0	9.1	10.3	15.0	4.8